Design, Numerical Analysis, and Fabrication of Laparoscopic Forceps with an Integrated Pneumoperitoneum and Suction Irrigation Feature

THESIS

Submitted in the partial fulfillment

of the requirements for the degree of

DOCTOR OF PHILOSOPHY

by

MD. ABDUL RAHEEM JUNAIDI

ID. No. 2016PHXF0119H

Under the Supervision of

Dr. RAM CHANDRA MURTHY KALLURI

&

Under the Co-supervision of

Prof. Y.V. DASESWARA RAO

BIRLA INSTITUTE OF TECHNOLOGY AND SCIENCE, PILANI

2022

BIRLA INSTITUTE OF TECHNOLOGY AND SCIENCE, PILANI

CERTIFICATE

This is to certify that the thesis titled **"Design, Numerical Analysis, and Fabrication of Laparoscopic Forceps with an Integrated Pneumoperitoneum and Suction Irrigation Feature"** submitted by **Md. Abdul Raheem Junaidi**, ID No **2016PHXF0119H** for award of Ph.D. of the Institute embodies original work done by him under my supervision.

Signature of the Supervisor:
Name in capital letters: Dr. RAM CHANDRA MURTHY KALLURI
Designation: Assistant Professor, Department of Mechanical Engineering, BITS-Pilani Hyderabad Campus

Date: 24/11/2021

Signature of the Co-supervisor:
Name in capital letters: Prof. Dr. Y.V. DASESWARA RAO
Designation: Professor, Department of Mechanical Engineering, BITS-Pilani Hyderabad Campus

Date: 24/11/2021

ACKNOWLEDGEMENTS

I express my sincere thanks to all those who directly or indirectly helped me in completing my Ph.D. in the Mechanical Engineering Department at Birla Institute of Technology & Science, Pilani (BITS Pilani), Hyderabad campus. Firstly, I express my gratitude to my supervisor, Dr. Ram Chandra Murthy Kalluri, and co-supervisor, Prof. Y. V. Daseswara Rao for their constant support, suggestions, and priceless guidance during the entire course of the Ph.D. program. Their timely guidance and sustained encouragement helped me in completing the thesis in time. I take this opportunity to thank my doctoral advisory committee members, namely Prof. Srinivasa Prakash Regalla and Dr. Supradeepan K., for their valuable suggestions during the entire course of my Ph.D.

I am grateful to Prof. Souvik Bhattacharyya, Vice-Chancellor, BITS Pilani, and Prof. G. Sundar, Director, Hyderabad campus, for giving me this opportunity and providing the facilities for research in the institute. I am thankful to Prof. S.K. Verma, former Dean, Academic Research Division, BITS Pilani, Prof. Vidya Rajesh, former Associate Dean, Academic Research Division BITS Pilani, Hyderabad campus and Dr. V.V. Vamsi Krishna, Associate Dean, AGSRD of BITS Pilani, Hyderabad campus, for their encouragement and co-operation in carrying out this doctoral work. I am thankful to Prof. N. Suresh Kumar Reddy, Head, the convener, and members of the DRC, for their continuous support in fulfilling the academic requirements. I would extend my sincere thanks to all the faculties and staff members of the Department of Mechanical Engineering, BITS-Pilani, Hyderabad campus, for supporting and helping me whenever needed.

Special thanks to Dr. Gopala Krishna Gokhale of Cardiothoracic Surgeon, Apollo Hospital, Hyderabad, Dr. M. A Saleem, Head, Laparoscopic Surgeon, Care Hospital, Banjara Hills, and Dr. Niranjan Ravuri, Laparoscopic Surgeon, NIMS Hospital, Hyderabad, and CEO

of Pinoty and care motto for allowing me to visit, observe different surgeries which helped me in setting the direction of this investigation and other research facilities. I am thankful to my fellow Ph.D. scholars at BITS-Pilani for their critical remarks and invaluable help. I am also thankful to the undergraduate students, Mr. Aakrit Patel, Mr. Krovvidi Anirudh, and Mr. Harsha Sista, for helping me in learning software.

I would like to take this opportunity to thank the management of Muffakham Jah College of Engineering and Technology (MJCET), Hyderabad, where I have been working as a faculty member for nine years. I express my regards to all my colleagues at MJCET. I extend my gratitude to Prof. Syed Ferhatullah Hussainy, Professor, Dean, and Head, MJCET, and Prof. Basheer Ahmed, Advisor cum Director, MJCET, Mohd. Abdul Samad, Asst. Professor, MJCET, for their help in the completion of work. I thank my family, especially my father, Late. Dr. Md. Abdul Khadeer Junaidi, Retired, Head Master, my mother Mrs. Afshan, Lecturer, who always supported me at every stage of my life. I would like to thank my Sisters Ms. Habeeba Bader, Scientist, Canada, and Haleema Sadia, Software Engineer, Australia, for helping me in difficult times. I'm also thankful to my wife, Mrs. Aliya Raheem, and my children, Syeda Ameena Fatima and Syed Md. Ibrahim Junaidi for their moral support. I thank SEED team members for providing a congenial environment. I thank Dr. Vikranth Kumar S, faculty–in-charge, and Mr. Rama Chandra Sharma, Programmer, CAD Lab, for carrying out my research activities in the laboratory. Lastly, I thank the Almighty Allah for giving me the courage to face challenges in every aspect of life.

Md. Abdul Raheem Junaidi

ABSTRACT

In the current scenario, minimally invasive surgery tends to be a leading surgical procedure in the medical area and has gained importance over open-cut surgery. Surgeries used by the traditional open-cut method are replaced with laparoscopic surgeries for cosmetic fineness. So, attention is now being turned to the latest equipment and surgical procedures to permit the surgeons and patients to use economic and environmentally friendly approaches based on instrument design and quality. A Minimally invasive procedure is used to perform surgery on the organs of the abdominal cavity of patients or to diagnose alterations. In minimally invasive surgery (MIS), laparoscopic surgical procedures are widely used as only small incisions are made during surgery. Despite its potential demand, the surgeons undergo fatigue and stress due to the existing design features of the instruments used. During laparoscopic surgery, the surgeons experience some difficulties due to a few deficiencies in the design of the laparoscopic instrument. The suction and irrigation, dissector, and CO_2 insufflator devices play an essential role in laparoscopic surgery. However, the amount of work done concerning these aspects by researchers worldwide is limited.

A laparoscope is used for manipulating the infected organ in minimally invasive surgical procedures. During surgery, blood often oozes out of the operated tissue, which has to be sucked out by the Suction-Irrigation (S-I) device. Thus S-I devices are used to clean and disinfect the abdominal cavity during surgery to enable safe and efficient inspection of the surgery area. Blood and other body fluids are sucked out as when required by the surgeon, and the site of surgery is irrigated with a disinfectant liquid, like saline water. In most surgeries, the dissector forceps, and S-I device are exchanged repeatedly and many times to operate and clean the site of surgery.

The objective of the research work is to introduce a new design of an instrument that combines the functionality of forceps with that of an S-I device. Currently, the above two

operations have to be carried out sequentially, which adds to the time and effort of the surgeon. Integrating these features within the same device will ensure that both processes can occur using a single device and may be repeated without exchange of additional devices through the incision as and when required, without unnecessarily removing the device. This reduces the time lost in swapping them, thereby reducing the surgery time and additional effort by the surgeon.

This research proposes a modified design by combining the suction-irrigation features and CO_2 features with the laparoscopic dissector. The modified design is first modeled in SolidWorks and then analyzed for fluid flow using ANSYS Fluent. Parametric analysis was performed to obtain the optimal design for the proposed multi-functional instrument, which will potentially improve the overall efficiency of the laparoscopic surgical process.

Computational fluid dynamics (CFD) studies were done on the modified laparoscopic instrument which is designed to work both as a suction-irrigation device and as a surgical forceps. Therefore, for a more comprehensive CFD flow analysis of the improved forceps, the flow of cleaning fluid is simulated in the present work for different driving pressures. Five different pressure differences have been used to study the performance of the new design in terms of the resulting mass flow rate in both suction and irrigation modes. Initially, the forceps were designed to achieve a better mass flow rate than the currently used S-I device. As the mass flow rate resulted was too less, then the protrusion design was moved from the connector end of forceps to the outer sleeve component, with which the mass flow rate showed similar results to that of the existing S-I device. However, to effectively achieve a more mass flow rate, four different types of forceps design were considered. The two designs of 8mm and 10mm outer sleeve diameters, which basically is meant to insert into patient's abdominal cavity were chosen and analysed consistently. Similarly, the results with two different protrusion angles $\phi = 45^o$ and $\phi = 60^o$ are compared both in suction and irrigation modes. The results show

that the mass flow rate is higher for $D = 10mm$ design compared to $D = 8mm$ designs. However, as the 8mm design resulted in sufficient mass flow rate and showed similarity in mass flow rates to that of the standalone S-I device and minimal size in the patient abdomen is preferred, hence 8mm design is selected. Among two different protrusion angles, the mass flow rate for $\phi = 60^o$ design is higher compared to $\phi = 45^o$ design in both Newtonian flow and non-Newtonian flow analysis. So, 60^o design was chosen for fabrication. These designs were evaluated based on mass flow rates they provided and how well they match with the existing S-I device for the range of pressure differences considered.

The non-Newtonian flow of blood has been simulated using Carreau model. The resulting flow rate of blood is compared with the prospective designs and the S-I device currently in use. The final improvised design of the forceps with D = 8mm and $\phi = 60^o$ design is proposed based on this analysis. Results for the flow of Newtonian fluid are investigated with the help of contours of velocity, pressure, turbulence kinetic energy, and turbulence eddy dissipation rate. In comparison, the results for the flow of non-Newtonian fluid are investigated with the help of contours of velocity, pressure, wall shear stress, strain rate, and viscosity. The proposed design of surgical forceps eliminates re-insertion of dissector and suction-irrigation device and is reusable, multi-functional, non-toxic, corrosion-resistant, toughened, and will be cost-effective. In addition, this forceps will potentially reduce the time of surgery, fatigue to the surgeon, and trauma to the patient. This can also potentially benefit single port and robotic laparoscopic surgeries.

The research work also included the analysis of the gas flow in a multi-functional laparoscopic instrument which can potentially serve as a pneumoperitoneum device. A comprehensive CFD flow analysis of the flow of CO_2 is presented for different driving pressures using ANSYS FLUENT software. The resulting flow rate of CO_2 is obtained for different driving pressures. The results are investigated with the help of contours plots of

different flow variables. Multi-phase simulations were carried out for completeness of the present study and look into the fluid flow behavior inside the instrument when both the fluids flow together. The results obtained are mainly qualitative in nature and help us visualize the interaction of two different fluids to get more insight of fluid flow and clear distinction among them.

Keywords: Computational fluid dynamics, Newtonian flow simulation, non-Newtonian flow simulation, Multi-functional instrument, CO_2 insufflation, Suction-Irrigation device, dissector forceps, laparoscopic surgery, numerical analysis, experimental validation.

TABLE OF CONTENTS

LIST OF TABLES

LIST OF FIGURES

Nomenclature

n	Number of operations performed
d	Duration
ϕ	Protrusion angle
D	Diameter
ΔP	Pressure difference
ϵ	Turbulence dissipation rate
M	Number of Mesh elements
γ	Strain rate
μ	Viscosity
μ_o	Zero shear viscosity
μ_∞	Infinite shear viscosity
ρ	Density

List of abbreviations

MIS	Minimally Invasive Surgery
CFD	Computational Fluid Dynamics
S-I	Suction-Irrigation
CO_2	Carbon dioxide
DOF	Degree of Freedom
CNC	Computer numerical control
OD	Outer diameter
ID	Inner diameter
SIMPLE	Semi-Implicit Method for Pressure Linked Equations
IAP	Intra-abdominal pressure

Chapter – 1

1 INTRODUCTION

1.1 General

Almost all the surgeries performed before the 20th century were open incision surgeries, i.e., the human body is cut wide open for surgery. In open incision surgery, surgeons cut open parts of the human body to operate on the affected tissue. After surgery, the opened part is stitched. Open surgeries have many disadvantages like significant recovery times, post-surgery pain, and a possible infection developed in the body. This affects the quality of life. In some cases, even after a couple of months, patients cannot resume a normal lifestyle due to blood loss and other complications.

To overcome all these deficiencies faced by patients, a new surgical technique was introduced in the late 19th century, namely laparoscopy, which was a game-changer in the entire surgical domain. Laparoscopy is a minimally invasive surgery that requires multiple small incisions of the order 5 mm to 10 mm, instead of broader cuts of sizes 150 mm to 200 mm in case of open surgeries, as shown in Figure 1.1. In order to have a clear view of internal organs, the abdomen of the patient is inflated by pumping an inert gas, like carbon dioxide (CO_2). CO_2 has a high diffusion coefficient, non-flammable, and is colorless. Hence, it is typically used for insufflation (capnoperitoneum) in minimally invasive surgeries like arthroscopy, endoscopy, and laparoscopy. It can also be rapidly cleared from the body as it is a natural metabolic end product and can reduce the risk of complications after venous embolism. Laparoscopic surgical techniques find applications in laparoscopic cholecystectomy (removal of gall bladder), laparoscopic myomectomy (removal of fibroids from uterus), laparoscopic hysterectomy (removal of the uterus), laparoscopic appendectomy (removal of the appendix), laparoscopic

splenectomy (removal of the spleen), diagnostic laparoscopy (viewing internal organs), Nephrectomy (removal of kidney), kidney transplantation, etc.

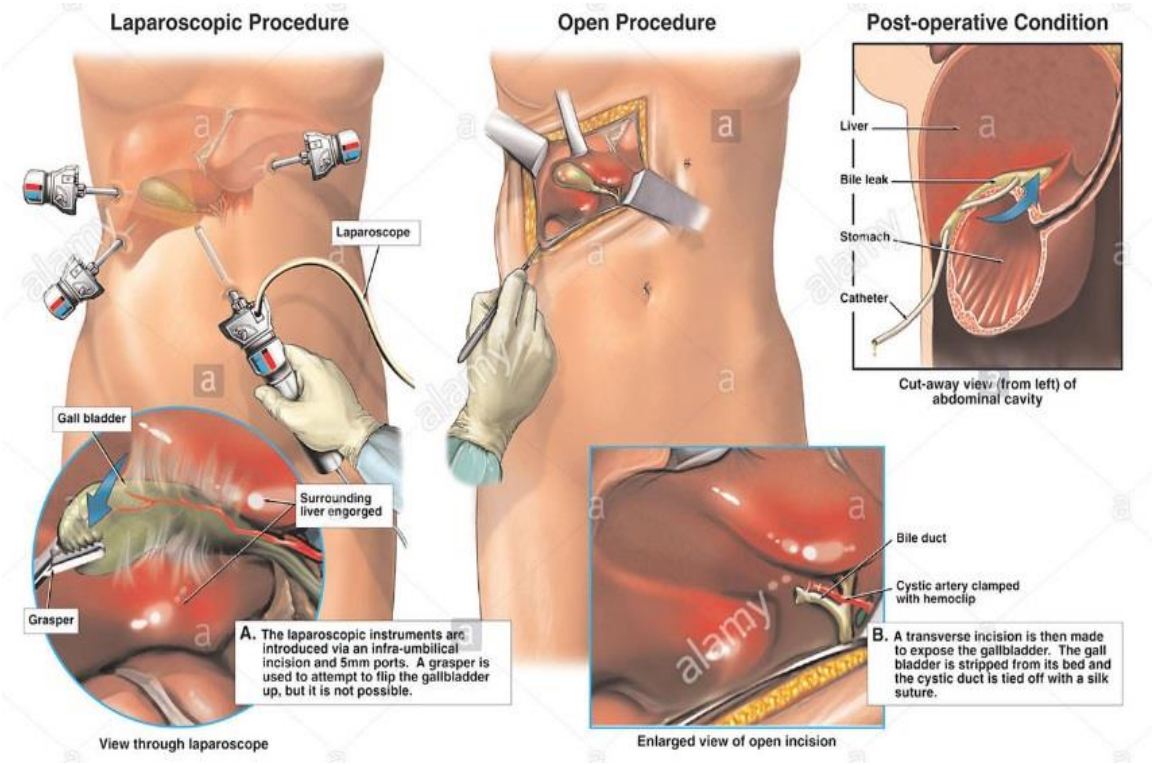

Figure 1.1: Laparoscopic cholecystectomy versus open incision surgery.

(Image source: Alamy stock photo)

An entire set of new instruments were developed in the 20th century and put to use in surgeries. A laparoscope is one such device used in laparoscopic surgeries. The modern-day techniques and state-of-the-art technologies from the fields of electronics, optics, and material science contributed to the development of a laparoscope. The idea behind the development of the laparoscope was to get dextrous access to internal organs of the human body by a surgeon, similar to the way a surgeon's hand accesses them from outside, yet have a complete vision of the area where surgery is happening with minimal incisions on the patient's body. Surgeons could hence make small incisions on the abdomen or other organs of a patient so that they can insert a trocar through incisions made to inspect and operate on the required internal organs. A Laparoscope, in the early periods, was a device similar to an endoscope with a high-intensity

light source and a digital camera. The material of the instrument has to be biocompatible, and the instrument has to be electrically insulated against contact between the device, internal organs, and fluids.

Laparoscopy has been widely put into practice since the 1990s and is gaining popularity in the field of surgery. Of late, it is very common to perform laparoscopic surgeries as the patient experiences less post-operative pain, minimum hospitalization duration, and lesser infection complications. Despite having these benefits from laparoscopy, surgeons continue to face other issues like longer surgery time and non-ergonomic laparoscopic instruments [1]-[4]. Other factors that affect surgical procedures are low or high surgery table height, poor positioning of the monitor, design of instrument handle, the posture of surgeons, usage of instrument multiple times, etc. These factors influence surgeons as they experience physical strain during laparoscopic surgeries. Some inventors came up with an ergonomic handle design for Maryland forceps, which improved the positioning of forceps at an appropriate location and orientation [5]-[8].

Laparoscopic instruments are classified depending upon their functionality as graspers, scissors, cauterizers, vessel sealers, etc. Maryland forceps belong to the category of grasping instruments, which facilitate ligating, positioning, and manipulating the tissue. The basic components of the Maryland forceps include jaws, end effector assembly, handle, outer and inner tubes. As shown in Figure 1.1, the handle lets the surgeon hold forceps and actuates the jaws to manipulate the tissue while performing surgery. The end effector assembly, jaws, is actuated using a four-bar linkage.

The saline water and other fluids are supplied during operation through another trocar. The removal of blood or fluid in the abdomen during surgery is called suctioning, while injection of fluid at the site of surgery to clear blood on the tissue is called irrigation. The suction and irrigation are done independently using another trocar. Suction-Irrigation (S-I)

device is used either to remove or add cleaning fluid at the site of surgery. As shown in Figure 1.2, William et al. [9] introduced a laparoscopic irrigation bottle pump, which mechanically regulates the liquid flow from a bottle into the irrigation line through pressurized CO_2 gas. This leads to a possibility of excessive CO_2 gas entering the irrigation line, causing severe health problems to the patient. Alternatively, the irrigation flow line could run out of CO_2 gas. Therefore, this requires continuous monitoring of the level of fluid in the bottles and hence prolongs the time required for surgery.

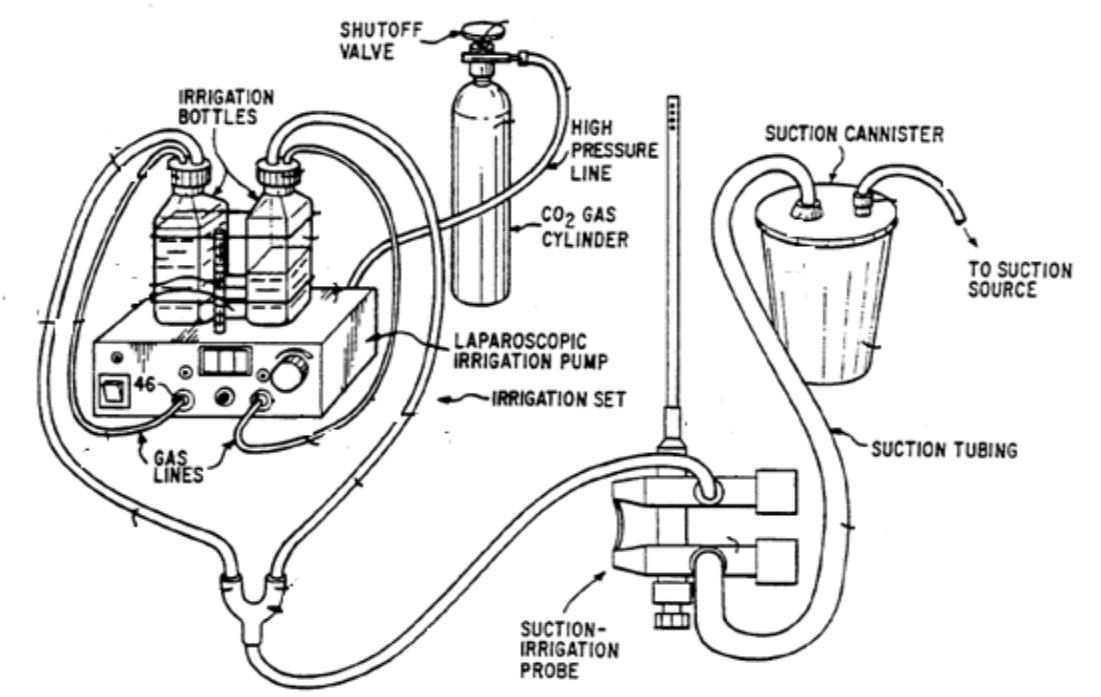

Figure 1.2: Suction-Irrigation bottle pump [9]

1.1.1 Overview of different laparoscopic instruments

There are many laparoscopic instruments used in laparoscopic surgeries. Different variations that came into existence in the design of commonly used forceps for micro-surgeries include surgical suction device [10], motion-compensated microscope [11], needle lock for jaws [12], endoscopic instrument [13], cupped forceps [14], laparoscopic kit [15], auxiliary forceps [16], Maryland forceps [17],[18], tissue retrieval forceps [19]. Some of the commonly

used instruments whose multifunctional aspects are relevant to our proposed design are briefly described below.

1.1.2 Suction-Irrigation pump

Figure 1.3: Suction-Irrigation Pump

(Source: http://www.endoscopechina.com/Electronics/suction-irrigation, *Retrieved on 26/09/2020*)

One of the commercially available Suction-Irrigation pumps is a pneumatically controlled device that provides the required pressures for suction and irrigation operations. It has two plug-ins, one for suction and the other for irrigation, as shown in Figure 1.3. The suction port tube is attached to a hydrophobic filter. The liquid bottles used for suction and irrigation are made of glass as they must sustain pressure fluctuations. The suction and irrigation pipes are connected to two different ports of the S-I device. After completing the self-test, the desired suction and irrigation power levels are set. The buttons on the suction and irrigation ports are used to close and open the flow to the respective lines. The unit can also be started and stopped using a foot-operated pedal.

1.1.3 Suction and irrigation device

Abraham et al. [10] invented a surgical suction device to control negative pressure. In this, they used sponge plugs to remove liquid inside the abdomen. Such traditional suction systems include the use of sponge plugs, which always had a chance of being left inside the

body, causing serious postoperative complications to the patient. Also, traditionally suction and irrigation systems were used separately, and this causes serious concerns regarding its handling time and complications. A suction instrument, shown in Figure 1.4, deals with the conventional problems associated with suction and irrigation mechanisms. It is a simple S-I device with an absorbent material at the distal end. The idea is to provide two different flow rates using what is known as direct suction and indirect suction. Direct suction is used when the required suction rate is high, and there is no risk of occlusion or tissue damage, whereas, for a lower flow rate, indirect suction is used. Indirect suction is achieved by the flow of fluid through the absorbent material, whereas unobstructed flow is achieved by the direct suction method.

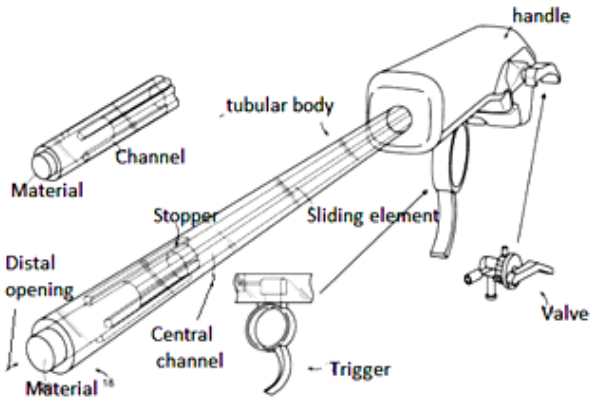

Figure 1.4: Direct and Indirect suction device [10]

The success of a laparoscopic procedure depends significantly on the skills of the surgeon because of the limited range of motion available to the surgeon in the body cavity and the reduction from real-world 3D vision to a virtual world 2D image on a screen to manipulate the tissues using surgical devices instead of directly using his hands. The suction tip is one of the few parts of an S-I device that has direct contact with the tissues inside the human body. Therefore, it exerts a large amount of pressure during suction and irrigation procedures. The modified design [20] has a bowed tip, unlike that in a conventional laparoscope. The curvature

of the bow tip covers more area during the circumferential movement of the tip and S-I tube. Further, it also helps in withstanding large pressure at the tip.

1.1.4 Electrosurgical forceps used for cutting and sealing

This forceps act as a plier to grasp, manipulate, and seal the tissue [21]. It has two levers that are joined at a pivot. It consists of a knife that extends between the jaw members with a handle to grasp and limit the movement of the two levers beyond the closed position. These forceps are employed for electrosurgical grasping, cutting, and sealing the tissue.

1.1.5 Endoscopic instrument

Schneider et al. [13], invented an endoscopic instrument that consists of an extended tube inserted through the trocar. It has two main parts, viz. inner push rod, and outer sleeve. The outer sleeve is insulated and has an irrigation attachment to clean and sterilize tissue inside the body. The handle actuates the inner push rod to manipulate the blades, known as the tool at the tip.

1.1.6 Maryland forceps

Maryland forceps are a crucial instrument in laparoscopic surgeries. Many patents are proposed based on different component's design and their usage by the researchers [6], [23]. Figure 1.5 shows Maryland forceps used in surgeries wherein the end effectors are pulled and pushed in order to manipulate the tissue. This is a disposable laparoscopic surgical instrument having end effectors manipulated by the handle. The handle is made of lightweight plastic or stainless steel, the inner tube is made of aluminum, the outer tube is made of plastic, the end effector & claws are made of cast bronze, and aluminum alloy is used for clevis. Plastic shrink is wrapped over the outer tube and handle to prevent electric shock. Insulation is also ferruled on the handle to ensure insulation from the handle to the tube. The tube and push rod imparts axial translation to the end effector. When the handle is closed inwards, the end effector moves

to the right and vice-versa. These forceps are either unipolar or bipolar and use an ultrasonic frequency electrical supply to dissect the unhealthy tissue.

Figure 1.5: Currently used Maryland forceps

(Source: https://www.teleflexsurgicalcatalog.com/surgical/pilling/contact, *Retrieved on 26/09/2020*)

Smith et al. [23] invented disposable Maryland dissectors used in minimally invasive surgery (MIS). Melzer et al. [24] described several devices that could be multifunctional like high frequency ultrasonic dissection and suction and irrigation. Sakurazawa et al. [25] undertaken a study to evaluate the safety and efficacy of forceps cum suction tube device useful in laparoscopic surgery for gastric cancer. No excess tissue damage was observed during operation with significant reduction in suction access time.

1.2 Problem description and motivation of the work

In the early periods, laparoscopic surgery is used rarely because of its cost expensive nature, and it operates with a digital camera and high-intensified light source. The laparoscopic material is completely electrically insulated and is biocompatible. The electrically insulating behavior of the instrument helps to be non-contactable between the instrument and the internal body organs during surgery. In due course, with positive feedback such as minimum duration of hospital stay, less pain after surgery, lesser infections, etc., patients gained faith in laparoscopic surgery; however, surgeons still face certain difficulties due to repetitive usage of the laparoscopic instruments and longer duration to complete the surgery. Some researchers came up to design the ergonomic model of the forceps used in laparoscopic surgery for enhancing the positioning based on its orientation and location [24].

So, a lot of research is focused on minimizing the limitation of the laparoscopic instrument by enhancing its handle design only. The S-I process requires repeated insertion and removal of multiple instruments, which results in prolonged duration in surgeries, and surgeons are very likely to feel exhausted. Moreover, a significant amount of time is spent in instrument exchange between the S-I device and the dissector forceps. The exchange of instruments also compromises the safety of the patient and disrupts the sequence of operation. The objective of the research is to enhance the multifunctional feature of the dissector forceps so that it aids in reducing the time of surgery, improving the ergonomics of the instrument, and the patient's safety. This is accomplished in the present work by merging the S-I feature with the dissector forceps. Chapter 2 of the literature survey reviews the latest developments in laparoscopic instruments, and shortcomings are addressed.

Even though inventors have introduced many instruments, only a few of them focused on the multi-functionality of the instrument. During surgery, the excess fluid and charred particles obstruct the field of view and require to be removed periodically. This requires the removal of one instrument and insertion of the S-I device. Also, continuous removal and insertion of instruments result in pressure drop in the abdomen. Consequently, after completing the S-I process, again, the abdomen must be inflated by supplying an additional amount of CO_2, which adds to the duration of surgery. A suction device creates negative pressure to suck the fluid inside the abdomen. If the suction pressure is increased, there may be a chance that the healthy tissue is sucked in the S-I device. In addition, due to the prolonged duration of surgeries which involves the insertion and removal of multiple instruments, surgeons, apart from fatigue, also suffer injuries after performing laparoscopic surgeries. Due to the removal and insertion of multiple instruments, there can be a risk to the patient if they are not inserted properly, disrupting the sequence of surgery. All of these contribute to the increase in the duration of surgery by up to 30% [26],[27].

Maryland forceps, one of the commonly used laparoscopic instruments, is an imported device, due to which the cost of procuring it is quite high. Previous attempts have been made, with several patents addressing the different laparoscopic instruments as detailed in Table 1.1. Many of them concentrate on improving the design of the forceps, and a few try to improve the efficiency of the S-I process by having absorbent materials integrated into the device. However, the combination of the Maryland Forceps with the Suction-Irrigation apparatus has not been addressed.

Table 1.1: Literature review and findings

Patent number/ Journal details	**Description**	**Drawbacks**
1. US8821377 B2, [15]	The invention discloses the kit to remove the tissues during laparoscopic surgery and robotic surgery. The inventor compares laparoscopic surgery to the modern surgical technique over laparotomy procedures. Laparoscopic procedures are advantageous due to fewer infections and pain, shorter stay in the hospital, less scar, less blood loss leading to fewer complications post-operation. However, there is difficulty in removing a large chunk of tissue. For this, a laparoscopic bag is introduced via a blunt instrument.	The limitation of the usage of a laparoscopic bag is a 15-20 mm incision. However, the procedure is still effective compared to open surgeries wherein there will be an incision of size more than 100 mm.

2. Royal Australasian College of Surgeons ANZ J Surg, [28]	This review explores current evidence on the cost and environmental impact of reusable versus single-use instruments. In addition, their quality, functionality, and associated clinical outcomes are compared.	The usage of disposable instruments shall be minimized to avoid waste disposal of surgical instruments that are not eco-friendly. Also, disposable instrument cost is not economical. However, reusable instruments face the problem of sterilization.
3. US20150038895A1, [20]	The patent discloses an irrigation and suction tip that moves in a circumferential trajectory to cover a large area in the abdominal region during laparoscopic surgeries. The device is used for suctioning and irrigating within a surgical cavity. It has a short distal end, tip, and a long proximal end.	The bigger diameter of the proximal end does not allow the instrument to traverse inside the trocar. The device is limited to its tip size, having a shorter end so as to move the tip inside the cannula of the trocar.
4. Article in Minimum Hindawi Publishing Corporation	The article studies to reduce the cost of laparoscopic surgeries by reviewing data from January 2012 to December 2013. In his study, he found a reusable instrument's cost to be one-tenth of that	Reusable instruments have many benefits over disposable instruments. However, it may lead to more medical issues if

Minimally Invasive Surgery, Volume 2014, [29]	of a disposable instrument's, without compromising the safety of the patient and the medical staff.	proper sterilization is not done.
5. EP2422720 B1, [30]	The present invention discloses forceps used for laparoscopic gall bladder surgeries. The stones in a gall bladder are crushed by the forceps and retrieved from the cannula of a trocar.	The invention is restricted to only the laparoscopic gall bladder. The forceps do not apply to other laparoscopic surgeries.
6. Current Problems in Surgery Vol 52, [5]	Surgeon faces issues from the energy settings to be used in an electro-surgical device due to which the patients are at risk. About 54% of surgeons in the American College of Surgeons have faced electrical injuries.	The choices of power settings and risks associated with radio-frequency electrosurgery depend on the experience and practice of surgeons in handling devices to minimize the risk of injury to the patients
7. US20140236147A1 [13]	The device comprises a rigid tube meant for suction and irrigation outside an endoscopic instrument. It has an inner transmission element that can move within the outer tube.	The instrument does not have laparoscopic applications.

1.3 Scope and objectives of the present study

Based on the detailed literature review and the research gaps as presented in sections 1.2 and chapter 2, the following are the scope and objectives of the present study,

1. To identify the shortcomings of laparoscopic instruments from observations of different laparoscopic surgical procedures.
2. To study the existing form of laparoscopic instruments.
3. To design and modify an existing form of Laparoscopic forceps which allows grasping of tissue while simultaneously manipulating, suctioning, irrigating and cauterizing.
4. To carry out Newtonian and non-Newtonian simulations of the proposed laparoscopic forceps and analyze the results using ANSYS Fluent.
5. To find out the provision for gas flow and analyze the carbon dioxide gas flow inside the fluid domain of the laparoscopic forceps.
6. To fabricate the prototype of the proposed design for Laparoscopic forceps.
7. To evaluate the ergonomics of the fabricated Laparoscopic forceps to meet the requirements of Laparoscopic surgeries.

1.4 Presentation of Thesis

The thesis has been presented in eight chapters, as outlined below.

Chapter-1 deals with the introduction, which focuses on various instruments used in conventional surgery to modern laparoscopic surgery. This chapter has been divided into four sections: general introduction, problem description, motivation of work, scope and objectives, and Presentation of the thesis.

Chapter-2 contains a literature study is made on conventional surgeries and laparoscopic surgeries, laparoscopic surgical instruments, ergonomic-based design, recent

trends and modifications in the surgeries, and the use of numerical analysis in surgical instruments. Gaps in the research are presented at the end of this chapter.

Chapter-3 describes the design modifications and modeling of the proposed laparoscopic instrument. The desired feature of the proposed design is studied to model all components in SolidWorks software. This chapter enlightens a detailed discussion on the construction, functionalities, mechanisms, and fabrication details of each component to get the desired forceps assembly.

Chapter-4 highlights the CFD analysis of the Newtonian fluid flow approach to compare existing designs to that of different proposed designs of laparoscopic forceps. Simulation results are compiled with regard to the different designs and compared. Simulation results are analyzed to check the pressure variation and mass flow rate within the fluid domain, which otherwise would be difficult to measure experimentally for 4 to 5 different proposed designs. The proposed forceps is re-designed further to facilitate the provision of carbon dioxide gas. The fabricated instrument is compared with a numerical analysis of the Newtonian fluid flow approach.

Chapter-5 describes the CFD analysis of non-Newtonian fluid flow to compare existing designs to that of different proposed designs of laparoscopic forceps. A combined effect of all these parameters using non-Newtonian and Newtonian approaches is also compared in this chapter. Based on this, the optimized model has been developed, and the prototype has been proposed for fabrication. Details of the prototype are given in this chapter.

Chapter-6 highlights the gas flow analysis, which is incorporated into the same proposed laparoscopic forceps. Initially, the geometry of the fluid domain is considered for mesh refinement studies. Later, boundary conditions are imposed and solved to obtain pressure and velocity changes at different mass flow rates.

Chapter-7 includes the multi-phase simulation where water is taken as the primary phase, and CO_2 gas is taken as the secondary phase. The inlet of the fluid domain is split into two that is 20 percent entry to the CO_2 gas passage area and 80 percent entry to the water passage area. Then, a simulation is carried out to obtain the results.

Chapter-8 includes the conclusions based on the preceding chapter and results presented in chapters 3, 4, 5, 6, and 7. The results obtained in these chapters describe the validation and simulation of the model used for a fluid domain by comparing the results with the previously published data. Scope for future work is also included at the end of this chapter.

The remaining sections contain the references, appendices, and referred published works in international journals and international conferences; those are relevant to the research topic, followed by brief biographies of supervisors and candidate.

Chapter – 2

2 Review of Literature

2.1 Introduction

Over the past 30 years, the procedures of minimally invasive surgery have become popular among the different conventional types of surgeries. In comparison with open-type conventional surgery, laparoscopic surgery is considered less invasive. In this surgical type, the surgical tools are passed into the abdomen of the patients through small and medium type trocars with 1 cm to 1.5cm of diameter level [31]. Many advantages are accomplished from the smaller incision surgery, such as minimum cost, smaller scars, faster recovery, and shorter hospitalization time [32]. This surgical type is considered the most widely used and earliest one among the several minimally-invasive techniques for proper diagnostics [33]. A skilled surgeon is required to establish the laparoscopic surgical procedures on the abdomen of the patients by inserting the laparoscopic surgical instruments through the port sites [34]. Certain standard sets of instruments, including dissectors, graspers, forceps, suction, and irrigation type devices, are widely employed in laparoscopic type surgical assistance. It has several more beneficial activities than the previously performed open surgical procedures, such as minimum surgical invasiveness, fewer mortality rates, and invisible scars [35]. Thus, the surgeons exercised their skills and enhanced their access to the laparoscopic surgical area more than the conventional surgery [36]. Typically, the laparoscopic instruments are employed with one limb during the operations of staple/cut/dissect; at the same time, navigation and visual field are maintained by other instruments. During the surgical, its actions or directions are altered as per the need [37].

Based on the factors of human input, several laparoscopic devices are designed with proper significant procedures. The design modifications are generally performed to enhance the level of usability, safety, and error minimization. Normally, the surgical instruments are reused [38]. However, it requires several disinfection procedures while using the instruments repeatedly. It may create the risk of incomplete results of disinfection. To overcome this, different disposable laparoscopic instruments are introduced into the market. In this, the cost of disposable type laparoscopic instruments is a little more when compared with the reusable type laparoscopic surgical instrument [39]. All the surgical instruments are made by adopting the applications of instrument mechanisms. The mechanisms are accomplished by the linkage assembly in which the links are connected through joints. The applied links are permitted to follow the controlled relative motion [40]. The laparoscopic instrument with several interactive mechanical components is not superior. Attaining the multiple functional features from the simple action of input may result in failure in the laparoscopic instrument because of its complex behavior. At the same time, this complex nature increases the total time spent and the cost for the overall mechanical parts of the laparoscopic instrument. Thus, it is counter-productive to design laparoscopic instruments with several mechanisms [41].

The robotic applications in surgical characteristics employ convenience for humans. Replacing the assistance of humans with the robot enhances the autonomy level of surgeons and limits the communication issues attain in the operating room [42]. For enhancing the clinical outcomes, robotic surgery has contributed as a minimally invasive technique, and it can restrict the limitations of the conventional type of laparoscopic surgery, such as reduced instrument movement and 2-dimensional imaging characteristics [43]. Instead of conventional laparoscopic surgery, robotic laparoscopic surgery can also be used because it performs well in complicated

situations within a short time duration. The surgical end actions and effectors are relatively similar between robotic and conventional laparoscopic surgery [44]. The robotic assistance is also done with the utilization of certain simulation kinds of approaches, namely CAD design and ANSYS analysis. Several types of research focused on the number of software programs for surgical analysis. It promotes the prediction of post-surgical outcomes from the performance analysis of several surgical instruments. 3D imaging provides a better and more convenient extraction of information about the patient by surgeons [45].

The main aim of this review is to enhance the functionalities of laparoscopic instruments in the view of available instruments. The various approaches of design modifications involved in the three different laparoscopic instruments, namely, grasper, forceps, and suction irrigation devices of the laparoscopic surgical applications, are categorized in this review. The present work gives the benefit of reviewing the options to designers to solve a particular design problem and provide an optimal solution to the problems in a shorter time. The performance is also analyzed at the terminal part of this study with the help of the performances of instruments.

This work focuses on improving the ergonomics of laparoscopic surgical instruments. By comparing with the existing works in laparoscopy, this is the first attempt to analyze the laparoscopic instrument based on the fluid flow behavior. In the present work, the need for laparoscopic surgery against open surgery is discussed in section 2.2. The existing reviews based on different laparoscopic instruments such as forceps, suction-irrigation, graspers, etc., are discussed in section 2.3. The failures in the laparoscopic instrument and the safety analysis of such an instrument are discussed in section 2.4. Section 2.5 discusses the various design modifications to enhance the ergonomic level and simulation software used for altering the laparoscopic design and analyzing its effect. From the overall analysis, the rarely researched laparoscopic instrument

is discussed in section 2.6**.** Section 2.7 discusses recent trends in laparoscopic instruments and concludes with the overall review and research gaps in the literature. This work helps surgical instrument designers modify the existing design of the laparoscopic device to benefit surgeons. This helps minimize the time taken to complete the laparoscopic surgery.

2.2 Conventional vs. Laparoscopy Surgical Instruments

In open surgery, the operation is handled manually by touching the organ or tissue in a body. Contrary to open surgery, laparoscopic surgery is performed using the laparoscopic instrument, which is mainly a device called a 'trocar' that is inserted into the body. Laparoscopy surgery is different from conventional open-type surgery, where a small incision is used for accomplished the operation. Certain invasive internal surgeries fail due to the required design specifications of the traditional surgical instruments. Besides, the laparoscopic instrument's overall cost is less than the open-type surgeries [46]. Gehrman et al. [47] analyzed the cost of laparoscopic and open surgery based on Health economics for rectal cancer. The cost was assessed for both short-term analysis (28 days) and long-term analysis (3 years). From the analysis, the author concludes that laparoscopy surgery was more efficient for a 3-year analysis than 28 days. Another analysis was done by Talha et al. [48], where the comparison took place based on the clinical outcome of both the open and the laparoscopy surgery. In this, the perforating appendicitis disease is considered for the entire analysis. In terms of fewer complications, a better score of pain, and earlier return to normal activities, laparoscopic surgery is considered a useful one when compared to open surgery.

2.2.1 Laparoscopic surgery

Laparoscopic surgery is a technique mainly used for abdominal surgery, in which the operation is performed by using small incisions nearly minimal 12 mm. Through these incisions,

narrow instruments, mainly trocars, are inserted to cut or sew the tissue. In this, the direct view of interior surgical sites is minimized by using a video camera approach, mainly a‘ laparoscope’[48]. A camera is inserted with one trocar, and other instruments are injected through other injection sites. During laparoscopic surgery, the Carbon dioxide gas is passed into the abdominal surgical site via a single trocar, and this helps to push the abdominal wall upward and creates a minor vacant area for the surgeon to operate. CO_2 gas is mainly used in certain minimally invasive surgeries such as arthroscopy, endoscopy, laparoscopy, etc., because of its non-inflammable and colorless characteristics. Besides, CO_2 gets completely cleared from the body and acts as an end product in natural metabolism [49].

2.2.2 Advantages and Disadvantages Over Laparoscopic Surgery

In open surgery, certain disadvantages such as metabolic stress over post-surgery, incisional pain, and tissue trauma are raised. Besides, a long incision is required for open surgery. Such disadvantages caused by open surgery get suppressed by laparoscopic surgery. In laparoscopic surgery, a patient recovers quickly due to small incisions compared to open surgery [50]. When compared to open surgery, there is no fluctuation in patient's weights after laparoscopic surgery. Minimal hospital stays, and less operating time is also considered superior benefits while carrying out laparoscopic surgeries [51],[54].

The laparoscopic approach to be used in several major surgeries such as removing the gall bladder (laparoscopic cholecystectomy), uterus removal (laparoscopic hysterectomy), cutting appendices (laparoscopic appendectomy), etc. Besides, it is used for kidney transplantation and removal of appendix and spleen, etc. [52].

The main disadvantage of laparoscopic surgery is larger operational procedures, duration of surgeries, infection rates, repetitive usage of instruments, and the cost of the materials. The

handle of the laparoscopic tool may fail to ergonomics in nature, so the surgeons face difficulties in gripping [53].

2.3 Laparoscopic surgical instruments

The contribution of surgical tools is superior to any surgical technique. Effective and secure surgery is accomplished by sufficiently equipped operating rooms. The secured procedures are performed only with the assistance of more advanced and suited reliable technologies.

2.3.1 Suction and Irrigation Instruments

The S-I device is used to clean and disinfect the operating region by removing blood and other bodily fluids through the suction feature and irrigating a disinfectant such as saline water through the irrigation feature. A typical S-I apparatus is shown in Figure 2.1

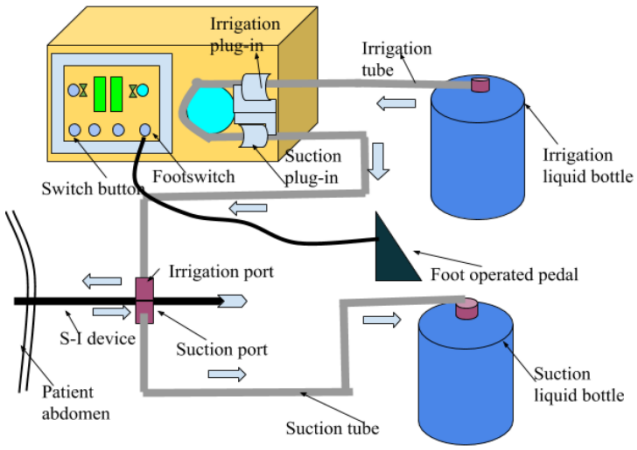

Figure 2.1: Suction-Irrigation apparatus

Carbon dioxide (CO_2) is insufflated into the abdomen before the procedure to maintain stable pressure and give more operating room for the surgeon, increasing his field of view as well. Multiple insertions and removals of instruments result in this pressure going down, due to which CO_2 has to be pumped into the abdomen again.

In current days, laparoscopic suction irrigation type is familiar in the way of surgery. The suction and irrigation laparoscopic procedures enabled to clear the blood and liquid in the abdominal cavity for promoting effective surgical behavior. The strong negative pressure is employed in the suction type of devices to damage the tissues in the body. It may fail due to delays and inefficiencies in the surgical procedure. To avoid this situation, Frech et al. [10] used sponge particles on the target area of the instrument before performing the suction behavior. It integrates the suction and irrigation characteristics through sponge applications. This process is also considered a time-consuming one. Nowadays, laparoscopic devices are formulated for both disposable and multi-use purposes. The single-use disposable items are sterile, and they cannot be recommended for reusing activities. So several types of research have focused on generating the new tool from the disposable one. It cost-effectively motivates us by producing a new tool type. The creation of different devices from the existing disposable ones proves to be financially friendly [54]. The disposal type suction and irrigation instruments with the integration of a monopolar hook are shown in Figure 2.2.

Figure 2.2: Disposable laparoscopic suction/irrigation with integrating monopolar Hook [54]

The irrigation type attains in laparoscopic surgery provides more benefits to adult patients than the child. It significantly improves the duration of the operation and is quite complex while operating in the abdomen. In addition to this, careful considerations must be followed by the

surgeons before performing irrigation to avoid the risk factors. From the analysis carried out by Siotos et al. [55], the performances of suction were a little more optimum than the irrigation level. From the existing randomized trial, it seems that the separate usage of suction and irrigation in the laparoscopic instrument is better than its combined actions. Peter et al. conducted randomized testing trials for perforated appendicitis that affected 110 children. In this, the outcomes from the individual operation process of suction and irrigation were approximately equal. There is an absence of considered variations between them [56]. The suction and the irrigation alone randomized trial test are listed in Table 2.1 with different output parameters such as operation duration, charge of the hospital, and the time taken for recovery.

Table 2.1: Randomized trial test conducted [56].

Parameter	Irrigation (n=110)	Suction (n=110)
Time taken for operation (min)	42.8 ± 16.7	38.7 ± 14.9
Hospital charges ($)	48.1 K ± 18.2 K	48.1 K ± 20.1 K
Time to regular diet (d)	3.5 ± 1.5	3.4 ± 1.7
Post-operative duration of safety (d)	5.4 ± 2.7	5.5 ± 3.0

Another way of Randomized test trial was conducted by Sun et al. [57]. In this, appendicitis disease is considered for 130 adult patients. This test was randomized to two streams, namely irrigation and suction group or suction alone group, with the help of a 3-port laparoscopic approach. The combined usage of suction and irrigation type laparoscopic instruments results in superior outputs in terms of charge and durational time of operation than the suction alone type.

The randomized trial test for the suction alone and the combination of irrigation and the suction type are listed in Table 2.2.

Table 2.2: Randomized Test Trial conducted [57].

Parameter	Irrigation and suction (n=130)	Suction only (n=130)
The volume of Irrigation (ml)	3063 ± 816	-
Hospital charge (¥)	14,592 ± 2,251	16,673 ± 2,163
Wound Infection (n)	1	3
Hospital stay Duration (d)	10.2 ± 2.5	12.5 ± 2.8
Operative time (min)	51.6 ± 16.1	41.5 ± 15.2

Due to the above limitations, we [58] developed a suction irrigation model combined with the dissector to minimize the time consumption during surgery. In this, ANSYS Fluent analysis is conducted to analyze the flow characteristic of the developed model. This approach helps to minimize CO_2 leakage and reduces the time during surgeries. Besides, the mass flow rates in the suction and irrigation process tend to increase with the increase in pressure differences, as discussed briefly in Chapter 4.

2.3.2 Grasping Tool

A laparoscopic grasping tool with multi-axis force-sensing capability is formulated for cost-effective, minimally invasive surgery. In which the tool is developed with 4 DOF, sense the

forces of single-axis- grasping and three-axis Cartesian manipulation. A wrist force sensor and two torque sensors are utilized for sensing the forces which are connected in the tool [59].

(a) Grasping Tips of the grasping instrument

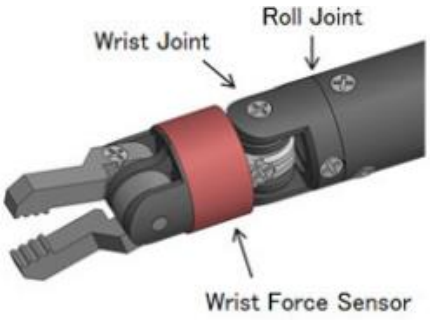

(b) 4-DOF grasper mechanism with 3-axis miniature force sensor of the grasping instrument

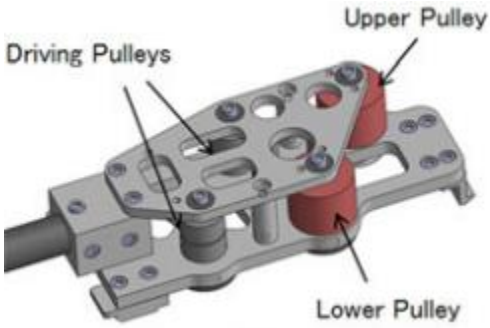

(c) Inner view of 4-DOF showing four pulleys installation at four locations

Figure 2.3: 4 DOF Grasper Instrument Model [59]

Figure 2.3 (a) represents the normal tips of the grasping tool; the 4 DOF and the pulley installation mechanism of the grasper instrument are shown in Figure 2.3 (b) and (c). Both the double and single jaw graspers with force models of tips are also developed by enabling the mechanism of graspers. In this, the grasper is designed based on ergonomic level by changing the handle orientation, tip forces, and grasper handle theoretically and experimentally. The other such type is an ergonomically developed grasper that creates the non-linear relation between the transmitted forces of the handle and tip [60]. The cable-less grasper with multi DOF has been performed for cleaning and sterilization purposes. For this, a detachable, fully functional cable-

less laparoscopic instrument with 5.3mm is designed with additional DOF at the tip. The components, namely, springs, pulleys, and cables, are hidden in the shaft of the instrument. By using the low-tech methods of cleaning, such a designed grasper instrument was assembled and disassembled for cleaning and sterilization cases [61]. Uysal et al. [62] developed a motorized model of grasping forceps with a high degree of freedom. The author concludes that the nature of ergonomics level and the weight of the instrument get reduced in the motorized model.

2.3.3 Laparoscope Forceps Models

The laparoscopic forceps is the major instrument for all simple and complex surgeries. The flexible, driven push-pull forceps manipulator for the Surgical Robot system with 3DOF is developed with the assistance of superelastic wires. The superelastic wire limits the contribution of the backbone available in the middle of the forceps model and the wire path errors. From the performances, the force is estimated experimentally at about 0.37 N [63]. The forceps manipulator plays a major role in minimally invasive surgery. Many types of research were carried out to develop a simple, reliable, and less expensive type of forceps. The development of 4-DOF based forceps reduced the interference with different surgeons and manipulators, which achieved a high power-to-weight ratio. In this, the mechanism is done by using the push-pull wire of superelastic alloy and the compact pneumatic cylinders [64]. Normally, surgeons face several issues when operating the occlusion region because of the rigid operating structure of endoscopic surgical tools. Zhang et al. [65] investigated the forceps manipulator with novel linkage bending mechanisms. This forceps manipulator is integrated with the function of the endoscope, maximum output force, and flexible bending potential. The different forceps models are shown in Figure 2.4.

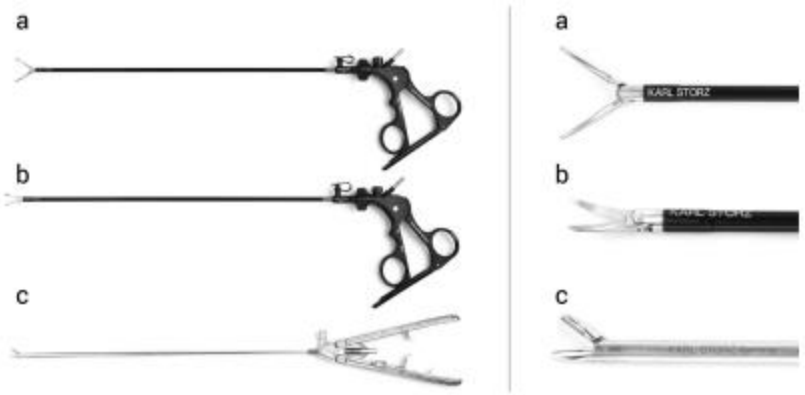

Figure 2.4: Photograph of laparoscopic dissector, scissor, and needle holder [66]

2.3.4 Maryland dissector forceps

The Maryland dissector is one of the mono-polar type electrosurgical instruments with a minimum of 3.2 millimeters of working channel diameter, and it is mainly used for dissection procedures. The efficient method of grasping design with curved and fine jaws is mainly accomplished in the double-action forceps model for the separation and dissection procedures of tissues. The stainless steel material in the forceps facilitates the durability of the instrument. The handle, insulated shaft, and collar locking are primary components of the Maryland dissector forceps. It promotes safe bipolar electrocauterization procedures, better coagulation results, brilliant tactile characteristics, etc.

The total force applied and its direction are essential during surgical operations. This is because, while applying the traction forces by the laparoscopic forceps to the internal organ, there is a risk for organ damage. At the same time, the weak forces limit the efficiency of the working performances. Maryland forceps is commonly used forceps, where the tips are made of several shapes and different thickness of about 3 mm, 5mm, or 10 mm. These different thicknesses and tip shapes were capable of altering the applied forceps forces. The forceps guiding correct operation is performed on the tips of the common type of Maryland forceps model with the shaft

thickness of 5 mm. Thus, we can achieve the ability to measure the forces used in surgical instruments. The assistance of sensors with the forceps guiding the correct operation of Maryland forceps contributes to the convenient use of the forceps model. In this forceps model, the pressure applied in the three different axes (X, Y, and Z) of the shaft and the jaw are measured in real-time [67].

The proper learning of surgeons about the direction and the levels of forces promotes efficient surgeries. In addition to this, the Maryland grasper dissector with disposable trocar type has been developed by Hemmati et al. [68]. This limits the reusability of the instrument and limits the sterile level. This type of instrument is utilized for a total of 10 patients to assure the patients' safety.

Figure 2.5: Currently used Maryland forceps

(Source: https://www.teleflexsurgicalcatalog.com/pilling/product/728014-maryland-dissector-forceps-rotating-monopolar**)**

The various applications and functions of different laparoscopic instruments are listed in Table 2.3 below.

Table 2.3: Applications of different laparoscopic instrument

Author/Year	Instrument	Aim
Lee et al. [59]	Grasper	A laparoscopic grasping tool with force sensing capability
Hardon et al. [61]	Grasper	The multi-DOF (degree of freedom) cable-less grasper can be assembled and disassembled for cleaning and sterilization
Peter et al. [56]	Suction and Irrigation alone	A randomized trial based on the laparoscopy surgical characteristics
Sun et al. [57]	Combination of Suction and Irrigation	Randomized test trial on 130 adults.
Haraguchi et al [63]	Forceps	Kinematic analysis of forceps manipulator with 3 degree of freedom.

Kanno et al [64]	Forceps	The development of 4-DOF based forceps for reducing the interference with different surgeons.
Zhang et al. [65]	Forceps	Forceps manipulator with novel linkage bending mechanisms
Sushmita et al. [60]	Grasper	To analyze the force model for both single and double jaw grasper tips.
Sawada et al. [67]	Forceps	Developing the forceps grinding operation on the tip of the tool.
Kanat et al. [54]	Suction Irrigation	Providing an economical friendly instrument from the existing one.
Kawamura et al. [73]	Forceps	Developing the mechanical design of the forceps manipulator when suturing operation.
Frech et al. [10]	Suction Irrigation	Formulating a sponge-assisted suction type technique.
Barrie et al. [74]	Grasper	To analyze the tissue damage thresholds.

2.4 Surgical Instrument Failures and Safety Analysis

The instruments may fail due to the presence of a lot of external disturbances. Insulation failure is one of the most important disturbances which influence the entire surgical instrument. During electro surgery, certain complications are involved due to defects that occurred in the insulation coat of the instrument. Insulation testing prevents the contribution of such failures in several ways [69]. Espada et al. [70] experimentally identify the prevalence, location, and incidence of the attained insulation failures in robotic and laparoscopic instruments. In this, 78 robotic and 298 laparoscopic instruments are tested at Mayo Clinic in Arizona for detecting the failures. The insulation testing is performed after the completion of each use of the instruments. The maximum attainment of prevalence and incidence of the laparoscopic instrument is determined according to the voltage specifications. In addition to the insulation failure, the position tracking error and coupled motion errors of the end effector are also found in the laparoscopic surgical robots. Liang et al. [71] used a feed-forward neural network to detect the movement behaviors of an end effector and predict the errors of coupling in grippers. The coupling angle is assessed from the feed-forward neural network outputs, the driving motor current, and the wrist angular displacement.

The risk of unsafe activation of electrosurgical instruments during laparoscopy is reduced by the application of image processing algorithms. The instrument performance was tested on the simulated environment, and it was measured against the skilled laparoscopic surgeon's decisions. The positions of the instrument were determined by an image processing algorithm with high precision for determining whether it was safe or unsafe with the manual inspection decisions [72]. Kim et al. [75] determined the temperature profile and emissivity of the laparoscopic ultrasonic devices, such as passive and active jaws of the device. They are determined in the real-time

operation of laparoscopic instruments (cutting and coagulation time). The LapaRobot has been introduced as the trainee for laparoscopic operations. It enables the playback capability of recorded surgical procedures. The recorded procedures are played back as a repetition mode to minimize the errors of the operator. In this way, the performance of the trainee was automatically detected and gained high-resolution behaviors [76].

Different failures which affect the laparoscopic instrument and the control measures taken to limit such issues are given in Table 2.4.

Table 2.4: Failure recognition and control of laparoscopic devices.

Author\ Year	**Application area**	**Contribution**
Tixier et al. [69]	Laparoscopic and non-laparoscopic electrosurgery instruments.	Analysis of insulation failures
Liang et al. [71]	Laparoscopic surgical Robots	Eliminating the coupled motion of the instrument
Seehofer et al. [77]	Bipolar and Ultrasonic scissors	Evaluation of burst pressure and thermal evaluation
Van et al. [72]	Laparoscopic grasper device	Preventing unwanted and harmful situations.
Prince et al. [76]	Robot assistance laparoscopic surgery	To develop a robot for a trainer of laparoscopic surgery

Espada et al. [70]	Robotic and laparoscopic instruments	Identification of prevalence, location, and incidence of the attained insulation failures
Kim et al. [75]	Laparoscopic ultrasonic devices	Determination of temperature profile and emissivity

2.5 Ergonomics based design

The ergonomics-based design of the instrument motivates in several ways of surgeons. In several existing types of research, the handles are designed based on ergonomic nature. The symmetrical type new laparoscopic handle was designed for convenient use of both left and right hands by the surgeons. A pair of levers on the instrument enables both the motions of end effectors (open and close) employing the thumb and index finger. In addition to this, the design of a precision grip on the instrument permits the instrument to be held tightly and enables the required control in it. This newly designed ergonomic laparoscopic handle provides better performance than the concept of a ring handle, and it reveals less time consumption and complexity for completing the task [78].

In addition to this, the contribution of ergonomics is extended to the design of endoscopic dissector handlers. The handles were designed based on modifications in the contact area. In between the fingers and thumb, the contact area of the handles was increased and altered in the eye rings. These modified handle models promote better efficiencies than conventional products [79]. Tsai et al. [80] explored the safety and feasibility of performing laparo-endoscopic single-site surgery with conventional laparoscopic instruments based on geometric and ergonomic

principles. The author concluded that the conventional type laparoscopic instruments are effective in single-site surgery mainly due to their cost-effectiveness.

Another type of lightweight, handheld, ergonomic type mechatronic instrument was developed by Hassan Suhrahee et al. [81], which has three degrees of freedom roll-pitch-roll end-effector. The instrument is designed on certain global aspects such as dexterity, control, and ergonomics, which enhances the dexterity level of surgeons in the ergonomic interface. A new pistol grip type ergonomic laparoscopic has been developed to surpass the performances of the traditional pinch type grip handle. It quantifies the considerations of ergonomic design, and performance is analyzed based on progressive operations such as peg transfer, cutting, and suturing of both pinch type and pistol-type handle design [82]. A novel gripper-based laparoscopic handle was proposed by Gonzalez et al. [83] for enhancing the ergonomic behavior by considering the muscular activity of the surgeons. Such a proposed handle model offers suppressed muscular fatigue and minimizes the large amplitude movements.

2.6 Contribution of software in surgical instruments

In surgical instruments, the utilization of simulation is more convenient for determining their performance. The researches with simulation are very rare in the area of laparoscopy. For example, in one of the studies [84], two main factors are important in the catheter such as push force and sleeve length of the catheter. Through the ANSYS simulation, the catheter length is varied to certain limits. In addition to this, the kinematic deformation of the catheter surgical device has been analyzed with the help of ANSYS software to determine the displacement error. The simulation work also prepares to compensate for the predicted errors in the future for the clinical safety operation. Another simulation work was carried out by Friedrich et al. [85] with the help of a CAD 3D tool in which suction tips of various surgical instruments are analyzed and optimized

in terms of flow-dependent suction noises. The factors such as complication reduction, quality enhancement, enhancement in patient safety, elimination of organ damage, and performance enhancement in the surgical team are gained from the noise-optimized 3D CAD device. The contribution of simulation and design software in the different surgical instruments are tabulated in Table 2.5.

Table 2.5: Simulation Analysis in Surgical Instruments

Author/ Year	**Software type**	**Purpose**
Guo et al. [84]	ANSYS	Analysis of catheter bending Interventional surgery.
Wain et al. [86]	ANSYS-CFX	Blood flow analysis through coupled and sutured microvascular anastomoses
Friedrich et al. [85]	Computer-Aided Design (3D)	Modifications on suction tip Geometry
Wu et al. [87]	Computational Fluid Dynamics	To predict the pressure distributions through the diffused fins and impeller.
Park et al. [88]	ANSYS	Strain analysis of structural instruments
Centenero et al. [89]	The CAD (3D)	To forecast the post-operative results in orthognathic surgery.

2.7 Research gaps in the literature

Medical devices and procedures elucidate the problem confronted during surgeries and should be favorable to the patient and surgeon with respect to safety and time reduction. There is a wider scope and a good opportunity in the medical field due to the advancement in the health care systems, changing lifestyle patterns, and new technology inventions. Hence, instruments with multi-functional features are highly desirable and can be efficient in eliminating the problems faced in the latest surgical developments.

The contribution of laparoscopic instruments in minimally invasive surgery is reviewed in the preceding sections. Based on the analysis, it is found that simulation activities are rare in the laparoscopic instruments when compared to the other conventional instruments. The CAD model is rarely used and applied for medical instruments. The application of FEA analysis was limited in the laparoscopic instrumental applications. Many existing designs of handle forceps are available with ergonomic-based modifications and their failure analysis.

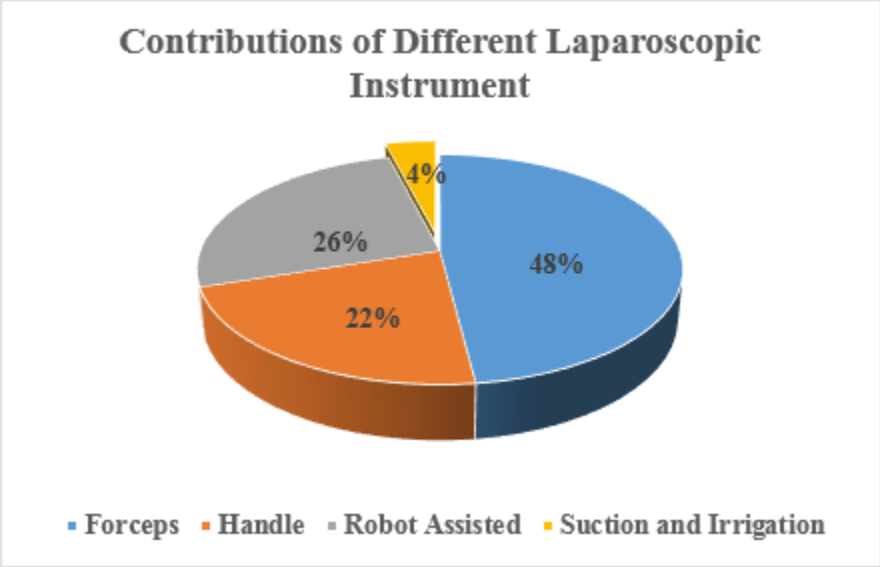

Figure 2.6: Contributions of laparoscopic devices

Figure 2.6 summarizes the different modular applications of laparoscopic instruments from the existing literature. The contributions are categorized in terms of four different devices; namely, the laparoscopic forceps model, handle design, suction and irrigation type, and the robot assistance model of the laparoscope. In which, the forceps are mostly used in several types of research. However, the laparoscopic suction and irrigation devices were limited in the existing reviewed researches. Thus, it will be seen that the research gap is attained in the suction and irrigation type of laparoscopic instrument when compared to the other available instruments.

The performances of laparoscopic instruments are analyzed based on the year-wise distribution in Figure 2.7. Here, three devices are considered for analyzing the performance such as Forceps design, suction, and irrigation device, between 2011 to 2020.

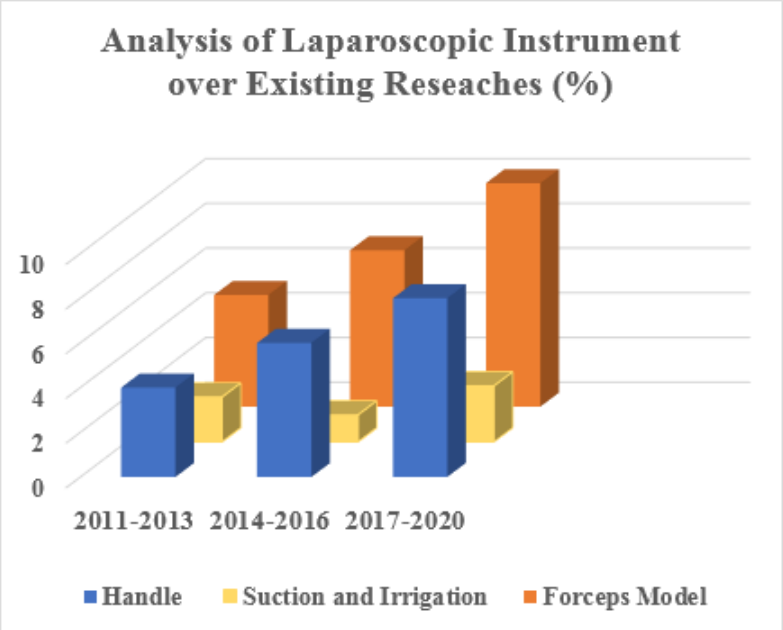

Figure 2.7: Year-wise Laparoscopic Instrument Analysis [84]-[89]

Among these three instruments, the performance of the forceps plays a supreme role in the present scenario. The work on handles is slightly lower when compared to that of forceps. Similar

to Figure 2.6, the utilization of the design modifications in the surgical applications is rare in suction and the irrigation type of device.

During the past decade, there has been a significant change in surgeries from open incision to single-incision surgeries. However, there is not much versatility in instruments. The incorporation of S-I devices with dissectors with the same mass flow rate can bring about the advancement in laparoscopic surgeries. S-I instrument is used in almost all surgeries like appendectomy, splenectomy, diagnostic laparoscopy, hysterectomy, and many more, which in combination with dissectors, can benefit the versatility of the instrument. With this improvement, there is a reduction in time due to the exchange of instruments resulting in a considerable reduction in time of operation theatre room and also patient safety for instrument mishandling due to continuous re-insertion.

Chapter -3

3 Design and Modeling of Laparoscopic Instrument

3.1 Introduction

During the 19th Century, people realized the hygiene benefits. Before and after surgery, doctors as well make sure to sterilize the equipment and wash their hands. Such a minor transformation brought about a drop in mortality rates. Different approaches were being made by the doctors to overcome the patient's death by a careful and persistent approach towards disinfection. This, together with the commencement of the Industrial Revolution, got to various essential standards in the surgical field. Standard devices in the surgeries were introduced, like scalpel and palpation tube. The surgeons brought about a change in this medical arena and were given the status of Gods.

Surgeons were able to cut open the 'patient's body and exchange or dissect unhealthy organs as per the requirement. The length of the incision made during this period was about 100mm to 150mm. But still, the patient was not satisfied as the operation time is more, the time of recovery is in years, and there is a chance of infection. The patient's life can be saved, but the quality of life was miserable due to post-operative pain and wound complications.

Later, at the end of the 19th Century, the field of minimally invasive surgery brought about a drastic change and eliminated laparotomy (open-cut surgeries) procedures. This surgery requires a laparoscope, a camera-enabled instrument to view the abdomen cavity by inflating CO_2 gas into it. The other instruments for dissection and grasping have to be introduced due to their smaller size of 10-15mm to insert and perform surgical operations. This gave a wide range of scope for the development of instruments used in minimally invasive procedures. The below section briefly

highlights the advancements made in laparoscopic surgeries and their instruments. However, an S-I instrument is taken for analysis, and suitable flow rates are mentioned with respect to five different pressure drops.

3.1.1 Forthcoming laparoscopic procedures

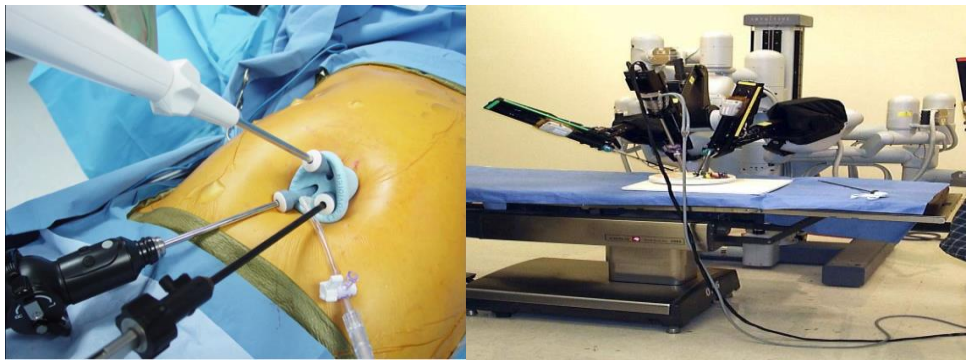

Figure 3.1 (a) & (b): Single Incision Laparoscopic Surgery

Due to the advancements made in Laparoscopic surgeries, there is a consistent requirement for instruments concerning ergonomics, versatile, lighter, reusable, and cheap. The future enhancement to laparoscopic surgeries can be Non-robotic hand-guided assistance surgery and Robotic laparoscopic surgery.

3.1.1.1 Non–robotic hand-guided assistance surgery

The non-robotic hand-guided assistance surgery can be categorized as laparoscopic single-incision surgery and single incision single port multi-instrument laparoscopy. They assist surgeons and their teams provided; the instruments must be multi-functional and versatile to save time and money. For such surgeries, surgeons suggested a necessity of instrument development and enhancement to the existing device and mechanisms.

3.1.1.2 Robotic laparoscopic surgery

This uses a Da Vinci Robotic-arm laparoscopic system, as shown in Figure 3.1. The machine here will perform surgery as per the instruction or signals given by the surgeon. In this, multiple incisions are made on the patient. So, the instrument should be robust, versatile, and easy to use.

3.2 Study area

Previously, the suction device and irrigation device were used as separate units. But, as technology advances, the S-I device became a single unit in almost all surgeries. The S-I device is typically made of either disposable or non-disposable. The non-disposable materials should be resistant to corrosive materials like alloys of stainless steel. During laparoscopic surgery, there is a consistent requirement for the S-I device either to suck the fluid from the abdomen or to irrigate the fluid to clear the vision for seeing on the monitor. It is basically due to Electro cauterization surgery that the blood oozes out from the abdomen and needs to clean with water through an irrigation device. As the fluid gets accumulated inside the abdomen, it gets sucked out by the Suction device. It is mandatory to view the organs on the monitor clearly to operate and complete the required surgery. Any unhealthy tissue, blood, or water obstructs the vision of a surgeon. This adds a considerable amount of time to the operation theatre room risking the patient's life. Thus, there is a requirement for an instrument that can suffice both cauterization and S-I device so that there can be considerable time reduction for both surgeon and patient. A multi-functional instrument is strongly recommended, which can facilitate a simultaneous operation without re-insertion of an instrument without a reduction in mass flow rate as per the surgeon's requirement. Thus, there is a broader scope in the development of surgical devices.

3.3 Maryland Forceps

This is commonly used to perform laparoscopic operations. Forceps are defined as hinged instruments that are used for grasping or holding objects. They are usually used by surgeons when the object in question is too small to be handheld or when other tasks need to be performed while holding a tissue. Maryland Forceps employ a scissor-like mechanism to open and close long, curved jaws with tapered tips, which are ideal for precise dissection [23].

3.3.1 Construction of Maryland forceps

Fan et al. [6] proposed laparoscopic forceps, which incorporate the features of grasping and dissection. The patented design provides spacing between jaws and uses a non-circular tube. With this feature, the forceps can move inside the abdominal cavity very conveniently in the available minimum space. Another design of laparoscopic forceps with a handle connected to the distal and proximal ends of the main body. A handle has a mechanism to operate the end effector, a pair of jaws connected to a tubular member.

During surgery, the blood and other fluids ooze out of the operated tissue, and an S-I device is used to clean and clear these fluids to have a clear vision of the area being operated on by the surgeon. For this, the laparoscopic forceps is removed from the trocar, and an S-I device is inserted into the abdomen through the same trocar. Saline water is irrigated through the S-I device to clean the tissue, and the same fluid is sucked out from the site of operation. This procedure is repeated as and when required. In order to have a clear view of internal organs, the abdomen of a patient is inflated by pumping an inert gas, like CO_2. During the S-I process, repeated insertion and removal of the S-I device causes CO_2 gas to escape leading to loss of abdomen pressure, which requires it to be inflated again to the required pressure. The re-insertion of the device consumes more time during the surgery leading to an increase in the overall surgery time.

In 2016, Andrew [28] suggested the 'Reusability' of laparoscopes and other instruments like trocars, ports, clip applicators, etc., to bring down the cost of surgery. While doing so, the reusability should not compromise the hygiene and other safety aspects of the instruments. In a study on 1803 laparoscopic cholecystectomy (LC) patients, the cost of a disposable instrument set per procedure was found to be 6.4 times the corresponding cost per procedure with a reusable instrument set. Further, disposing of wastage accounts for 20% of the hospitals' average budget on environmental services, and this can be reduced drastically by using reusable instruments.

3.4 Modified design of Laparoscopic forceps

As stated in the preceding sections, repeated insertion and removal of the S-I device poses safety issues, consumes the considerable time of surgery, and causes loss of CO_2 gas, which is required to keep the abdomen inflated. Hence, there is a necessity to modify the existing design to incorporate the S-I feature.

3.4.1 Desired Design Features

The proposed design modification uses the outer tube as a conduit for the passage of fluids, which is an S-I feature. When the suction-irrigation feature has to be used, the outer tube is slid forward, and when the jaws are in operation, it is retracted back. This will obviate the requirement for another incision in the patient's body for one more trocar. The following are different aspects considered in the modified design.

Functional:

- The modified design is aimed at multiple functions like the ability to grasp, pick, hold, manipulate, electro cauterize, seal, suck, and irrigate the fluid present inside the abdomen of the patient.

- When the sleeve moves towards the distal end, the jaws grasp and dissect the tissue. When the sleeve rests near the proximal end, it acts as a suction-irrigation device by enclosing the jaws inside it.
- Assembling and disassembling all the parts has to be easier in the modified design. This will enable the replacement of individual parts and facilitate ease of sterilization and reusability of the instrument.

Geometry:

- The outer diameter of the main body has to be between 10-13 mm, as this is the maximum diameter that a trocar can generally accommodate.
- The length of the instrument has to be around 300-350 mm from its tip to the handle end, as shown in Figure 3.3 (Also, all figures with dimensions are enclosed in the appendix).

Mechanisms:

- The jaws, which manipulate the tissue, are actuated by a mechanism similar to the Lazyman mechanism. The jaws are opened and closed by movement of the inner rod forward and backward.
- The modified design has an outer tube or sleeve which can slide inwards and outwards. When the jaws are in use, the outer sleeve has to remain in a locked position.

Fluid Mechanics:

- The suction-irrigation feature allows the instrument to suck out the fluids from the abdomen of a patient body and clean the blood oozing out by irrigating the tissue

area with saline water for clear vision. This is achieved by pumping pressurized fluid using a suction and irrigation pump.

- The forceps should have a passage that acts as a two-way valve. During irrigation, the pressurized saline water is pumped at a regulated pressure from the distal end into the patient body to clean, thereby having a clear vision of the internal organs. Whereas from the same passage, the fluids from the abdomen are sucked out from the proximal end. Thus, the passage is the same for both operations.
- The cleaning fluids must be discharged from the instrument at an appropriate velocity while accurately targeting the affected tissue without interfering with the other parts.
- A steady flow of saline water has to be ensured during irrigation.

Material:

The material selected for the proposed design should be suitable for repeated use, non-disposable type, and must resist physical and chemical effects due to body fluids, secretions, and sterilization. The material chosen for all the components of the forceps, except the handle, is stainless steel of the Austenitic 300 series or Martensitic 400 series. Aluminum is not preferred due to its thermal properties, reactivity to body fluids, and poor ductile properties. In general, the 420 series stainless steel is used for surgical cutting tools. Hence, 400 series stainless steel is preferred in surgical equipment due to the addition of Molybdenum, which gives anti-corrosion properties. For the inner tube, Austenitic 316 series steel can be used as it also has 2-3% Molybdenum content, which provides better conductivity. The material used for the handle head and handle link is Polyether ether ketone (PEEK), as it has better chemical and abrasive resistance. Listed in Table 3.1 are different parts of the forceps with their material and quantity.

Table 3.1: Material for different components of the modified laparoscopic forceps

ITEM NO.	PART NAME	MATERIAL	QTY.
1	Inner Rod	Stainless steel	1
2	Pin	Stainless steel	5
3	Clawbar	Stainless steel	2
4	Actuating Connector	Stainless steel	1
5	Head	Stainless steel	1
6	Outer Tube	Stainless steel	1
7	Knob	Stainless steel	1
8	Connector	Stainless steel	1
9	Outer Sleeve	Stainless steel	1
10	Fixed Handle	Stainless steel	1
11	Movable Handle	Stainless steel	1
12	Link	Stainless steel	1
13	Outer Cap	Stainless steel	1
14	Locking Pin	Stainless steel	1
15	Top Claw with Bar	Stainless steel	1
16	Bottom Claw with Bar	Stainless steel	1

3.4.2 The Proposed Design

The initial proposed design, as seen in Figure 3.2, is similar to the Maryland Forceps with modifications to incorporate the S-I feature. This is accomplished by introducing an additional hollow pipe (sleeve) over the existing Maryland forceps. A gap between the outer pipe of the existing forceps and the sleeve serves as an annular region through which the S-I fluids flow. The S-I fluid can be fed to or removed from the device through a small pipe protruding from the outer

tube at the distal end, as shown in Figure 3.2**.** In addition, the design facilitates the outer sleeve to slide along the axis of the pipe so that when surgery has to be performed, the sleeve is pulled backward, that is, towards the distal end, such that the jaws are allowed to move and perform the actions like holding & cauterizing during surgery. Whereas, when the irrigating fluid has to be pumped into the abdomen, the sleeve is pushed forward, that is, towards the proximal end of the instrument, and the jaws are enclosed within the sleeve. This enables suction or irrigation to be carried out without the jaws interfering with the process. The sleeve is held locked at the extreme ends of its motion. A complete description of the components of the proposed design, along with their functionality, is detailed in the patent [99].

The diameter of the second tube in the proposed initial design shown in Figure 3.2 is too small for proper fluid flow through the conduit. To accommodate the end effector and its actuating mechanism, an enlarged part, called the mouth of the tube, has to be provided at the distal end of the outer tube. This requires a cap-like arrangement on the frontal (distal) end of the outer tube. This requires additional space to accommodate the end effector and its mechanism, which may further constrict the space available between the inner and outer tubes. This resulted in a reduced mass flow rate, and hence the initial design was rejected.

An additional tube is required over the outer tube to act as a conduit for the fluid flow. This new tube will be outside the jaws, and the grasping mechanism, and the suction and irrigation are done through the outermost tube. The size of the trocar increases slightly due to this additional tube. In order to overcome this problem, an alternate design with an extendable stick arrangement used in an umbrella is proposed. This umbrella stick mechanism is built using a third outermost concentric tube, which tapers towards the distal end.

Different trocar sizes commercially available are 2mm, 3mm, 5mm, 10mm, 11mm, and 12 mm. However, surgeons in general use two 5mm trocars and one 10mm trocar, the choice of which may depend on several factors [96]. In the present design, the outside diameter of the instrument is 8mm or 10mm, and this requires the usage of 10mm or 12 mm trocar sizes. The present design is multi-functional and is more useful in surgeries where excessive bleeding or ejection of body fluids is expected.

The proposed design incorporates the S-I functionality into the conventional Maryland Forceps. This task is challenging as the final design must possess the same functionalities of an already existing Maryland Forceps with an S-I tube incorporated for simultaneous suction and irrigation as per the demand of the surgeon. On the other hand, this feature also addresses the limitations of the conventional Maryland Forceps described in section 2.3.4.

Repeated insertion and removal of multiple instruments results in prolonged duration of laparoscopic surgeries, and surgeons are very likely to feel fatigued [94]. There is invariably a requirement for a suction irrigator and dissector in most of the laparoscopic surgeries [90]. About 13% to 30% of the operative time is wasted in instrument exchange between the S-I device and the dissector forceps [26],[27]. Besides, exchanging instruments during surgery compromises the safety of the patient and disrupts the sequence of operation. Therefore, the proposed design of forceps would improve surgical performance by functioning as a dissector, grasper, or suction-irrigator during the surgery.

3.5 Modeling of the modified laparoscopic device

Several useful features for the proposed design of forceps have been discussed in the previous sections. Based on these requirements, a modified design was conceived and modeled using SolidWorks Software. Overall, 16 components are designed, namely, head, claw bar & claw,

pins, claw bar to claw connector, Inner tube, Outer tube, Capslock, Claws (top and bottom), Handle Head, Handle Mover, outer cap, rod connecting capslock to Handle Mover, two tapered, concentric flow tubes to enable suction & irrigation. The fluid flow domain of the assembly of these components is shown in Figure 3.2 and Figure 3.3. The angle of inclination of the protrusion with the axis of main flow tubes is denoted by ϕ. The diameter of the sleeve at the proximal end is denoted by D. The total length of the assembly is 330mm, and the diameter of the instrument varies along its length between 8-10mm at the distal end and 13mm at the proximal end.

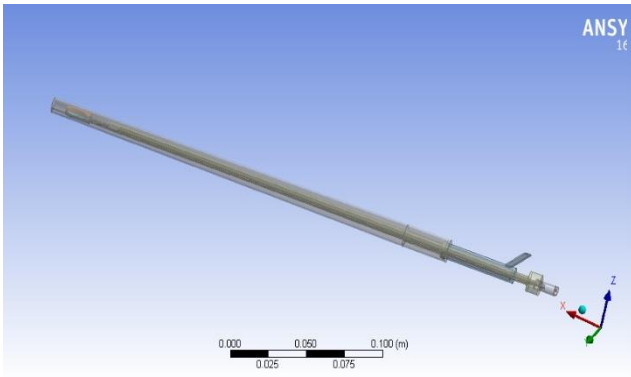

Figure 3.2: Initial design of the laparoscopic instrument

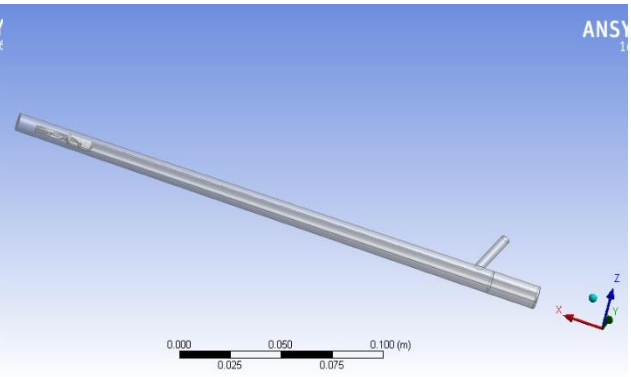

Figure 3.3: Modified design of the laparoscopic instrument

Figure 3.2 shows the initial design of the laparoscopic instrument, which is analyzed using ANSYS Fluent software. The design is such that the jaws are exposed by sliding the outer tube backward. In this mode, it is similar to Maryland forceps and can be used to perform related operations. After completion of the surgery, the tube can be moved towards the distal end. In this position, the outer tube acts like an S-I device. The left extreme end and the right end with protrusion shown in Figure 3.3 are the inlet and outlet for the fluid in suction mode. The outer tube can be slid toward the distal end for performing the S-I operation. The tube at the distal end is tapered so that the incision made in the patient's body could be minimal.

Figure 3.3 shows a modified version of the design shown in Figure 3.2, where the protrusion is moved away from the proximal end. In addition, only one of the four possible designs from different combinations of D and ϕ is shown here. The modified instrument is analyzed for two different values of D, 8mm and 10mm, each for $\phi = 45^{\circ}$ and 60°. The optimal design among these four designs is decided based on the fluid flow analysis of the cleaning fluid, as illustrated in the following sections.

3.6 Essential components and manufacturing details of the proposed instrument

Our proposed instrument combines the functionality of the forceps, the S-I device, and the CO_2 insufflator into a single instrument, which can be sterilized and re-used with ease. This instrument does not require multiple re-insertions, leading to a stable CO_2 pressure in the abdomen. Each component has its specific purpose and contributes to the overall functionality of the instrument. The characteristics, features, functions, and materials of every component are explained briefly in this section. The details of this instrument are described in the patents [6,7]. The fits and tolerances of each of the components described below should ensure that the entire mechanism operates smoothly without play.

3.6.1 Jaws

Jaws are one of the essential components of the instrument as they directly operate on the tissue. As shown in Figure 3.4, the jaws are used to grasp, manipulate, cauterize, and seal the tissue. They are replaceable with other suitable forceps heads for other laparoscopic procedures. Stainless steel of the martensitic 420 series is a preferred material for the jaws. The jaw's outer edges and corners are manufactured initially in a CNC machine, then tooths are programmed and made in the wire-cut machine. The required features of the jaws are:

- outer edges and corners of the jaws have to be smooth and rounded to avoid injury to tissues.
- withstand sterilization and surgical procedures, as they are subjected to thermal, chemical, and mechanical stresses.
- a high surface finish, strength, and toughness.

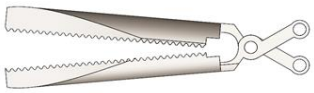

Figure 3.4: Pair of jaws

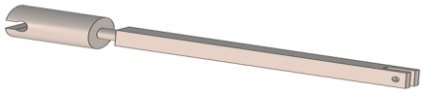

Figure 3.5: Actuating connector

3.6.2 End Effector Assembly

The end effector comprises the jaws that facilitate the four-bar mechanism, as seen in Figure 3.4. The head encases the four-bar linkage and is used to open and close the jaws. Two of the four bars are connected to the jaws, while the other two bars are hinged to the head. The end effector continuously comes in contact with different fluids; hence it is made of 304 series stainless steel. This complete assembly is step by step made into proportionate size in CNC machine, then finally programmed and given in wire-cut machine, as the dimensions are of the order of 1mm. The required features of this end effector assembly are:

- should be sleek and strong enough to bear the stresses exerted during the operation.
- links should be compact to fit inside the head and should have better machinability.
- head, jaws, and four-bar linkage are subjected to a high-frequency current supply and are constantly in touch with body fluids. So, the material should be non-corrosive and be able to withstand damage over multiple sterilization cycles.

3.6.3 Inner Rod and Outer Tube

The inner rod and the outer tube are significant components of laparoscopic forceps. The inner rod is 2.5 mm in diameter and transmits the motion of the handle to the four-bar mechanism near the jaws. A metallic outer tube of 3.5 mm outer diameter encloses the inner rod, as shown in Figure 3.6. The inner rod and outer tube are made of austenitic stainless steel of 316 series due to material requirements like corrosion resistance, toughness, rigidity, hardness, and mechanical strength. The inner rod and outer tube are procured as per their dimensions of diameters. Then inner rod's ball end is rounded off in a CNC machine. The threading operation is performed on a lathe machine. The required features of the inner rod and outer tube are:

- should incorporate threading and small drill holes for dimensional accuracy.
- the inner rod should be able to transmit the motion of the handle to the jaws.
- the outer tube should be biocompatible to prevent inflammation or allergic reactions as it comes in contact with the tissue.
- both of them should be easily sterilizable.

3.6.4 Outer Sleeve

The outer sleeve is important because it acts as a suction-irrigation channel to either irrigate disinfecting saline or suck the body fluids from the patient's abdominal cavity, as shown in Figure 3.6. It is restricted in two extreme positions over the connector to serve multiple purposes. At the extreme left end position of the sleeve, the suction or irrigation process is carried out. While, at the extreme right end of the sleeve, the jaws are exposed, and grasping, dissection or cauterization is performed. The recommended material is 304 series stainless steel. The outer sleeve available in the market is 8mm inner diameter (ID) and 12mm outer diameter (OD). However, our designed outer sleeve has 13mm OD. Since the instrument is mainly preferred for lesser OD as the rupture

in the abdomen can still be reduced. So, 12mm OD is selected. However, the inner diameters (ID) are not changed. The ID at the left end is 6.5mm and at the right end is 11mm. Only the difference in the design and fabrication is the thickness is reduced to 1mm. The IDs are made in a wire-cut machine as a tapered hole from 11mm at the right end to 6.5mm to the left end. A wire-cut machine is used to achieve smoothness and accuracy. The OD's are tapered on a lathe machine with 12mm at the right end and 8mm at the left end. The required features of the outer sleeve are:

- must ensure the fluid is sucked or irrigated within the channel only, and leakage should be avoided.
- ease of assembling, disassembling, and effective sterilization.
- the distal end near the jaws should be rounded without sharp edges to avoid injury while inserting it inside the abdominal cavity.

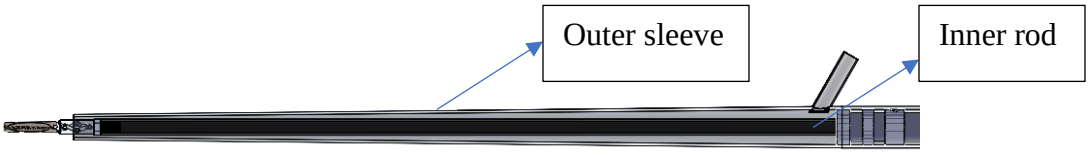

Figure 3.6: Outer sleeve enclosing the inner rod

3.6.5 Actuating Connector

The actuating connector is a link that connects the inner rod and the handle, as shown in Figure 3.5. A small ball and socket joint are used to connect the inner rod to the actuating connector. Stainless steel of 304 series is a recommended material. The actuating connector is fabricated in a tool and cutter machine to make a combination of rectangular and circular profiles. The required features of the actuating connector are:

- should be rigid, tough, and strong enough to bear the loads.
- it should impart rotary motion of the knob to the jaws using a ball and socket joint.

3.6.6 Handle

Figure 3.7: Design of handle.

Figure 3.8: Knob

The handle, as shown in Figure 3.7, is a primary component that is held by the surgeon and provides access to the instrument functions. The end at which the handle is located is known as the 'proximal end.' It comprises the fixed handle and movable handle. The fixed handle is used to rest the surgeon's fingers, while the movable handle is used to transmit the motion to a four-bar mechanism near the jaws. The conventional instrument handle uses different grades of stainless steel and Poly ether ether ketone (PEEK) material. Here, the handle is machined in combination of manual and CNC lathe machines, then the die is made and moulded with rubber material. The desirable material properties of a handle are chemical resistance, toughness, rigidity, hardness, and mechanical strength. The required features of the handle are:

- Provision to accommodate the high-frequency electrical power cable for electro-cauterization operation.
- Ergonomically designed to enable surgeons to hold it longer durations without causing strain or injury.
- It should be properly insulated against electrical shock to both surgeon and patient during electro-cauterization.

3.6.7 Knob

As shown in Figure 3.7, its purpose is to facilitate the surgeon to orient the jaws in the desired direction. It is connected over the outer tube and imparts 360^{o} rotation to the jaws. Stainless steel material is also used for the knob. The knob has a beautiful aesthetic look of gear profile and so is machined in a CNC machine, whose required features are:

- should have a firm grip over the outer tube such that the rotation of the knob rotates the outer tube and, eventually, the jaws.
- the spacing between the protrusions should be ergonomically suitable for the surgeon to operate using fingers.

3.6.8 Connector

Its function is to restrict fluid flow in one direction and to hold the outer sleeve in two extreme positions. The outer sleeve slides over the rubber washers, which prevents the leakage of fluids. The connector is provided with a groove on the collars for the locking pin to slide into, which restricts the axial motion of the outer sleeve, as shown in Figure 3.9. The recommended material for the connector and collars is 304 series stainless steel, which has good corrosion resistance. Biocompatible rubber is recommended for the two washers close to the left end. The connector is step turned and drilled a hole in a lathe machine, and locking pinholes are made in a wire-cut machine. The required features of the connector are:

- must prevent fluid from oozing out of the device during surgery.
- rubber washers must facilitate the easy movement of the outer sleeve.

3.6.9 Link

The purpose of the link, as shown in Figure 3.10, is to convert the angular motion of the handle to the translatory motion of the actuating connector such that it imparts movement to the end effector assembly. The link is machined in a CNC machine, as the size is too small to be held, and holes are drilled carefully on a drilling machine. The preferred material is 304 series stainless steel.

Figure 3.9: Connector

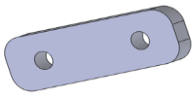

Figure 3.10: Link

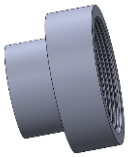

Figure 3.11: Outer cap

3.6.10 Outer Cap

The outer cap, as shown in Figure 3.11, is threaded to hold the inner rod and the handle assembly together. The preferred material is 304 series stainless steel. The complete operations of the outer cap are manufactured in a lathe machine.

3.6.11 Locking Pin & Pins

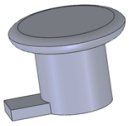

Figure 3.12: Locking pin

Figure 3.13: Pins

The locking pin, as shown in Figure 3.12, is used to fix the outer sleeve at two extreme positions by sliding into the grooves on the collars of the connector. The locking pin is fabricated in a CNC machine due to the complexity of handling the small piece. Pins, like those in Figure 3.13, are used to join the four bars of the end effector assembly at the two ends of the link and the pivot of the handle. The preferred material for locking pins and pins is 304 series stainless steel.

The pins should withstand forces experienced during the actuation of the handle and the jaws. The pins are taken directly from the market of 1mm diameter, and length is proportionately cut to fix in an assembly.

3.7 Construction of the modified laparoscopic device

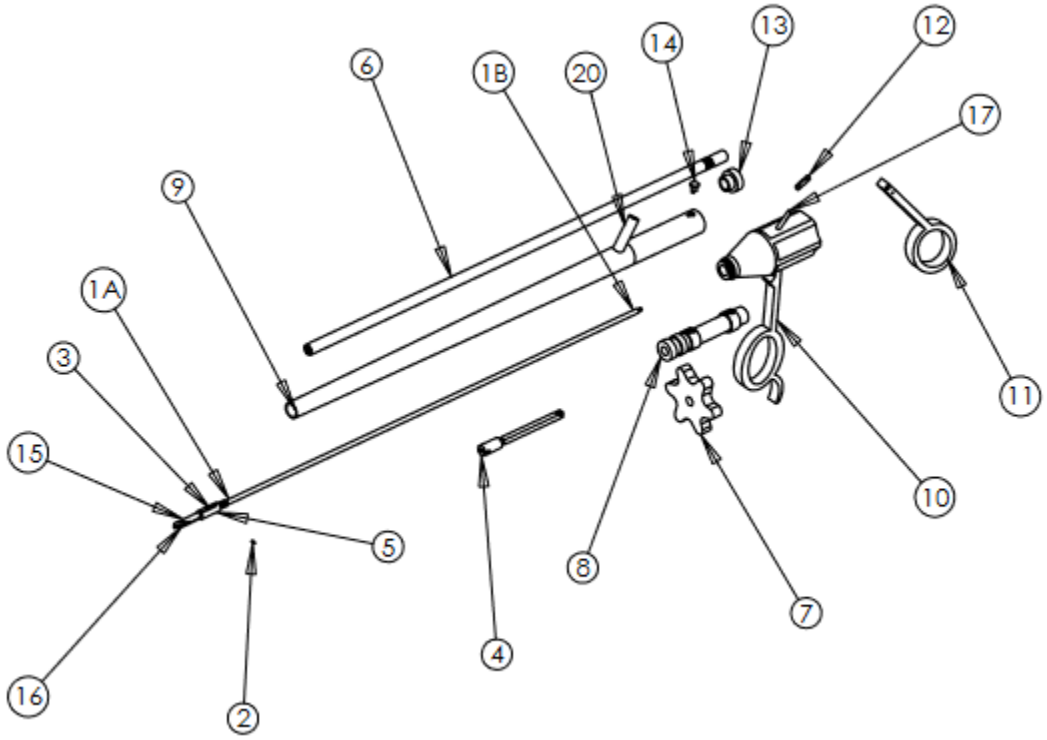

Figure 3.14: Exploded view of component parts of the device assembly

Referring to Figure 3.14, the laparoscopy device of the present invention comprises of an inner rod (1), a pin (2), a claw bar (3), an actuating connector (4), a head (5), an outer tube (6), a knob (7), a connector (8), an outer sleeve (9), a fixed handle (10), a movable handle (11), a link (12), an outer cap (13), a locking pin (14), a top claw with bar (15), a bottom claw with bar (16) and a terminal (17).

- The top claw with bar (15) and the bottom claw with bar (16) forms a jaw assembly. The fixed handle (10) and a movable handle (11) form a handle assembly.
- The inner rod (1) transmits the motion of the fixed handle (10) and movable handle (11) to the top claw with bar (15) and bottom claw with bar (16). The claw bar (3) is used to activate the motion of the top claw with bar (15) and the bottom claw with bar (16) by connecting with the inner rod (1). The actuating connector (4) connects the fixed handle (10) and movable handle (11) with the inner rod (1) through a ball and socket joint. The head (5) encases a jaw assembly comprising of a top claw with bar (15) and a bottom claw with bar (16). The outer tube (6) encloses the inner rod (1) and contains threading for attaching the connector (8).
- The knob (7) is connected to the outer tube (2) to change the orientation of the jaw assembly. The knob (7) comprises a plurality of symmetric grooves, which can be rotated either clockwise or anticlockwise. The grooves also ensure that they can be operated using only one finger, usually the index finger of the same hand which holds the instrument.
- The connector (8) is fitted with rubber washers to restrict flow in one direction. The connector (8) acts as the extreme position for the outer sleeve (9) and has a groove for the locking pin (14) to slide into, fixing the outer sleeve (9) in place.
- The outer sleeve (9) acts as a suction-irrigation conduit. The motion of the outer sleeve (9) is restricted to two extreme positions using grooved metallic collars to house a locking pin (14). The locking pin (14) affixes the outer sleeve (9) in the two extreme positions by attaching it to the connector (8) and locking it in place.
- The laparoscopic device of the invention operates in two modes, depending on the position of the outer sleeve (9), namely suction-irrigation (S-I) mode and forceps mode. In suction

irrigation mode, the outer sleeve (9) can be locked into the grooves on the connector (8) through a locking pin (14). When the locking pin (14) is rotated, the outer sleeve (9) is fixed in a position, allowing the surgeon to handle the device without dislodging the outer sleeve (9). When the outer sleeve (9) is pulled back, the jaw assembly is uncovered, and the forceps mode of the laparoscopic device is activated.

- The fixed handle (10) connects the jaw assembly with the actuating connector (4) near the handle, whereas the movable handle (11) transmits the motion of the surgeon. The link (12) is used for converting the angular motion of the movable handle (11) to the translatory motion of the actuating connector (4). The outer cap (13) joints the inner rod (1) and jaw assembly, and the handle assembly via threading. The jaw assembly is used primarily for grasping the tissue or an organ and cauterizing. Pins (2) are used for affixing various components of the laparoscopic device.
- The handle assembly has been ergonomically designed to be comfortably held and operated with a single hand. The movable handle (11) is operated using the thumb, while the index finger rests on a groove near the hub of the fixed handle (10).
- The device of the present invention has an outer sleeve (9) over the laparoscopic forceps known in the art. A gap between the outer tube (6) of the forceps and the outer sleeve (9) serves as an annular region through which the suction irrigation fluids flow. The suction irrigation fluid can be fed to or removed from the device through a small pipe protruding from the outer tube at the distal end, as shown in Figure 3.14.
- In addition, the design of the laparoscopic device of the present invention facilitates the outer sleeve (9) to slide along the axis of the outer tube (6) so that when surgery has to be performed, the outer sleeve (9) is pulled backward, i.e., towards the distal end. The jaw

assembly is then actuated using the handle assembly to move and perform various surgical operations.

- Whereas, when the irrigating fluid has to be pumped into the abdomen, the jaw assembly is first brought to a closed position using the handle assembly. Then the outer sleeve (9) is pushed forward, that is, towards the proximal end of the instrument, enclosing the jaws within the sleeve. This enables suction or irrigation to be carried out without the jaws interfering with the process. The outer sleeve (9) is held locked at the extreme ends of its motion, as shown in Figure 3.19.
- The jaws can also be rotated by rotating the knob (7) located near the handle for adjusting the orientation of the jaws. In addition, electro-cauterization can be carried out by electrically activating a terminal (17) located on the handle and passing an electric current through it.
- In an embodiment, the inner rod (1), the outer tube (6), and the outer sleeve (9) can all be made flexible to increase the flexibility of the laparoscopic device so that the device itself can be bendable during the operation. In another embodiment, the locking pin (14) mechanism of the device is automated for locking the outer sleeve (9). In another embodiment, carbon dioxide (CO_2) gas can be passed through the annulus in the outer sleeve (9) itself by duly modifying the valve, which controls suction or irrigation inlets from the pump.
- During surgical operations, a surgeon can push the outer sleeve (9) forward, covering the jaw assembly to activate the S-I mode. The device can be used to disinfect the operated region, reducing the chances of infection or inflammation after the surgery, in addition to obtaining a clear view. The supplied fluid includes saline water or any other disinfecting

fluid as required by the surgeon. The outer sleeve (9) is a homogenous tapered tube with different diameters at the proximal and distal ends. It has a protrusion that acts as the outlet during the suction operation and an inlet during the irrigation operation.

- In the conventional procedure, after the dissection operation, the forceps are removed from the trocar, the suction irrigation tube is introduced, and the suction irrigation process is carried out. This exchange of forceps and the suction irrigation tube has to be done multiple times, as and when required.
- The laparoscopy device of the invention eliminates the need for multiple insertions and can potentially minimize the cost of surgery to suit medical needs, particularly of the rural population, and can improve the ease of usage to carry out surgery smoothly and effectively.

3.8 Mechanisms

The previous section describes the various components and their working. In this section, the different mechanisms connecting the components are described. The basic mechanisms in our current design of forceps include a four-bar mechanism, a sliding mechanism for an outer sleeve, the outer sleeve locking mechanism, a knob to change the orientation of the jaws, and the handle mechanism with suitable linkages.

3.8.1 Handle Mechanism

It comprises three distinct parts, namely the fixed hub, the movable handle, and the link. The movable handle is pivoted to the fixed hub so that it can rotate around that point within the constraints of the geometry of the hub when moved by the surgeon. The link joins the movable handle to the connector, transforming the angular motion of the movable handle into the translatory motion of the connector. The default position of the handle is shown in Figure 3.15. Therefore,

when the handle is moved towards the fixed handle, the link transmits the motion to the connector, which is affixed to the inner rod, making it move towards the jaws. This movement activates the four-bar mechanism encased in the head, which is explained below.

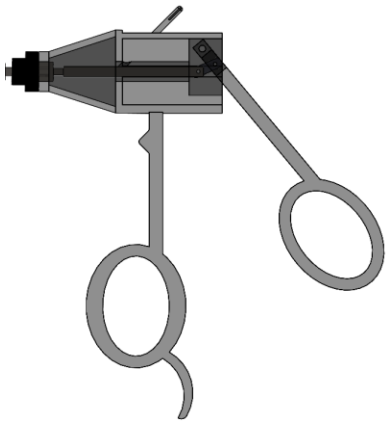

Figure 3.15: Handle in default position

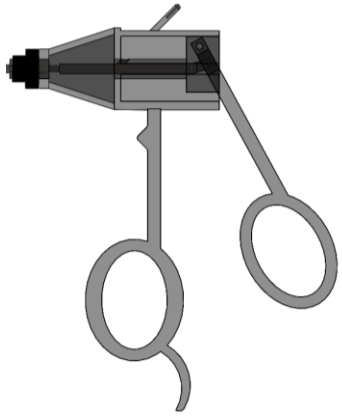

Figure 3.16: Handle position when actuated

3.8.2 Four-bar Mechanism

The head encloses a four-bar mechanism that connects the two jaws to the end of the inner rod. The main function of this mechanism is to open and close the jaws. The bars extending from the two jaws are held together at their center using a pin, which is one end of the four-bar mechanism. The other end of this mechanism is attached to the inner rod, as shown in Figure 3.17. When the surgeon actuates the handle, the inner rod moves to the left, resulting in the jaws being opened, as shown in Figure 3.18.

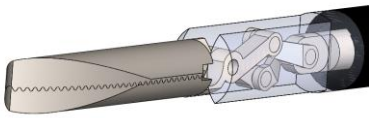

Figure 3.17: Closed configuration of jaws

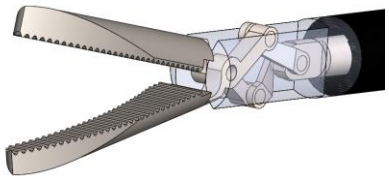

Figure 3.18: Open configuration of jaws

3.8.3 Outer Sleeve and Locking Pin Mechanism

The outer sleeve is capable of sliding over the outer tube of the forceps. It has two extreme positions, which are defined by the grooves in the connector, as shown in Figure 3.19. The locking pin fixes the outer sleeve into either of these grooves, ensuring that the outer sleeve cannot move during operation. When the outer sleeve completely covers the jaws, it is in the S-I mode, as shown in Figure 3.19. When the sleeve is retracted to the other extreme position, and the jaws are uncovered, the device is in the Forceps mode, as shown in Figure 3.20.

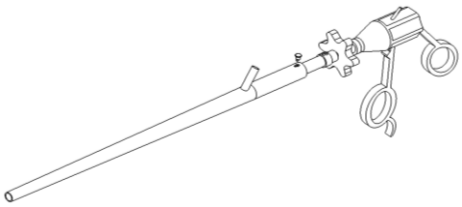

Figure 3.19: Device in S-I mode

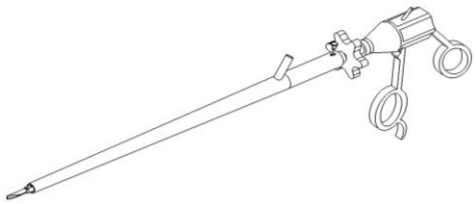

Figure 3.20: Device in Forceps mode

The locking pin depicted in Figure 3.19 is inserted within the groove in the outer sleeve and the connector. Then the pin is rotated to lock the outer sleeve in either of the positions described above. This arrangement ensures that the outer sleeve does not move and disrupt the surgery.

3.8.4 Knob

The surgeon can change the orientation of the jaws as and when required by rotating the knob clockwise or anticlockwise, as shown in Figure 3.7.

Thus, all the above components constitute an assembly of the modeled laparoscopic forceps and are fabricated accordingly as per the dimensions. These are manufactured using different machines such as three-axis CNC lathe machines, three-axis CNC milling machines, surface grinding machines, drilling machines, and CNC wire-cut machines.

Chapter- 4

4 CFD Analysis of the Newtonian Fluid Flow in the Proposed Forceps

4.1 Methodology

4.1.1 Existing device: Suction-irrigation (S-I) instruments

Abraham Frech et al. [10] designed a suction instrument that overcomes the problem of occlusion by introducing a sponge near the instrument tip. However, if sponges are misplaced or kept in the abdomen may result in a severe challenge to the patient after post-operative pain. In some cases of appendectomy surgery, an irrigation instrument is compared and examined with a suction instrument [10],[90], while others have concentrated on the SI instrument for pressure recommendation [55]. Studies have also been conducted on wound complications during negative suction pressure [91],[92].

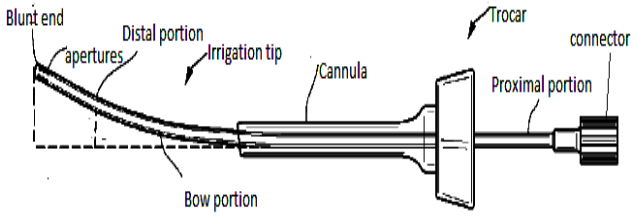

Figure 4.1: Bowed tip inserted into trocar during suction in Laparoscopic surgery

The success of laparoscopic procedures is subject to the surgeon interacting in 2D vision with the tissues using surgical tools rather than open-cut 3D vision. During surgeries, a standard S-I instrument most commonly used is either a 5mm or 10mm diameter extending up to a length of 330mm [93]. This S-I instrument has a problem with repeated insertion during the surgery whenever there is an obstruction in the field of view from the monitor [94]. The blockage can be basically due to blood clots or any charred particles during cutting, dissection, and fulgurating the

tissue. It so happens that the abdomen is filled with CO_2 gas, and there is a chance of escape of gas when multiple instruments are re-inserted. It can be avoided by introducing a new instrument that can dissect, grasp, suck or irrigate with the same instrument. Before doing this, the preliminary results of the S-I device will facilitate the modified instrument to incorporate S-I device results and compare them effectively.

4.1.2 Existing device: Preliminary Results and discussion

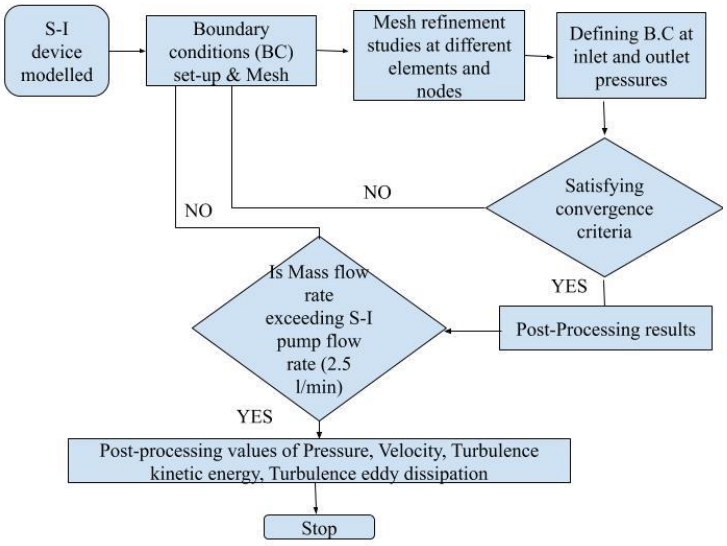

Figure 4.2: Flow steps in the numerical analysis of the S-I device

Based on the design given in the Aesculap manual [95][96] and other German manuals, the S-I conduit shown in Figure 4.3 with a 5 mm inner diameter and 330 mm length is modeled in SolidWorks. This S-I conduit is analyzed in ANSYS Fluent to compare the flow features with that of the modified forceps.

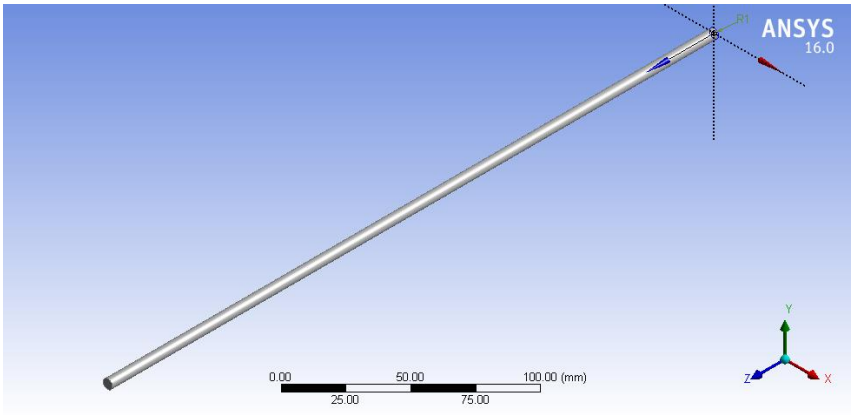

Figure 4.3: Model of S-I conduit having 5 mm inner diameter and 330 mm long

Table 4.1: Properties of the fluid used

	Properties of the fluid used (water)	
	Units	Values
Density	kg/m^3	998.2
Viscosity	kg/m-s	0.001003

Figure 4.3 shows the modeled S-I conduit, which is used to clean the site of surgery by pumping fluids. As shown in Figure 4.4 and Figure 4.5, for irrigation, the inlet is on the right side, i.e., the proximal end and the outlet is on the left side of the instrument, i.e., the distal end. In the case of irrigation, the pressure difference between the right (pump) and left (abdomen) ends of the device is ΔP. Inlet-outlet pressure difference, ΔP, is defined such that it is always positive. In our analysis, ΔP is taken as 5mm, 10mm, 15mm, 20mm, and 25 mm Hg. In case of suction, fluid from the abdomen (left) end enters into the device and leaves from the right (pump) end. Therefore, ΔP is defined here as the pressure difference between the right and left ends of the device. As mentioned before, the abdomen is inflated to 10mm Hg gauge pressure with CO_2, which is imposed

as a boundary condition at the distal end. The pressure boundary condition at the proximal end of the device can be computed from this abdominal pressure and the imposed ΔP.

ANSYS Fluent is used to carry out CFD simulations for flow analysis in both the S-I conduit and the proposed laparoscopic instrument. The model is analyzed using a steady-state pressure-based Navier-Stokes solver with the SIMPLE algorithm. Standard k – ε turbulence model with enhanced wall treatment is used to simulate the flow of water at standard temperature and pressure conditions. Given in Table 4.1 are the properties of the fluid (water) used. The right side, left side, and the outer surfaces of the S-I conduit are given inlet, outlet, and wall boundary conditions, respectively, in irrigation mode. In both suction and irrigation modes, and for all five sets of pressure variations, mass fluxes are computed and compared in this analysis.

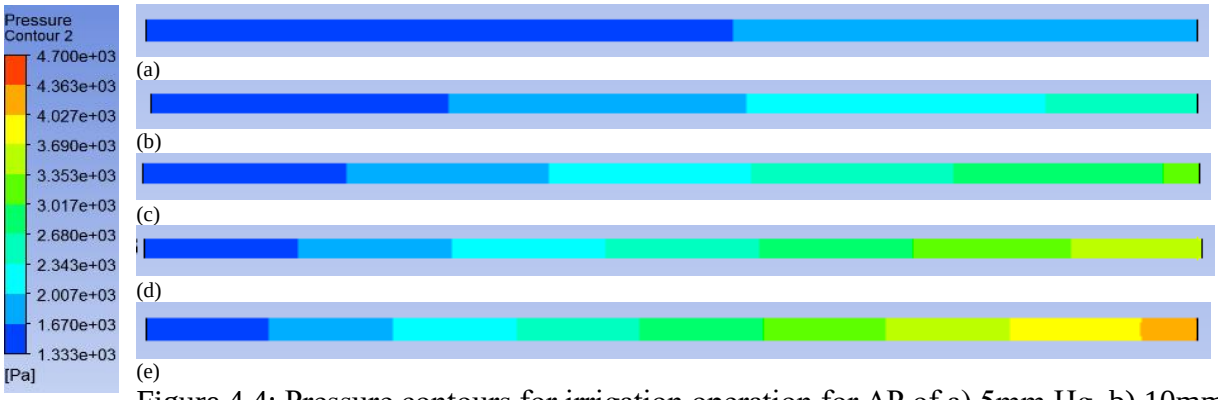

Figure 4.4: Pressure contours for irrigation operation for ΔP of a) 5mm Hg, b) 10mm Hg, c) 15mm Hg, d) 20mm Hg, and e) 25 mm

The pressure and velocity contours in the S-I conduit are shown in Figure 4.4 and Figure 4.5 for the above-mentioned ΔP. From Figure 4.4 we see that the pressure decreases uniformly over the length of the tube as expected. The velocity contours in Figure 4.5 show that the flow is developing at the inlet for a short distance, after which it assumes a fully developed profile. As the applied pressure difference, ΔP, across the instrument increases, we can see that the maximum

fluid velocity also increases in it. These results obtained in the case of irrigation mode are also applicable for the suction mode with the flow direction reversed.

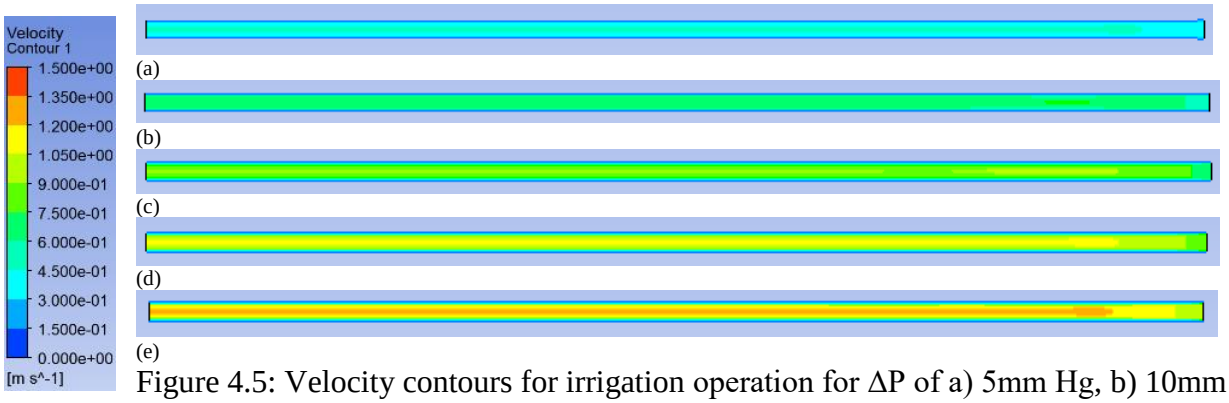

Figure 4.5: Velocity contours for irrigation operation for ΔP of a) 5mm Hg, b) 10mm Hg, c) 15mm Hg, d) 20mm Hg, and e) 25 mm Hg

Since very few computational analysis is carried out in medical instrument, the novelty of work lies in the determination of mass flow rates with the help of ANSYS Fluent from the medical perspective. It is clear that with an increase in pressure difference, the mass flow rate also increases. The suction irrigation pump used in laparoscopic surgeries has a maximum flow rate of 1.8 lit/min [8] in both suction and irrigation processes. The ideal pressure to be sent to the abdomen is 1333 Pa. So, the inlet pressure is set at this pressure, as shown in Figure 4.4, but the outlet pressure in case of suction is decreased in steps of 5mm Hg (666 Pa) so as get the flow rates. The flow rate in the abdomen is varied from patient to patient, depending on the obesity. However, negative pressure can suck the tissue from the abdomen. Hence, 10 mm Hg (1333 Pa) is considered the maximum safe limit within which the fluid can be irrigated or sucked from the abdomen cavity. The mass flow rate of 0.0179 kg/sec is equal to 1.07 lit/min, which is well below the S-I pump limit and can be irrigated or sucked for effective tissue rinsing. From the analysis, at maximum pressure difference at -2000 Pa, corresponding velocity, turbulence eddy dissipation, and turbulence kinetic energy are found to be 1.354 m/s, 1294 m^2/s^3, and 0.08247 $m^2/s^{2,}$ respectively.

With these S-I device results, the work shall be further proceeded to incorporate dissection and grasping features to make an instrument more useful in the field of modern laparoscopic surgeries.

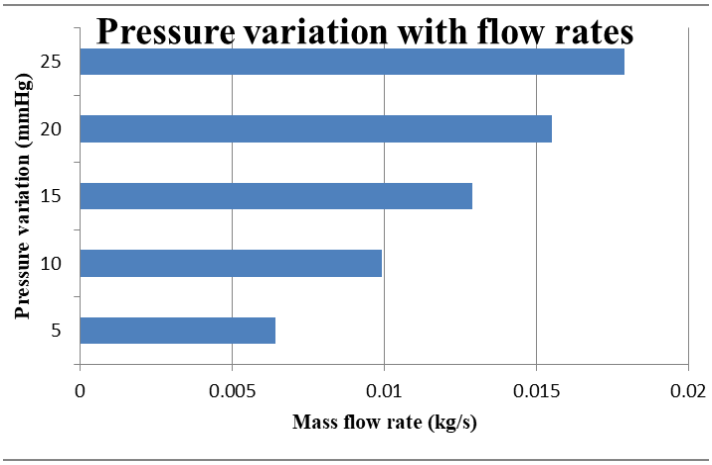

Figure 4.6: Mass Flow rate at different pressure variations across the device

With this analysis and findings in this chapter, further research study has been carried out to study other laparoscopic instruments and their utilization in the operation theatre.

4.2 Analysis of Laparoscopic device

For the flow analysis of the proposed laparoscopic device, similar steps as that of the modeled S-I conduit are followed. 267,393 nodes and 672,744 elements are used to mesh models shown in Figure 4.8 to Figure 4.10. Four different cases are considered for fluid flow numerical analysis with a combination of D =8mm & 10mm, and $\phi = 45^{\circ}$ & 60°. For each of these four cases, five different ΔP values ranging from 5mm to 25 mm Hg (gauge pressure) are used in steps of 5mm Hg in both suction and irrigation modes. In the case of suction and irrigation modes, the direction of fluid flow is essential for the modified design of forceps, as the geometry is not symmetric about its center, in contrast to that of the S-I conduit.

For each of the four designs mentioned above, the fluid flow region is imported from the SolidWorks model shown in Figure 4.7 and applied boundary conditions are similar to those of the S-I conduit. Despite carrying out mesh convergence studies with 672,744, 745,051, and

874,163 elements, the results are found to be independent of the mesh refinement used. Each of these four models mentioned above is simulated using ANSYS Fluent and post-processed for pressure, velocity, turbulent kinetic energy, dissipation rate contours, and mass flux rates.

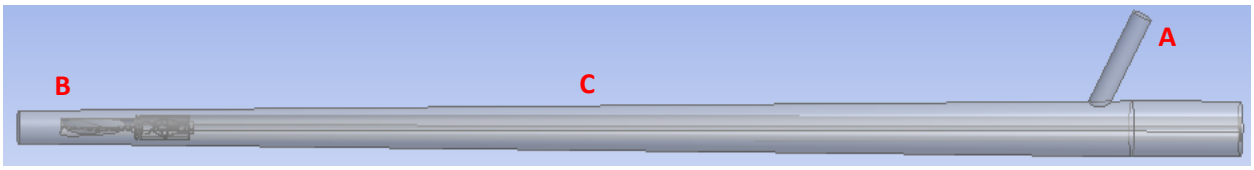

Figure 4.7: Suction Irrigation in the modified design of laparoscopic forceps

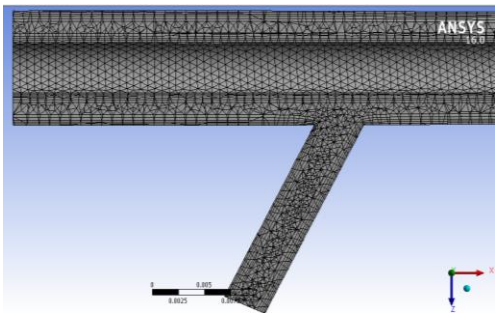

Figure 4.8: Mesh used near the protrusion

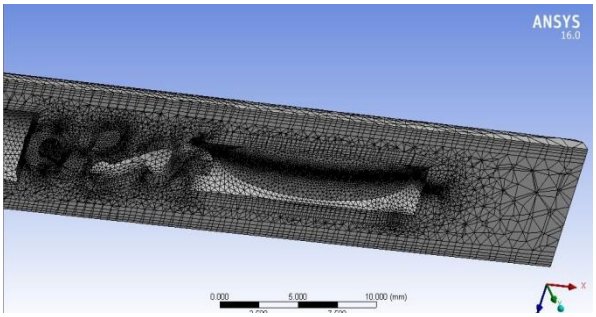

Figure 4.9: Mesh used near the jaws

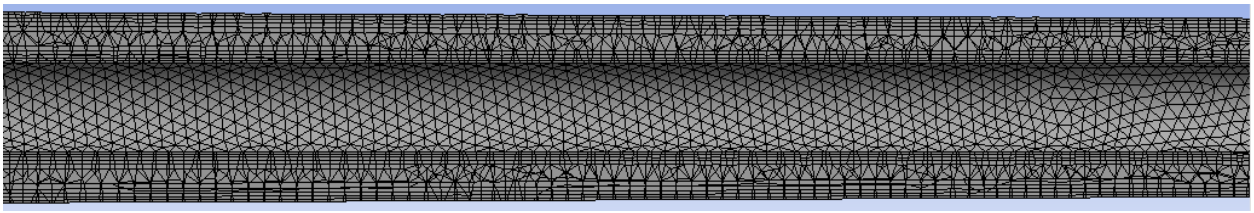

Figure 4.10: Mesh used in the flow tube

4.3 Results and discussion

Shown in Figure 4.11 to Figure 4.26 are the contour plots of pressure and velocity used to compare flow features in the four different designs. Suction and irrigation cases together, pressure and velocity contours for three different ΔP values are presented instead of all the five cases as a matter of convenience. Contours for turbulent dissipation rate with ΔP values of 25mm Hg are shown in Figure 4.28. For ease of comparison, in each set of plots, the contours are plotted with the same minimum and maximum legend values.

4.3.1 Geometry model D = 8mm case with $\phi = 60^{\circ}$

In the modified design with $D = 8$mm and $\phi = 60^{\circ}$, the S-I channel has a 2mm passage for the fluid to flow. For fluid flow analysis, in the case of irrigation, with $\Delta P = 5$mmHg, the pressure at the inlet (point A, Figure 4.7) is set to 15mm Hg, and pressure at the outlet (at point B, Figure 4.7) is set to 10mm Hg. Whereas in the suction case, the same analysis is repeated, considering point B as inlet and point A as an outlet under the same pressure conditions.

Contours of pressure (Suction):

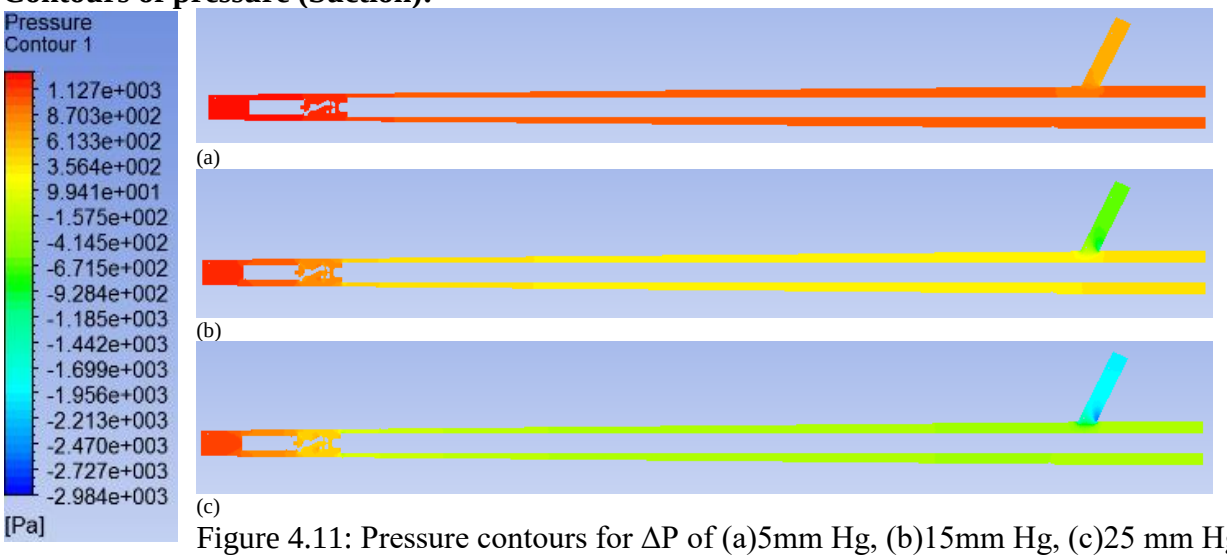

Figure 4.11: Pressure contours for ΔP of (a)5mm Hg, (b)15mm Hg, (c)25 mm Hg

Contours of velocity (Suction):

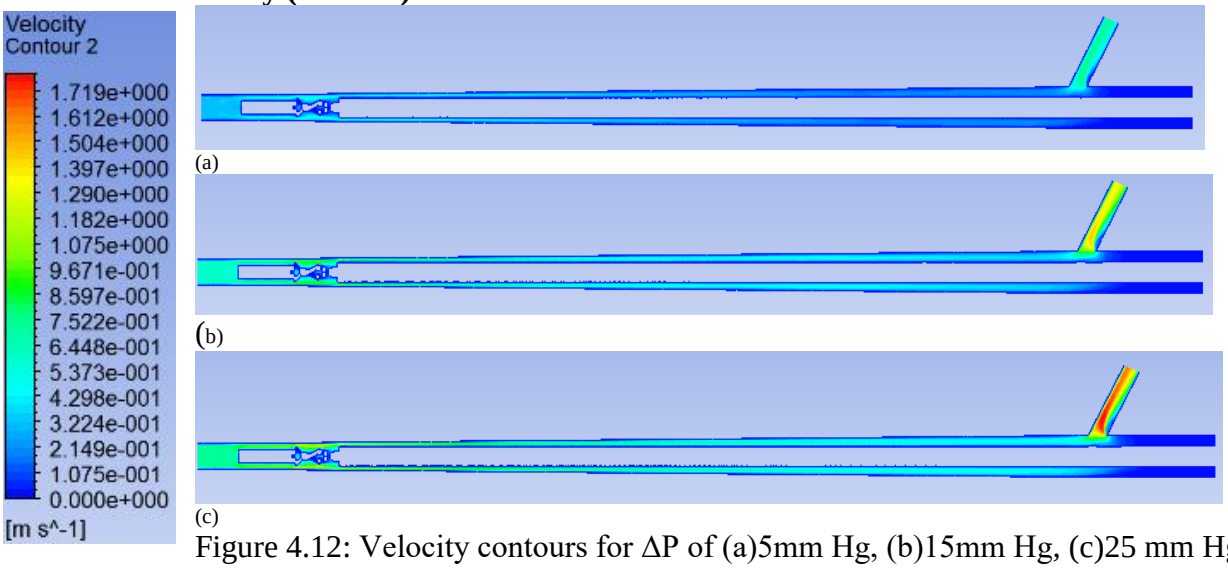

Figure 4.12: Velocity contours for ΔP of (a)5mm Hg, (b)15mm Hg, (c)25 mm Hg

As seen from the contour plots shown in Figure 4.11 to Figure 4.14, both in suction and irrigation, the pressure variation from inlet to outlet increases as ΔP increases as expected. From the pressure contours in Figure 4.14, it is clear that the pressure drop in the device occurs primarily at two locations for the suction process. The first pressure drop occurs at the flow inlet (near the jaws) and the second one at the flow exit (near the protrusion). At the inlet, the fluid has to navigate the complex geometry around the jaws and the actuating mechanism to get into the annular tube, which results in a pressure drop. In addition, the flow cross-section suddenly reduces at the inlet due to the presence of jaws, which in turn results in increased velocity and reduced pressure. Near the flow exit, the flow takes a sharp turn due to protrusion and results in a drop in pressure. Due to flow through the long annular section, pressure drops along the flow path. However, this pressure drop is small compared to the two minor losses mentioned near the flow inlet and outlet. Similar pressure contours are observed for all suction cases with five different ΔP values.

Figure 4.12 shows the velocity contours for three different ΔP values in case of suction. For all three cases, we see that the velocity of flow attains peak values at the centrelines of both protruding pipe and the annular section. The velocity of flow is less in the annular region and increases near the jaws because it is more constricted. The flow velocity to the right of the protrusion (proximal end) is negligibly small, which is like a stagnant zone as no flow occurs there. Similar flow velocity contours are observed for irrigation, too, with minor variations. Further, the magnitude of velocity in the flow domain also increases with an increase in pressure drop, as expected.

Contours of pressure (Irrigation):

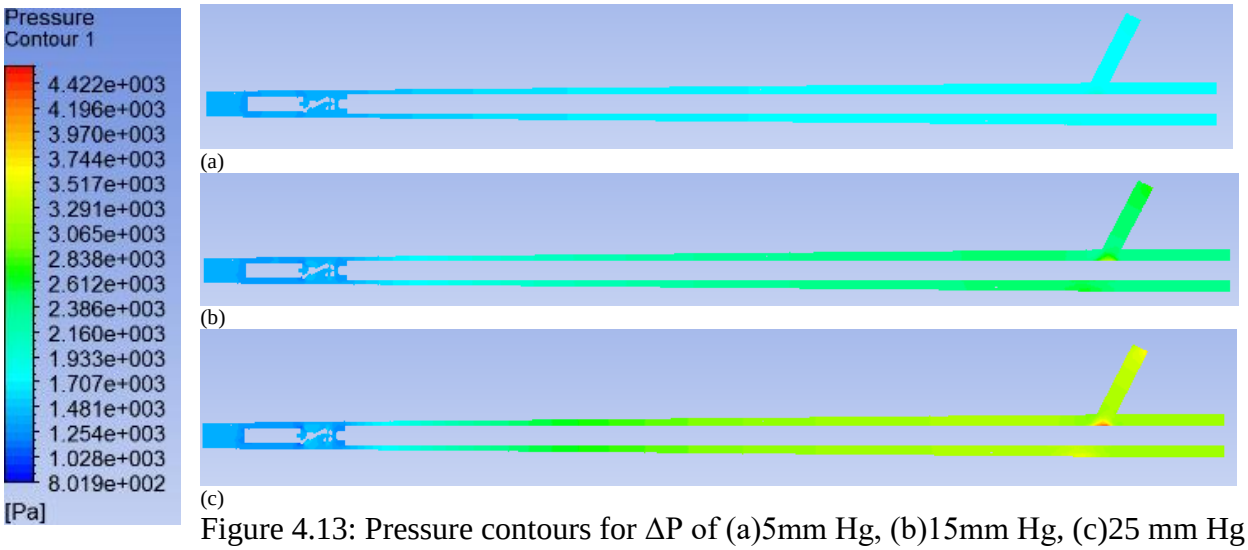

Figure 4.13: Pressure contours for ΔP of (a)5mm Hg, (b)15mm Hg, (c)25 mm Hg

Contours of velocity (Irrigation):

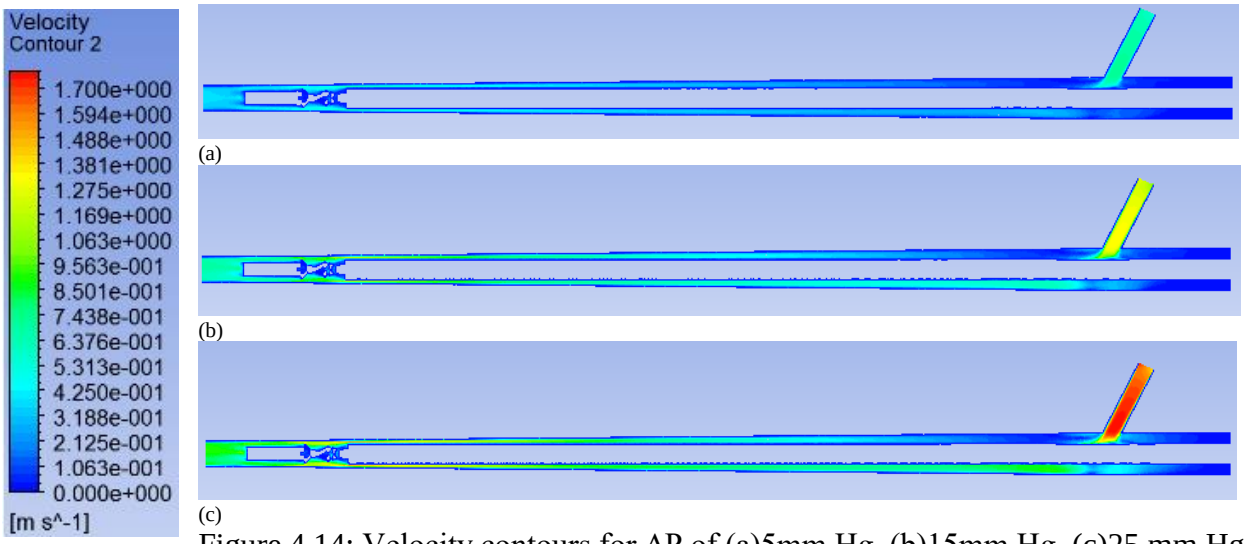

Figure 4.14: Velocity contours for ΔP of (a)5mm Hg, (b)15mm Hg, (c)25 mm Hg

The pressure contours shown in Figure 4.13 for the irrigation cases are slightly different when compared with the suction cases. The corresponding pressure drops at different sections are relatively more minor and more uniform throughout the length of the flow domain.

4.3.2 Geometry model D = 8mm case with ϕ =45°

Figure 4.15 to Figure 4.18 show the pressure and velocity contours for the modified design with $\phi = 45^{\circ}$. The boundary conditions applied are the same as those for $\phi = 60^{\circ}$. The overall variations of pressure and velocity contours are similar to those for $\phi = 60^{\circ}$, with small variations.

Figure 4.11 and Figure 4.15 depict the pressure variation with $\phi = 45^{\circ}$ and $\phi = 60^{\circ}$ repectively. For $\phi = 45^{\circ}$, the pressure variation is observed to be more than that for $\phi = 60^{\circ}$. In both the cases, pressure drop near the jaws (where the geometry is complex), during suction is more than that during irrigation (Figure 4.13 and Figure 4.17). This is seen in the contour plots for suction when there is a distinct change in the pressure. This is, however, not observed in the contour plots of irrigation where the pressure changes are less near the jaws, as the fluid flows over them are in a more streamlined manner. A similar trend is also observed near the protrusion end.

Contours of pressure (Suction):

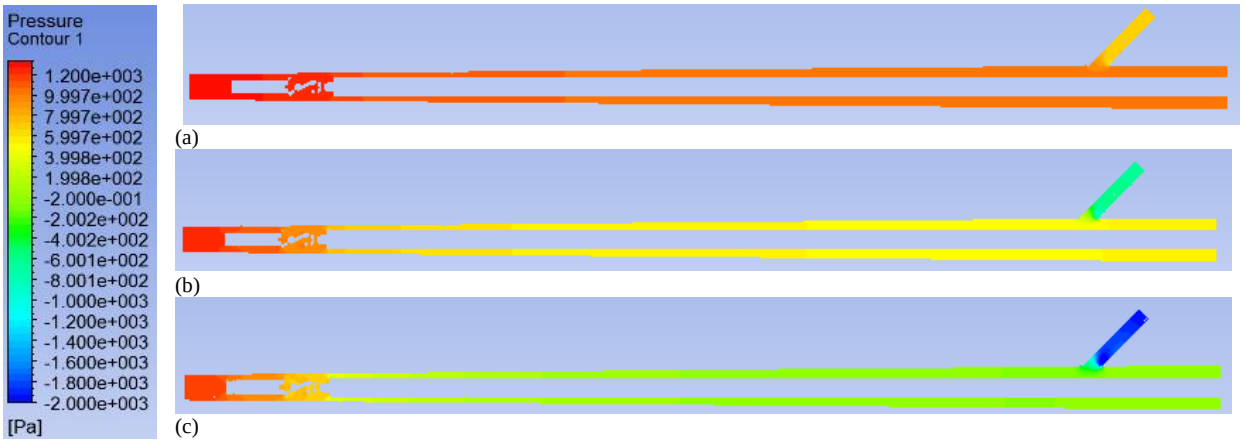

Figure 4.15: Pressure contours for ΔP of (a) 5mm Hg, (b)15mm Hg, (c)25 mm Hg

Contours of velocity (Suction):

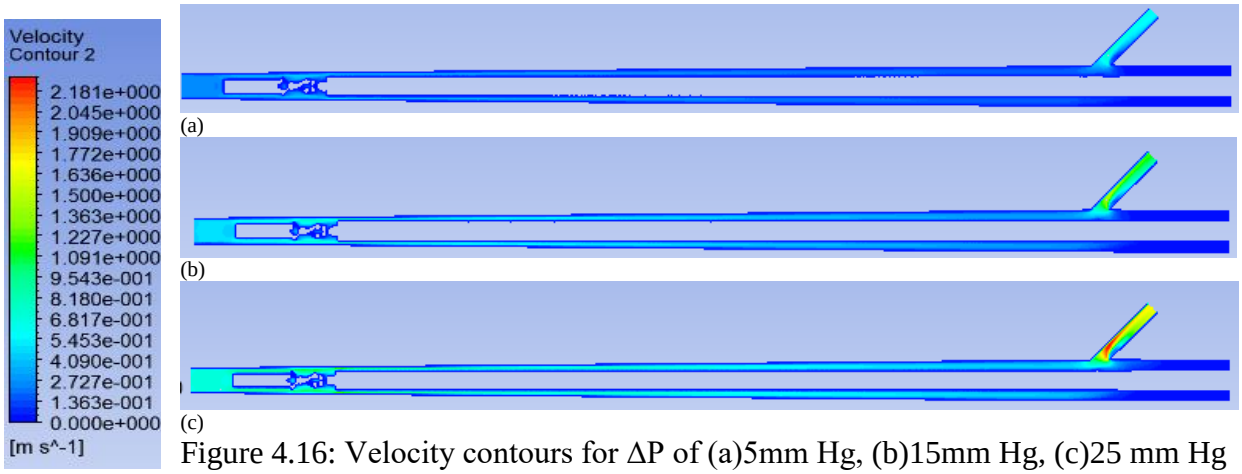

Figure 4.16: Velocity contours for ΔP of (a)5mm Hg, (b)15mm Hg, (c)25 mm Hg

Contours of pressure (Irrigation):

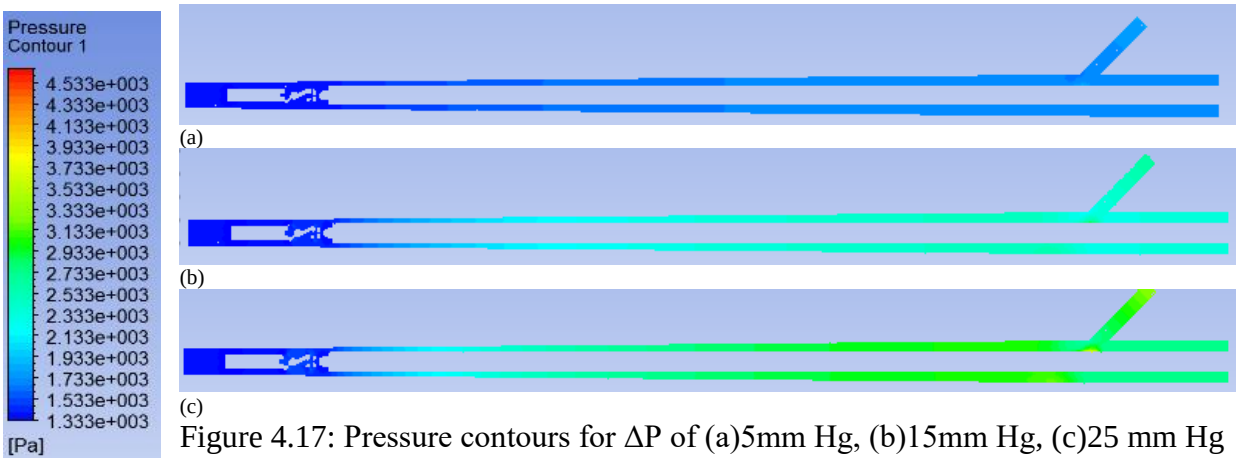

Figure 4.17: Pressure contours for ΔP of (a)5mm Hg, (b)15mm Hg, (c)25 mm Hg

In the velocity contours, the magnitude of the peak velocity for $\phi = 45^{\circ}$ (Figure 4.14 and Figure 4.18) is larger compared to that for $\phi = 60^{\circ}$ (Figure 4.12 and Figure 4.17) in both suction and irrigation modes. This is primarily seen inside the protrusion, where the pressure drops are higher for $\phi = 45^{\circ}$, which result in larger velocities. Hence, it may be concluded that the design with $\phi = 60^{\circ}$ is better compared to that of $\phi = 45^{\circ}$, as lesser pressure drop for the same flow rate is desirable.

Contours of velocity (Irrigation):

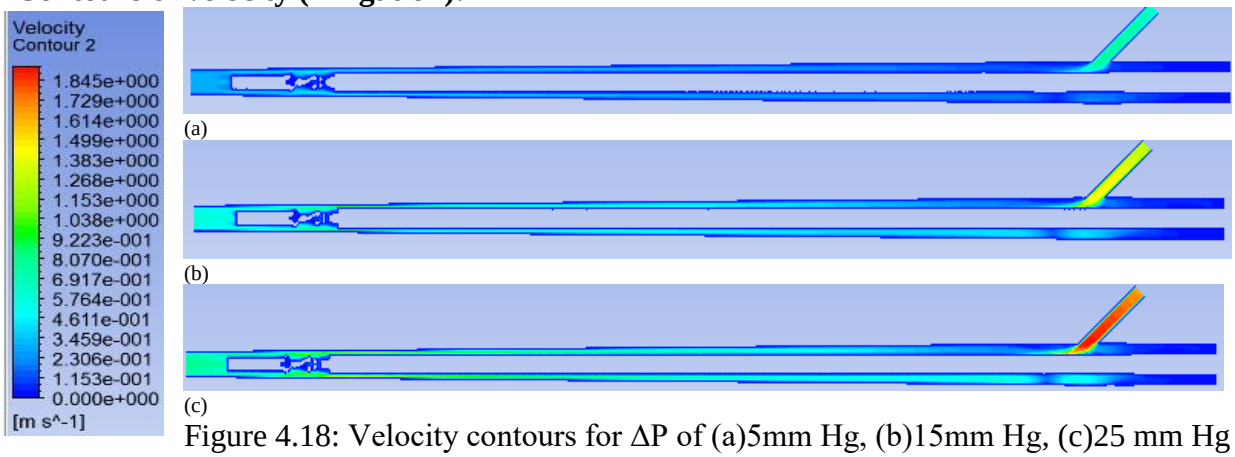

Figure 4.18: Velocity contours for ΔP of (a)5mm Hg, (b)15mm Hg, (c)25 mm Hg

4.3.3 Geometry model D = 10mm case with $\phi = 60^{\circ}$

Contours of pressure (Suction):

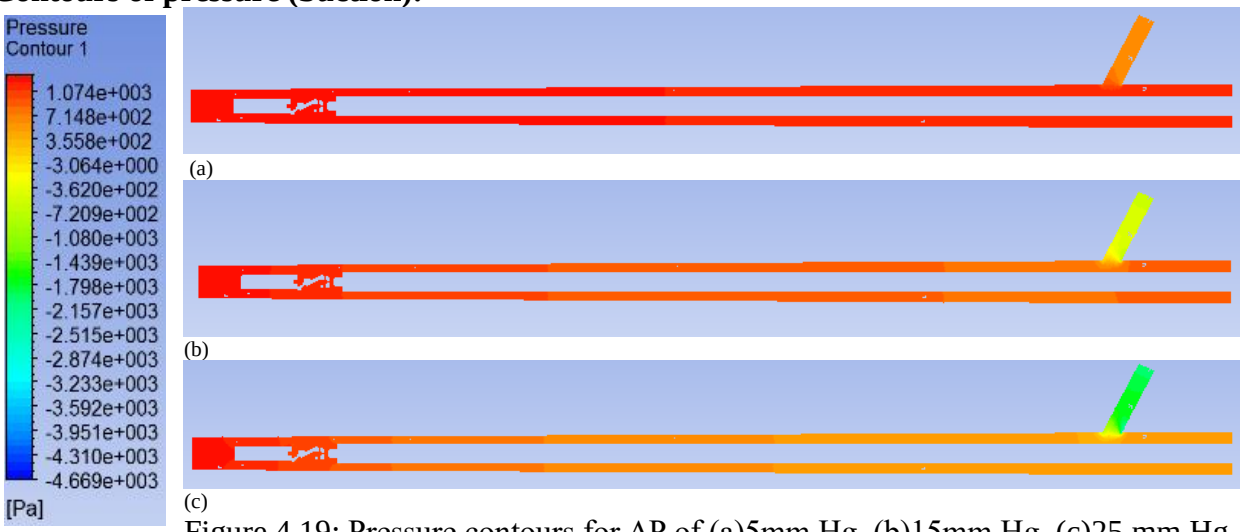

Figure 4.19: Pressure contours for ΔP of (a)5mm Hg, (b)15mm Hg, (c)25 mm Hg

Figure 4.19 to Figure 4.22 illustrates the results for the modified forceps of 10mm diameter, which has only 2.5mm thick annular passage for the fluid flow. As shown in Figure 4.7, the boundary condition for suction is set at the distal end (point B) at a constant 10mm Hg, and pressure at the proximal end (point A) is reduced in steps of 5mm Hg from 5mm Hg to -15mm Hg. While in the case of irrigation, the same procedure is repeated except that point A will act as an inlet, and point B is the outlet.

From Figure 4.19 and Figure 4.21, the pressure drop across the jaws and the protrusion are observed to be significantly more in suction mode compared to that in the irrigation mode. The peak velocities in the fluid domain are higher for suction compared to irrigation. Similar trends in pressure and velocity are observed for $D = 8mm$.

Contours of velocity (Suction):

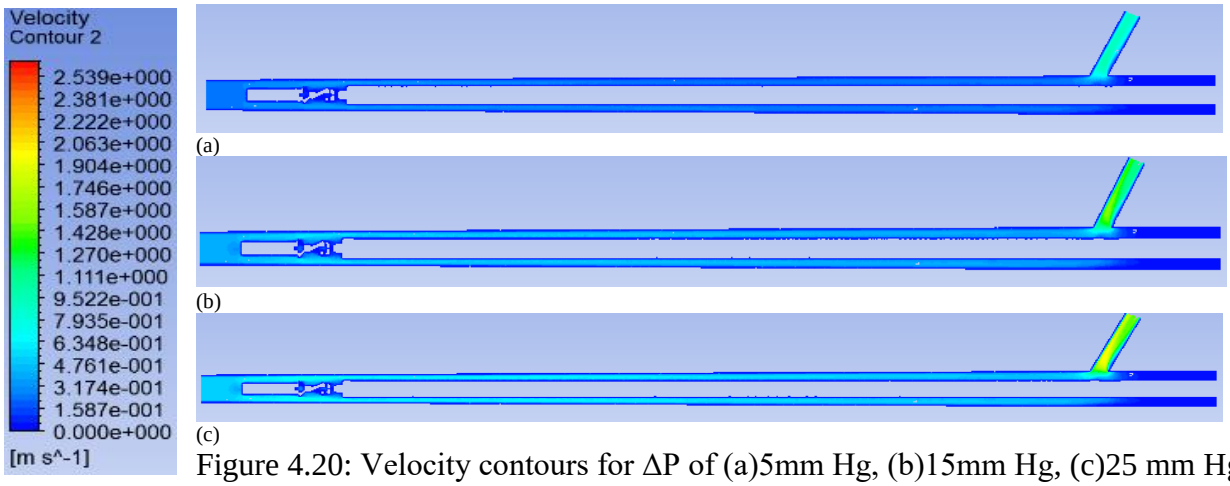

Figure 4.20: Velocity contours for ΔP of (a)5mm Hg, (b)15mm Hg, (c)25 mm Hg

Contours of pressure (Irrigation):

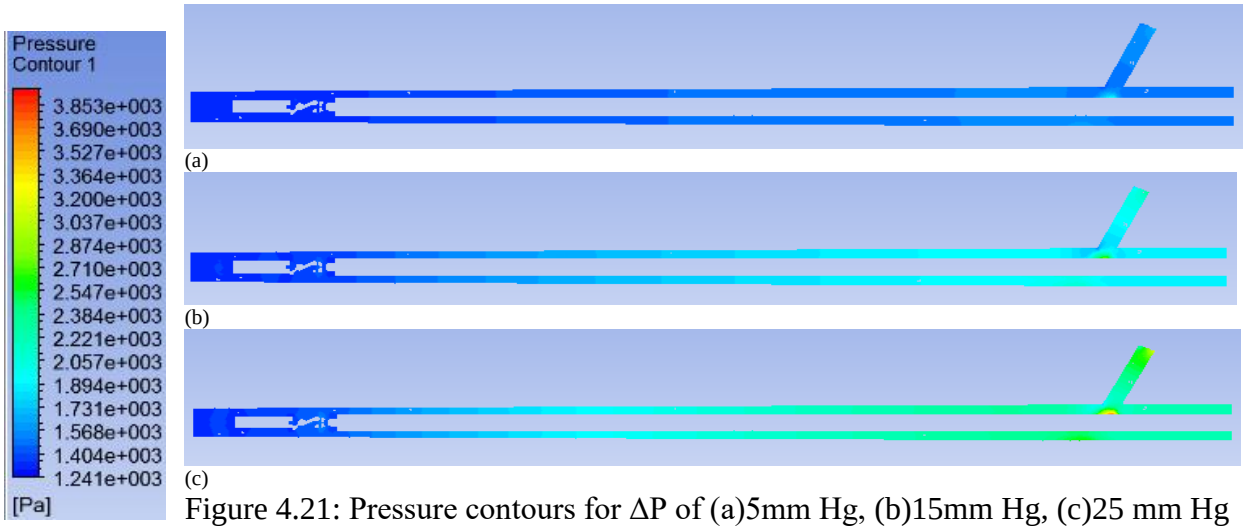

Figure 4.21: Pressure contours for ΔP of (a)5mm Hg, (b)15mm Hg, (c)25 mm Hg

Contours of velocity (Irrigation):

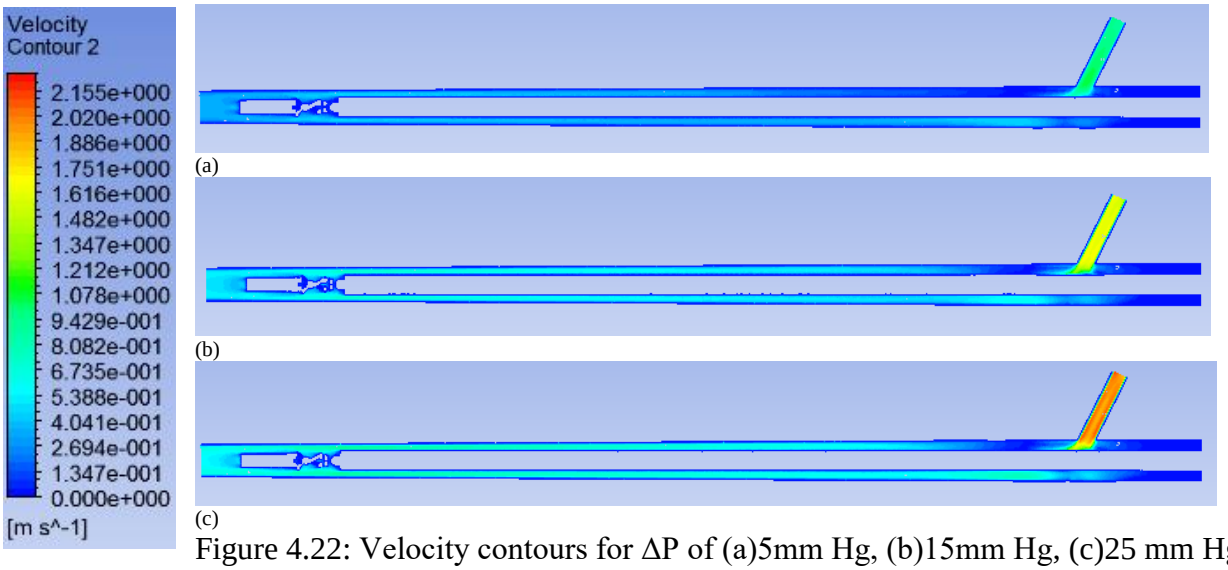

Figure 4.22: Velocity contours for ΔP of (a)5mm Hg, (b)15mm Hg, (c)25 mm Hg

4.3.4 Geometry model D = 10mm case with ϕ =45°

Figure 4.23 to Figure 4.26 illustrates the results for modified forceps with a 10 mm annular diameter and 2.5 mm passage. The boundary conditions remain the same as that of the design with $D = 10mm$ and $\phi = 60^{\circ}$.

Contours of pressure (Suction):

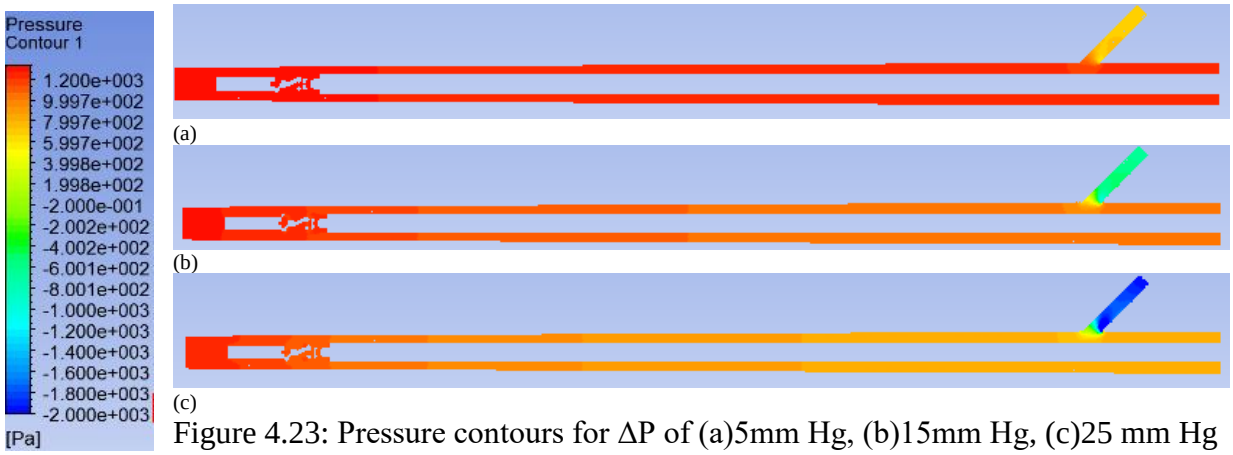

Figure 4.23: Pressure contours for ΔP of (a)5mm Hg, (b)15mm Hg, (c)25 mm Hg

Contours of velocity (Suction):

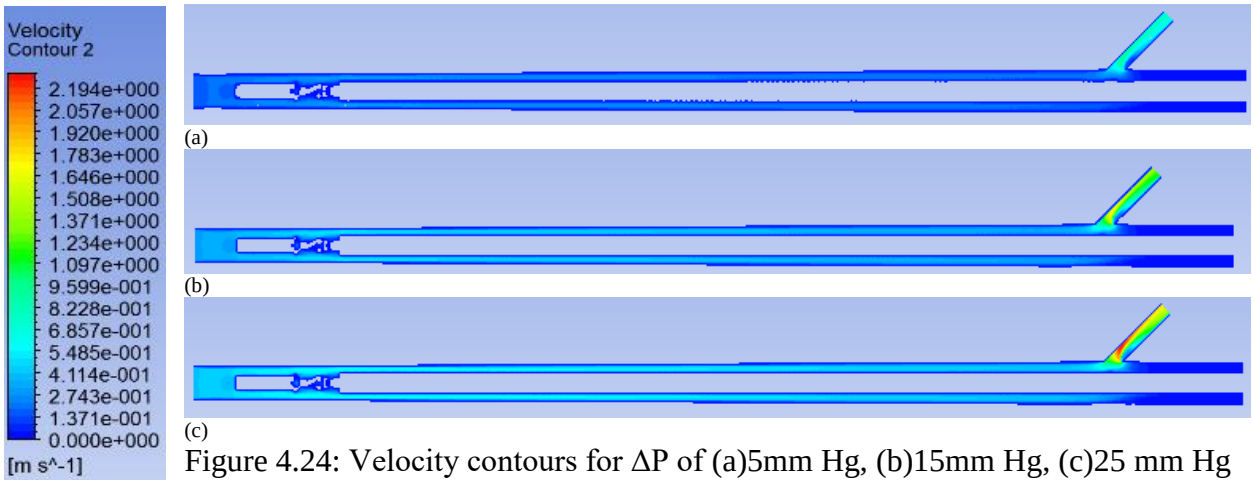

Figure 4.24: Velocity contours for ΔP of (a)5mm Hg, (b)15mm Hg, (c)25 mm Hg

From Figure 4.23 and Figure 4.25, pressure drop across the jaws is found to be less compared to that near the protrusion, even though the geometry of the jaws is more complicated. This trend is found to be consistent for both 8mm and 10mm designs during suction and irrigation modes with $\phi = 45^{\circ}$ and $\phi = 60^{\circ}$. This may be attributed to two reasons. Firstly, the fluid flow takes a sharp turn near the protrusion, thereby developing a recirculation region. Secondly, since the flow is through an annular region before entering protrusion.

Contours of pressure (Irrigation):

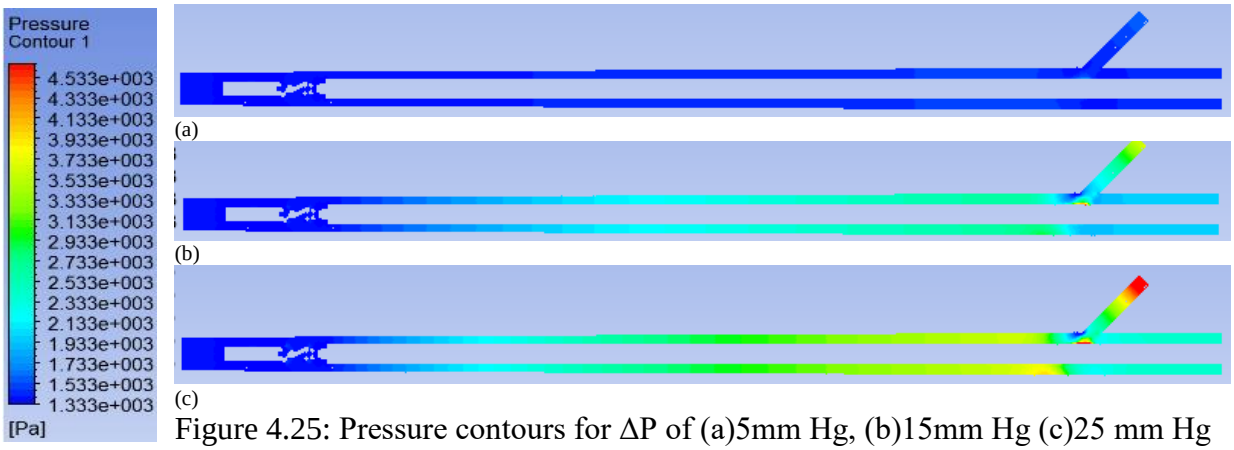

Figure 4.25: Pressure contours for ΔP of (a)5mm Hg, (b)15mm Hg (c)25 mm Hg

Contours of velocity (Irrigation):

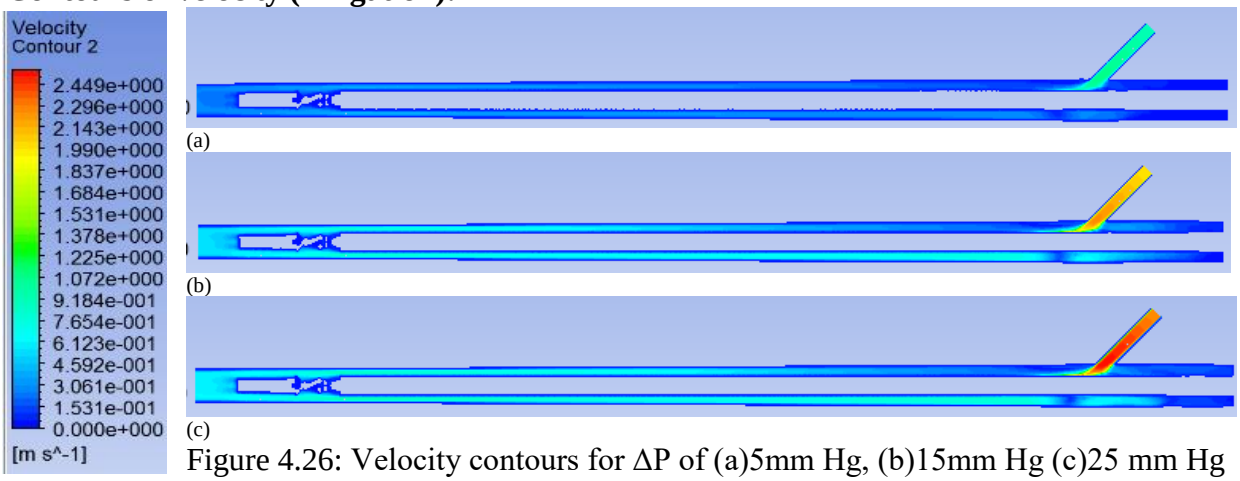

Figure 4.26: Velocity contours for ΔP of (a)5mm Hg, (b)15mm Hg (c)25 mm Hg

4.4 Summary of different designs: Variation of mass flow rate through the devices with applied pressure difference.

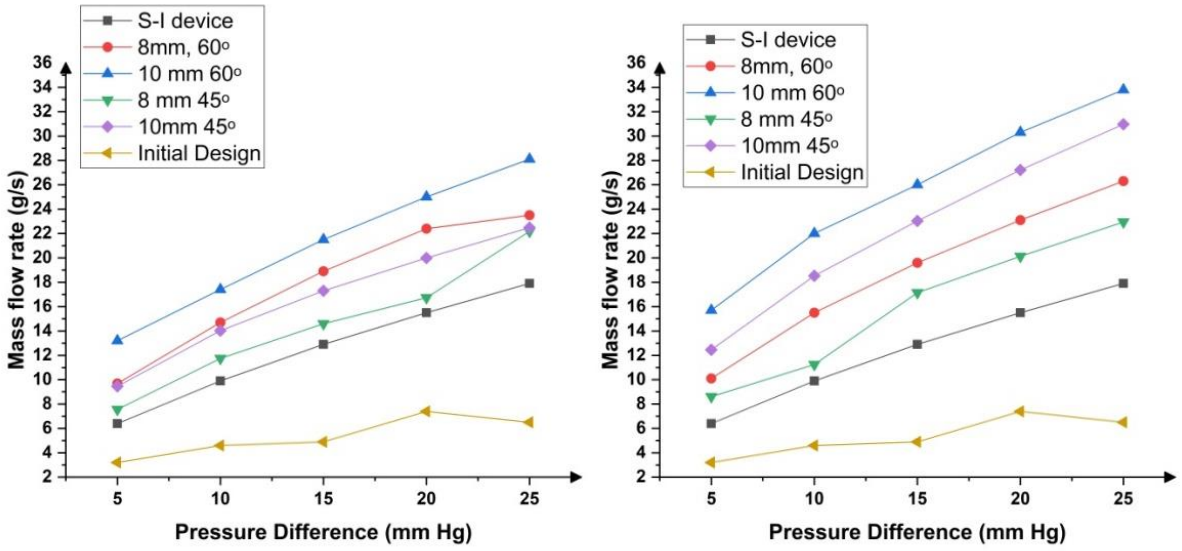

Figure 4.27: Comparison of mass flow rates through different devices in (a) suction and (b) irrigation modes of operation

The mass flow rate variation with respect to the applied pressure difference is shown in Figure 4.27. Four types of forceps designs with two different diameters (8mm total diameter, which has 2 mm annular region, 10mm total diameter, which has 2.5 mm annular region) and two

different protrusion angles $\phi = 45^{\circ}$ and $\phi = 60^{\circ}$ are compared both in suction and irrigation modes. These designs are, in turn, compared with the initial design.

From Figure 4.27, we note the following salient points. The mass flow rate

- for all the modified designs and SI conduit is higher than that of the initial design.
- for all the modified designs are higher than that of the SI conduit.
- is higher for $\phi = 60^{\circ}$ design compared to $\phi = 45^{\circ}$ design for both $D = 8mm$ & $10mm$.
- is higher for $D = 10mm$ design compared to $D = 8mm$ designs.
- increases with an increase in pressure difference across the device.

All the observations mentioned above hold for both suction and irrigation modes of the device.

Table 4.2: Comparison of mass flow rates through different devices in suction and irrigation modes

Mass flow rate (g/s) in Suction Mode						
Pressure difference (mm of Hg)	**S-I device**		**$\phi = 60^{\circ}$**		**$\phi = 45^{\circ}$**	
		Initial Design	D=8 mm	D=10 mm	D=8 mm	D=10 mm
5	6.4	3.2	9.69	13.20	7.56	9.45
10	9.9	4.6	14.70	17.40	11.74	14.03
15	12.9	4.9	18.90	21.50	14.59	17.30
20	15.5	7.4	22.40	25.00	16.73	20.00
25	17.9	6.5	23.50	28.10	22.18	22.48
Mass flow rate (g/s) in Irrigation Mode						
Pressure difference (mm of Hg)	**S-I device**		**$\phi = 60^{\circ}$**		**$\phi = 45^{\circ}$**	
		Initial Design	D=8 mm	D=10 mm	D=8 mm	D=10 mm
5	6.4	2.9	10.10	15.70	8.61	12.46
10	9.9	4.4	15.50	22.00	11.25	18.53
15	12.9	5.7	19.60	26.00	17.14	23.03
20	15.5	6.8	23.10	30.30	20.12	27.22
25	17.9	7.8	26.30	33.80	22.95	30.97

The mass flow rates for different designs in suction and irrigation modes are listed in Table 4.2. The tabulated values show that the mass flow rates through different designs are consistently more in irrigation mode compared to those in suction mode.

Contours of turbulence dissipation rate (ϵ):

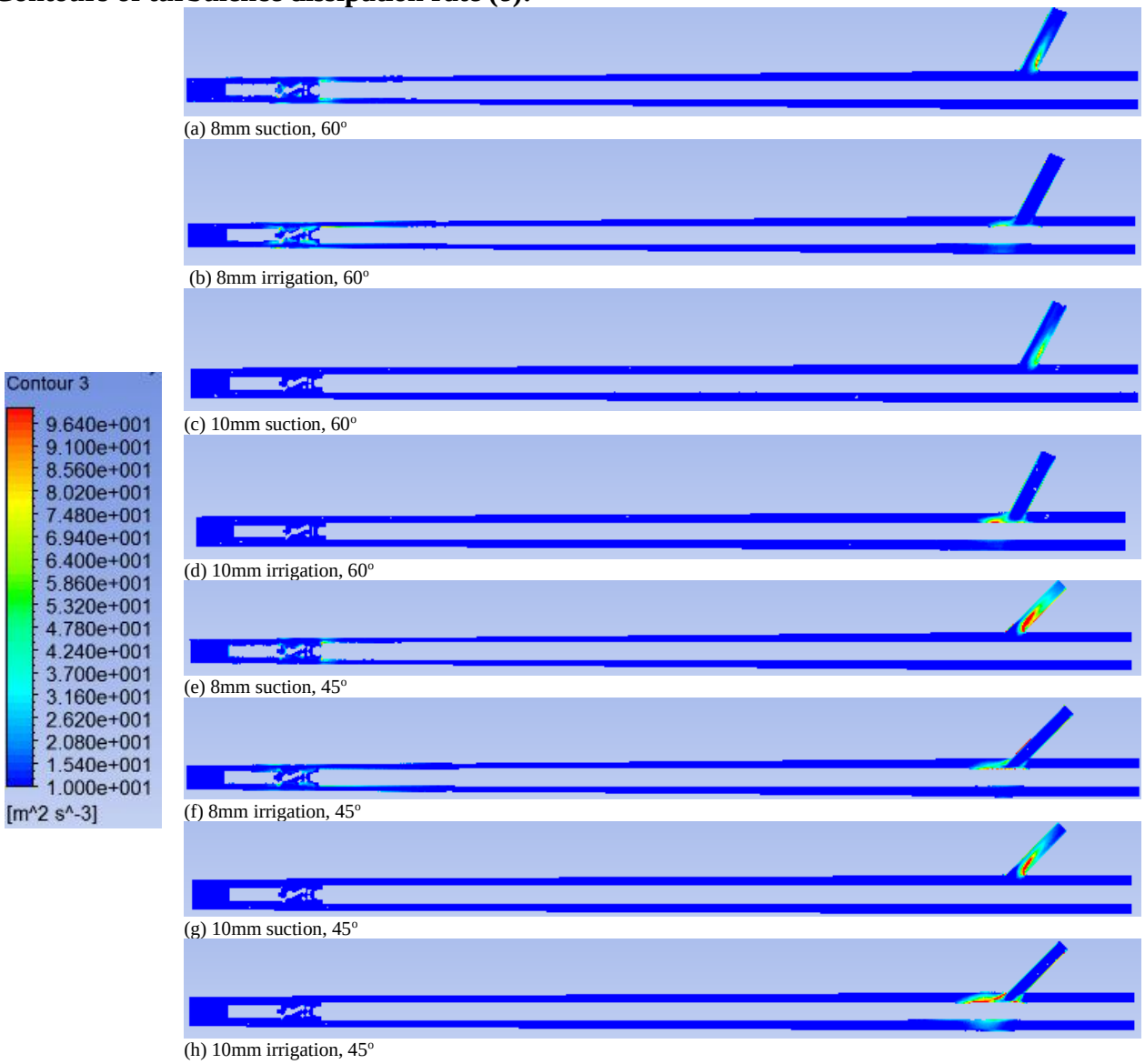

(a) 8mm suction, 60°

(b) 8mm irrigation, 60°

(c) 10mm suction, 60°

(d) 10mm irrigation, 60°

(e) 8mm suction, 45°

(f) 8mm irrigation, 45°

(g) 10mm suction, 45°

(h) 10mm irrigation, 45°

Figure 4.28: Turbulence dissipation rate contours for 25 mm Hg pressure difference

Several conclusions drawn in the preceding discussion are also reflected in the contours of turbulence parameters like turbulent kinetic energy and dissipation rate. Figure 4.28 shows the contour plots of energy dissipation rate for different diameters and protrusion angles designs in both suction & irrigation modes. The contour plots of turbulent kinetic energy closely resemble

those of the energy dissipation rate and are hence not shown here. From these contours, we observe that,

- Suction *vs.* irrigation modes: ϵ is high in the suction mode for all the designs in the protrusion and forms a bottleneck for the outgoing fluid resulting in lower flow rates. In contrast, in the irrigation mode, though the dissipation rate is high in the region where incoming fluid from the protrusion strikes the inner annular wall, the flow can continue past the annulus to its diametrically opposite end resulting in less pressure drop and relatively higher flow rates.
- $D = 8mm$ *vs.* $D = 10mm$ designs: ϵ is smaller near the jaws for the $D = 10mm$ design as the fluid can flow through a greater cross-sectional area with lower velocities. This also increases the mass flow rate for the $D = 10mm$ designs, as observed in Figure 4.28. ϵ is also higher in the region where the incoming fluid strikes the inner annular wall for $D = 10mm$ design than the $D = 8mm$ design in irrigation mode. This is because the corresponding mass flow rate is high for the same cross-section (for $D = 10mm$ design) and results in larger turbulence.
- $\phi = 45^o$ *vs.* $\phi = 60^o$ designs: ϵ is similar near the jaws but higher near the protrusion for the $\phi = 45^o$ designs in comparison with $\phi = 60^o$ designs. This results in a more substantial pressure drop and decreased mass flow rate for the $\phi = 45^o$ designs near the protrusion region.
- Jaws *vs.* protrusion regions: ϵ is high near the jaws and protrusion when compared with that in the straight annular pipe flow. ϵ is also high near the protrusion when compared with that near the jaws for all the cases. This can be related to high-pressure drop near the regions of high ϵ (i.e., the areas of high turbulence), as illustrated in the pressure contours, as shown in Figure 4.28.

4.5 Experimental study

The proposed laparoscopic device modeled in SolidWorks is fabricated as per the design with $D = 8$ mm and $\phi = 60^o$ S-I channel for the fluid to flow. Initially, to prepare the set-up for experimentation, carpentry work is done to hold the instrument in place, as shown in Figure 4.29. To measure the pressure drop at two extreme ends, a T-junction is attached at both ends. One end of the T-junction is attached to the manometer, and the other end is connected to pass the fluid. A similar T-junction is set up at the other end of the instrument, as shown in Figure 4.30. For fluid flow, in the case of irrigation, the pressure drop is calculated between these two ends (point A acts as an entry and point B acts as an outlet, as shown in Figure 4.7). A T-junction is required at both ends for connecting the manometer and passage of the fluid channel. The schematic diagram for irrigation process is shown in Figure 4.31. Whereas in the case of suction, the same analysis is repeated, considering point B as an inlet and point A as an outlet under the same pressure conditions as shown in Figure 4.33.

Figure 4.29: Stand for holding laparoscopic instrument in place

The water is passed from the tap water pressure and is regulated through the butterfly valve. The valve is opened slowly and set at a pressure difference in the manometer. A beaker is used to measure the flow rate by measuring the time taken for 700 ml of water to flow. Gradually, the flow

rate is increased by adjusting the valve, and the resulting pressure difference in the manometer is noted down. Similarly, the suction results are noted down by reversing the entry and exit points.

Figure 4.30: Experimental set-up of the instrument

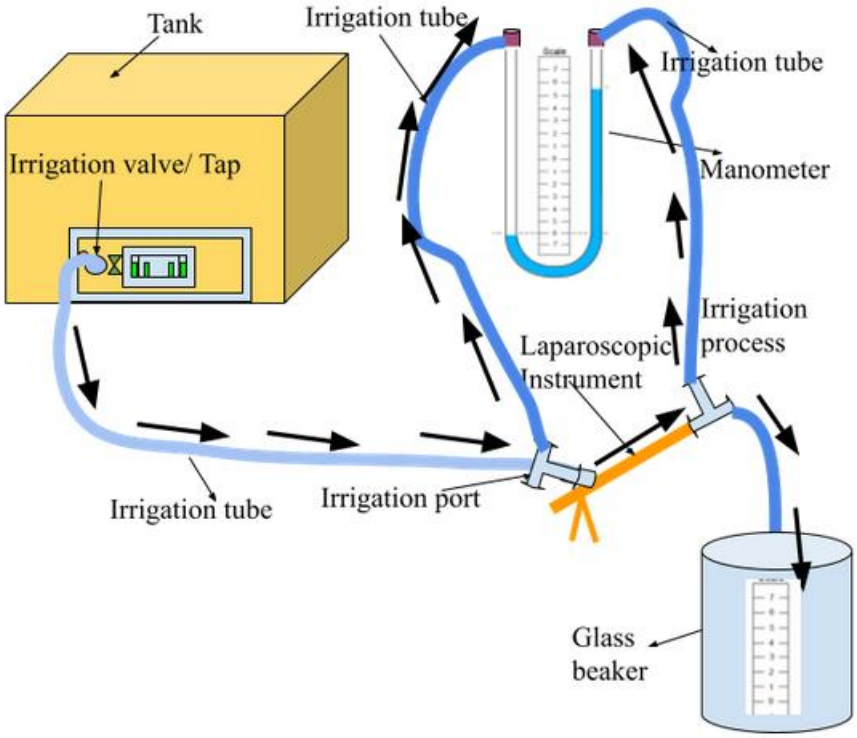

Figure 4.31: Experimental setup for schematic diagram during irrigation process

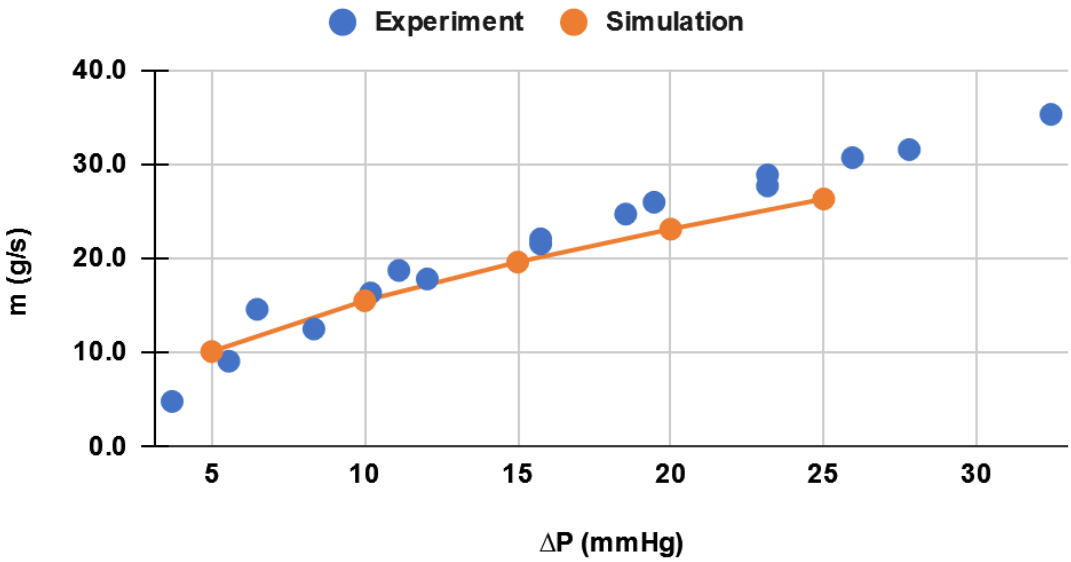

Figure 4.32: Comparison between experimental and simulation results of Irrigation process in the laparoscopic instrument

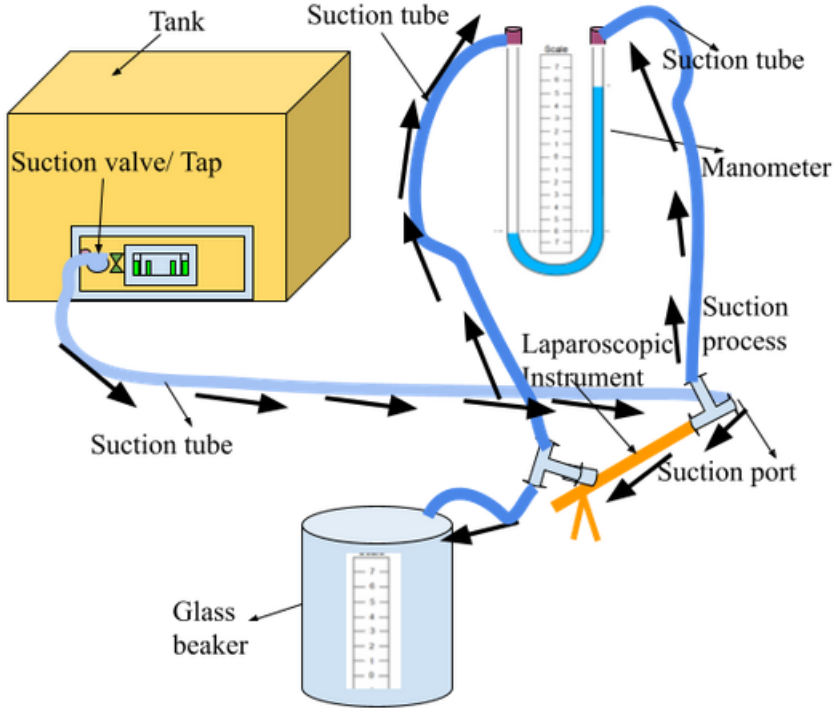

Figure 4.33: Experimental setup for schematic diagram during suction process

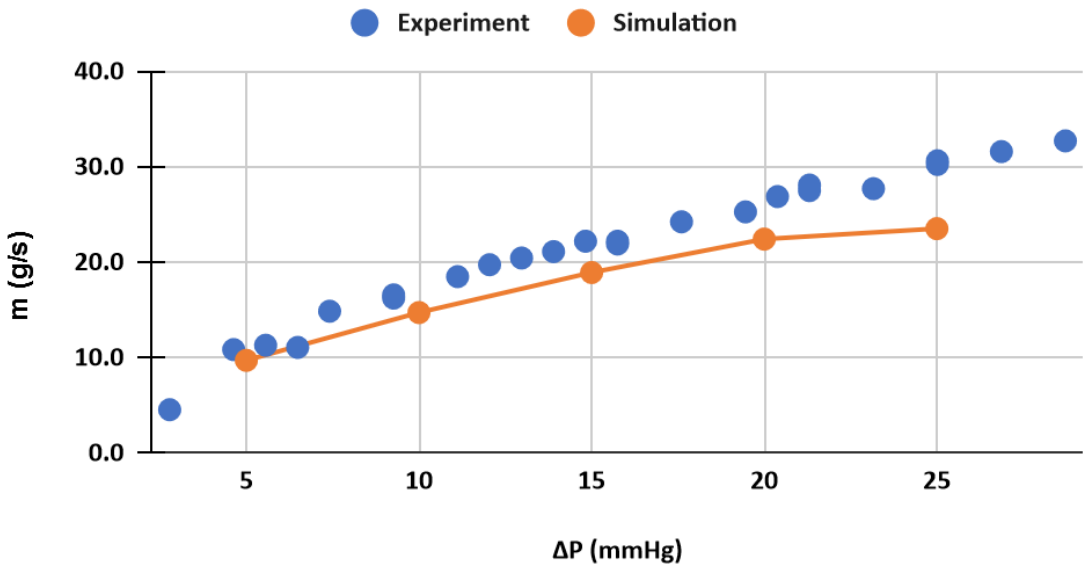

Figure 4.34: Comparison between experimental and simulation results of Suction process in the laparoscopic instrument

Figure 4.32 and Figure 4.34 compare numerical analysis and experimental results of the Irrigation and Suction process, respectively. It is seen from both figures that the experimental result is slightly more than the simulation results, particularly for larger pressure drops. It is possibly because of the following differences:

1. The flow is simulated using $k-\epsilon$ model, assuming it is fully turbulent. However, there are regions of the flow domain, which are laminar or regions where the flow transitions from laminar to turbulent flow. The $k-\epsilon$ model effectively adds higher viscosity to the fluid resulting in smaller flow rates in the simulation. This primarily explains the observed differences.
2. The fabricated device is of similar dimensions as the modeled one and given a smooth surface finish using a wire and cut machine. Despite this, there could possibly be a minor mismatch in the dimensions, particularly for the small internal components and surface finish, due to tolerances in the fabrication processes.

3. In the numerical analysis, simulation is considered with some part beyond the protrusion end of the instrument up to a stopper in the connector component. But, in actual experimentation work, the washers are immediately placed at the connector such that there is no leakage and passage of fluid beyond the protrusion end. This eliminated the backflow of water inside the fabricated instrument.

Since the purpose of fabrication was to meet the mass flow rates of the existing used instrument in laparoscopic surgeries. From numerical analysis, different designs and protrusion angles were compared to result in more mass flow rates. However, during fabrication, a few changes like reduction in the outer diameter without compromising the instrument quality and the addition of washers at the connector part to avoid leakage of fluid in the fabricated device resulted in more mass flow rate.

Chapter-5

5 Non-Newtonian Blood Flow analysis

5.1 Introduction

Even though advances in laparoscopic surgeries have resulted in the accelerated development of surgical techniques, a few instruments currently in use are yet to be improved. The reason is that due to the repetitive exchange of instruments, the surgeon experiences fatigue and strain-related injuries in hand and shoulder [97]. In addition, patients are subjected to the risk of injury because of multiple instrument exchanges. Studies [98] show that around 17-30% of the operation time is wasted in instrument exchange during laparoscopic surgeries. Also, wound closure and port insertion contribute to 26% of the operating time, whereas the actual surgical procedure only requires 57% of the total duration. This highlights the need to develop multi-functional forceps ergonomically designed for ease of use and reduce surgery duration. A more comprehensive overview of the literature, laparoscopic procedure, and recent advances in this field have been presented in chapters 2 and 3.

The above discussion emphasizes the importance of designing the instrument for safety, high quality, cost, feasibility, and functionality. The feedback obtained from practicing surgeons in this field also reinforced the need for modifying the existing design. These limitations of the existing design of dissector forceps commercially in use were addressed in our new multi-functional design [99],[100] that integrates the dissector forceps and suction irrigation device into a single instrument. The new design introduces a hollow pipe (sleeve) over the Maryland forceps in use. The S-I fluids can be pumped in and out of the device through the gap between the sleeve

and the forceps. More detailed engineering of this new design is required to prescribe the dimensions and other functional aspects of it completely and confidently.

Several researchers have successfully employed an analytical approach to model the physical problems ranging from microflows to macro flows in the recent past [101][103]. Such a methodical analysis, which gives insight into the physics of the problem, and aids in the design and development of laparoscopic devices, is largely missing in the literature. Therefore, a similar flow analysis was carried out numerically on the new design, using water as a working fluid, in our first work [104]. This was done to ensure that the flow rate in the new design is similar to that of the existing S-I device. The objective of the current work is to further extend the fluid flow analysis to simulate the non-Newtonian flow of blood inside the new design. This is done to get a better insight into the actual behavior of blood flow rather than its first approximation as water. Moreover, the current work also points to the improvements that can possibly be made to the new design and its operating conditions. Finally, it also ensures that the flow rate of blood provided by the new design is similar to that provided by the existing S-I device.

5.2 Methodology

As mentioned above, the proposed modified design of the forceps was selected out of different possible designs based on the flow analysis using water as the medium. This was done to mimic the flow of cleaning fluid, typically saline, in the S-I device. However, during surgery, in the suction process, typically, blood that oozes out of the tissue could also mix with the cleaning fluid. In reality, the flow could be transient, multiphase, and non-Newtonian in nature due to the formation of blood clots or air bubbles. However, this full-scale simulation is beyond the scope of the present work. Since blood has a higher viscosity than that of water, it is expected to result in a lesser mass flow rate for the same pressure difference across the S-I device. Therefore, in the

present work, simulations are performed to explore the flow behavior of blood alone, to quantify the lower limit of flow rate in the modified instrument. The flow of blood is assumed to be laminar with a constant density of 1060 kg/m^3.

The study of non-Newtonian fluid flow properties is important for simulating the flow phenomena better and accurately predicting them before the fabrication of instruments. Several studies have suggested the applicability of computational fluid dynamics (CFD) on different medical fronts [105]-[107]. In their work, a finite volume method is used to describe the blood flow properties passing in the aortic arch. Some authors initially considered blood as a Newtonian fluid. However, since the viscosity of blood is affected by the shear and flow rates, they suggested rheological models that treat blood as a thixotropic, non-Newtonian fluid. At lower mass flow rates, the viscosity of blood increases as the shear rate is very less. This is because, at a lower shear rate, there is an increase in the adhesiveness that causes red blood cells to adhere to the surface boundary resulting in more viscosity. Similarly, if the temperature decreases, the viscosity of blood increases. Taking blood as non-Newtonian fluid in arteries and blood vessels, theoretical results were also validated with the experiments [107],[108].

Non-Newtonian flow analysis is carried out for the S-I device incorporated in the proposed forceps design for $D = 8mm$ with two different protrusion angles $\phi = 45^\circ$ and $\phi = 60^\circ$. The most suitable design is selected such that it yields a mass flow rate similar to that of the existing S-I device.

5.3 Geometry and mesh generation

The S-I instrument currently used in laparoscopic surgeries is 5 mm in diameter, with a length of 330 mm [95]. Figure 5.1 shows the boundary layer mesh used to simulate the flow in the

S-I device, which is modeled and meshed in ANSYS Fluent. The mesh refinement studies were conducted for a maximum pressure difference of 25 mm Hg across the device, as shown in Table 5.1. The mass flow rate is chosen as the determining parameter in the mesh independence studies for three meshes: M1, M2, and M3. It is found to be consistently independent of nodes and elements used in the mesh. The deviation in mass flow rate, measured with respect to that in the fine mesh M3, is less than 2%. So, an intermediate mesh M2 with 255,583 elements and 118,160 nodes is used for all simulations.

Table 5.1: Mesh refinement studies for S-I instrument

Suction Pressure (25 mm of Hg)	**Nodes**	**Elements**	**Mass flow rate (g/s)**	**% error w.r.t M3**
M1	74,764	171,976	23.47	2.0
M2	118,160	255,583	23.83	0.5
M3	214,856	447,115	23.94	0.0

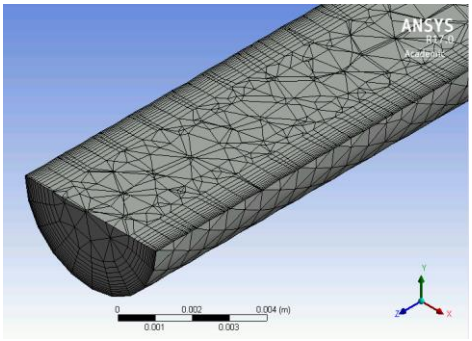

Figure 5.1: Cross-sectional view of mesh used in the S-I conduit.

The modified laparoscopic forceps is modeled in SolidWorks, and its fluid domain is imported in ANSYS Fluent to carry out meshing and run simulations. The mesh sensitivity studies are carried out in the fluid domain extracted from the assembly. Table 5.2 shows the mesh studies

for both $D = 8\ mm, \phi = 45^{\circ}$ and $D = 8\ mm, \phi = 60^{\circ}$ geometries. We see that the mesh is independent of nodes and elements used since the deviation in mass flow rate with respect to the fine mesh M6 is lower than 1.5%. So, the mesh M4 is chosen to simulate the flow for different pressure drops across the device. Figure 5.2 shows the mesh created near the protrusion end.

Figure 5.3 shows the mesh around the jaws, while Figure 5.4 shows the mesh in the flow conduit.

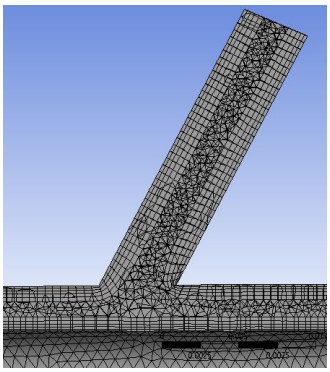

Figure 5.2: Mesh near the protrusion

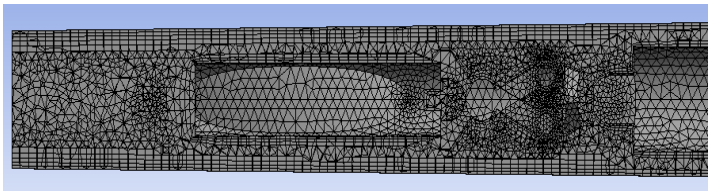

Figure 5.3: Mesh near the jaws

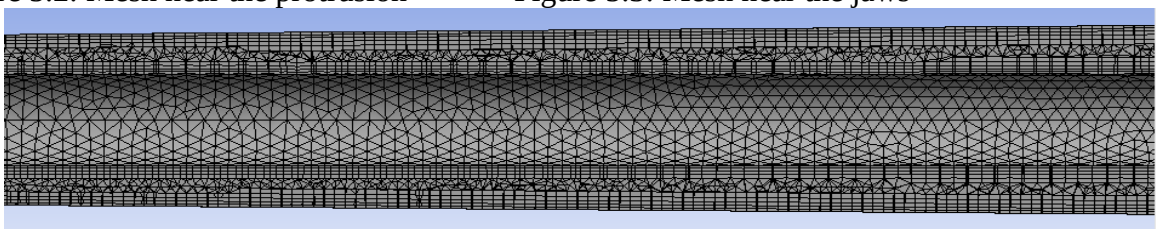

Figure 5.4: Mesh in the flow conduit

Table 5.2: Mesh refinement studies for modified laparoscopic forceps for 8mm, 45° and 8mm, 60° geometries

	8 mm, 45° geometry				8 mm, 60° geometry			
Suction Pressure (25 mm of Hg)	**Nodes**	**Elements**	**Mass flow rate (g/s)**	**% error w.r.t M6**	**Nodes**	**Elements**	**Mass flow rate (g/s)**	**% error w.r.t M6**
M4	266822	671864	15.3	0.26	267393	672744	18.92	-1.39
M5	319756	786955	14.89	2.93	393163	951471	18.78	-0.64
M6	600711	1398843	15.34	0.00	562044	1266821	18.66	0.00

5.4 Boundary conditions used and the proposed design parameters

The flow through the fluid domain is simulated using a steady-state, pressure-based solver. As shown in Figure 4.7, while performing suction tasks in laparoscopic surgeries, the distal end (point A) acts as an outlet, the flow channel (point B) acts as the fluid passage area, the proximal end (point C) as an inlet. It means that the fluid inside the abdominal cavity is sucked out from the proximal end of the forceps, enters the flow channel, and leaves from the distal end. The proximal end is fixed at a pressure of 1333 Pa (in suction mode), and the pressure at the distal end is decreased in steps of 666 Pa (5 mm Hg) till -2000 Pa. Table 5.3 shows the boundary conditions set at different pressure differences.

Table 5.3: Boundary conditions at inflow and outflow surfaces of the flow domain in suction mode

Pressure Difference (mm of Hg)	Inlet Pressure (Pa)	Outlet Pressure (Pa)
5	1333	666
10	1333	0
15	1333	-666
20	1333	-1333
25	1333	-2000

5.5 Simulation methodology

In our study, the blood flow is assumed to be laminar and simulated in steady-state, using a pressure-based Navier-Stokes solver. The SIMPLE algorithm is used with second-order modeling of the pressure and momentum terms. The flow chart, shown in Figure 5.5, explains the simulation procedure adopted for analysis. The output of the flow simulation has been post-processed to visualize the field variables like velocity, pressure, strain rate, and wall shear stress.

As discussed earlier, blood exhibits non-Newtonian characteristics and has many non-Newtonian models to describe its rheology. The commonly used non-Newtonian Models are Carreau [107],[109]-[120], Carreau-Yasuda [108],[109],[112]-[118],[119],[121]-[119], Oldroyd-B [122], Casson [109],[112],[116],[123],[120], Power-law [109],[112]-[114], Cross [109],[112],[124], Powell-Eyring [112], Walburn – Schneck [114], Quemada [116],[125] and many more. The literature on these models reveals that the Carreau model is the most popularly used one, followed by the Carreau-Yasuda model. In this analysis, the simulation results from both models are compared, and the Carreau model is chosen out of the two. It is used to simulate non-Newtonian flow and study its behavior in laparoscopic forceps. The equations defining the fluid viscosity [109] according to the Carreau and Carreau-Yasuda models are described below.

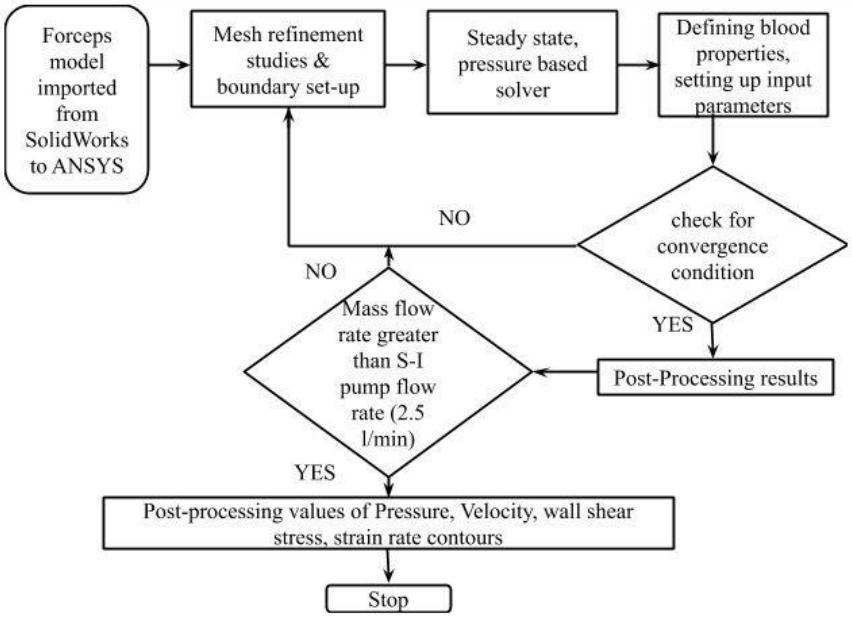

Figure 5.5: Flow chart of the simulation procedure adopted in the present analysis

(a) Carreau model

The flow of blood is defined by its viscosity. The Carreau model defines the dynamic viscosity η, as a function of strain rate γ, zero shear viscosity μ_o, and infinite shear viscosity μ_∞, as given by equation (1).

$$\mu = \mu_\infty + (\mu_o - \mu_\infty)[1 + (\lambda\gamma)^2]^{(n-1)/2} \quad (1)$$

(b) Carreau-Yasuda model

The Carreau-Yasuda model is a more generic non-Newtonian model, as the Carreau model can be derived from it. The Carreau-Yasuda is described by equation (2) below.

$$\mu = \mu + \frac{(\mu_o - \mu_\infty)}{\{1 + (\lambda\gamma)^x\}^{(1-n)/x}} \quad (2)$$

A User-Defined Function (UDF) is created, imported in ANSYS, and executed during simulations. The methodology and simulation procedure applies to both models, as explained in Figure 5.5. The properties studied, their values, and units of different parameters for the Carreau and Carreau-Yasuda models are listed in Table 5.4.

Table 5.4: Model parameters used in Carreau and Carreau-Yasuda models [109].

Properties	**Carreau model**	**Carreau Yasuda model**	**Units**
Blood density, ρ	1060	1060	Kg/m^3
Time constant, λ	3.313	1.902	sec
Power law index n	0.3568	0.22	-
Zero shear viscosity, μ_o	0.056	0.056	kg/m-s
Infinite shear viscosity, μ_∞	0.00345	0.00345	kg/m-s
Constant, x	-	1.25	-

5.6 Validation

5.6.1 Comparison of the non-Newtonian models

Using the procedure described in Section 5.3, simulations are carried out using the Carreau and the Carreau-Yasuda models to calculate the resultant mass flow rate.

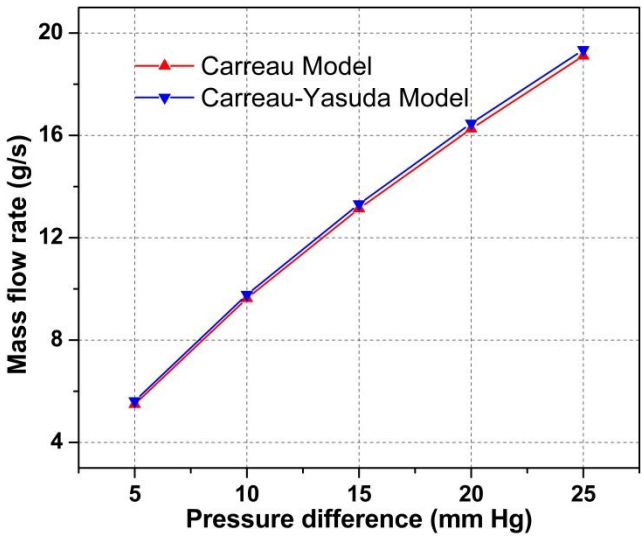

Figure 5.6: Comparison of mass flow rates obtained using Carreau and Carreau-Yasuda models for different pressure drops

Figure 5.6 shows the mass flow rates obtained using the two models for the pipe of the uniform cross-section that are consistently similar for various pressure drops across the device. Therefore, either model can be used for the non-Newtonian simulation of blood flow in the present study. The Carreau model is selected in this case because it is more popularly used in literature.

5.6.2 Model validation with experimental results

In the published work [108],[126], the authors considered a supra-aortic branch of an artery (with a 6.35 mm inner diameter, 1828.8 mm length, and an inlet velocity of 19.45 mm/sec) and validated with experimental results for two-phase non-Newtonian simulations. Studies [107],[109]-[120] reveal that the different authors used the Carreau model numerically and validated it experimentally with the rheological blood flow. Also, Carreau-Yasuda models [108],[109],[112]-[119],[121] are used popularly to analyze the blood flow in small arteries. In their studies, the previous concept of blood as Newtonian fluid is rejected, and different non-Newtonian models are proposed and validated. Figure 5.7 compares the results of the present study with published experimental and numerical results (using the Oldroyd-B model). Therefore, it

shows that the results of the present study closely match both the experimental and theoretical results available in the literature.

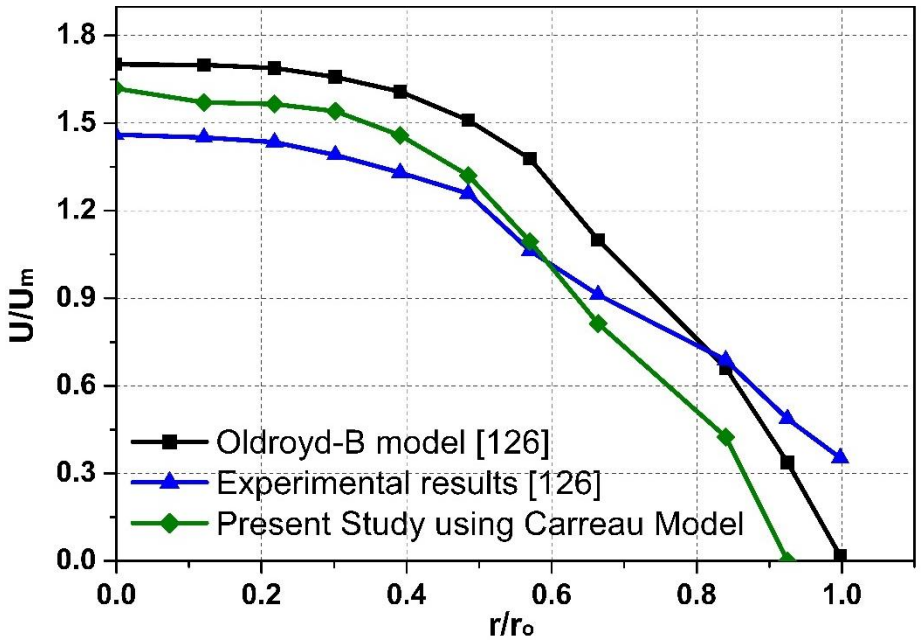

Figure 5.7: Comparison of velocity profiles from the present study with that of the Oldroyd-B model and experimental results [126]

5.7 Comparison of flow through different geometries using different working fluids

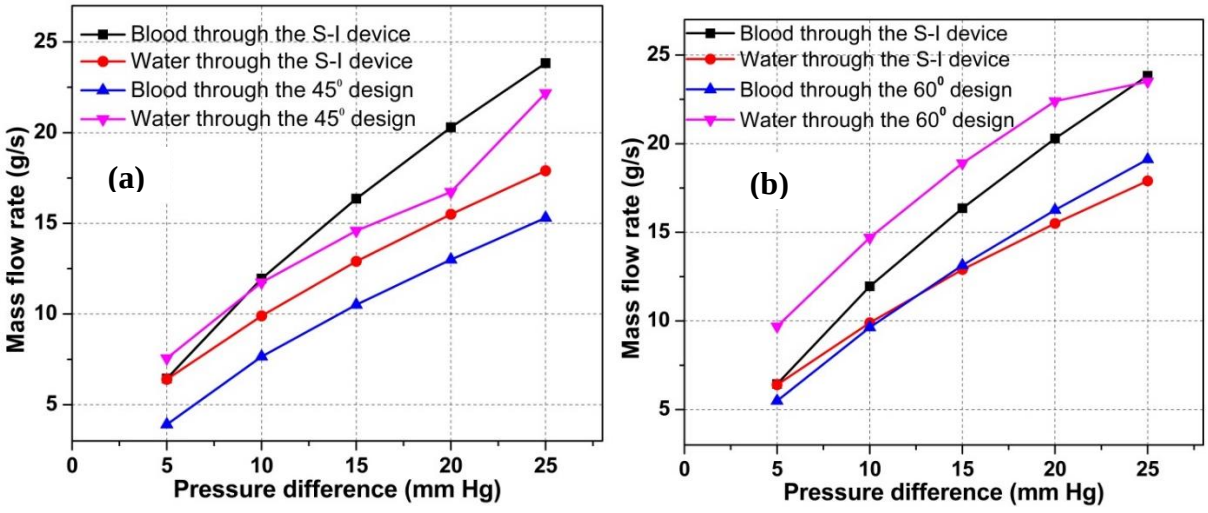

Figure 5.8: Variation of mass flow rate with the applied pressure difference for (a) ϕ=45^o and (b) ϕ=60^o designs

Figure 5.8 shows how the mass flow rate varies with the applied pressure difference in the proposed design of forceps using water and blood as working fluids for $\phi = 45^{\circ}$ and $\phi = 60^{\circ}$ geometries. Results with water as the working fluid [104] are shown here to aid comparison. These flow rates are compared with those of blood through an S-I device. The results show that the flow rates through the $\phi = 45^{\circ}$ design are lower than those through the corresponding $\phi = 60^{\circ}$ design.

For the $\phi = 60^{\circ}$ design, though the flow rate of blood is lower than that through the existing S-I device, the flow rate of water can be seen to be higher than through the existing S-I device. The same conclusion holds only marginally for the $\phi = 45^{\circ}$ design. Therefore, $\phi = 60^{\circ}$ design can better cater to the flow rates of both blood and water provided by the S-I device. The marginal difference between the desired and the actual flow rates delivered by the device by adjusting the suction or irrigation pressure applied by the S-I pump.

Table 5.5: Comparison of mass flow rates (g/s) in suction mode

	Carreau model			Carreau-Yasuda model	Water	
Pressure difference (mm of Hg)	S-I device	$\phi = 45^{o}$	$\phi = 60^{o}$	$\phi = 60^{o}$	$\phi = 45^{o}$	$\phi = 60^{o}$
5	6.44	3.91	5.49	5.62	7.56	9.69
10	11.95	7.65	9.63	9.78	11.74	14.7
15	16.36	10.51	13.14	13.32	14.59	18.9
20	20.29	13.0	16.26	16.47	16.73	22.4
25	23.83	15.3	19.11	19.35	22.18	23.5

5.8 Results and discussion: non-Newtonian flow analysis of the Suction-Irrigation device and surgical forceps

Figure 5.9 to Figure 5.11 show the contour plots of simulation of blood flow through the geometry with $D = 8$ mm and $\phi = 60^{\circ}$, modeled using Carreau model. The contour plots are shown only for pressure differences, ΔP of 5 mm, 15 mm and 25 mm Hg for reference. The contour plots of ΔP of 10 mm and 20 mm Hg follow similar trend and hence are not shown. Each of the contour plots in these figures is shown to use the common legend for ease of comparison.

i) Velocity contours:

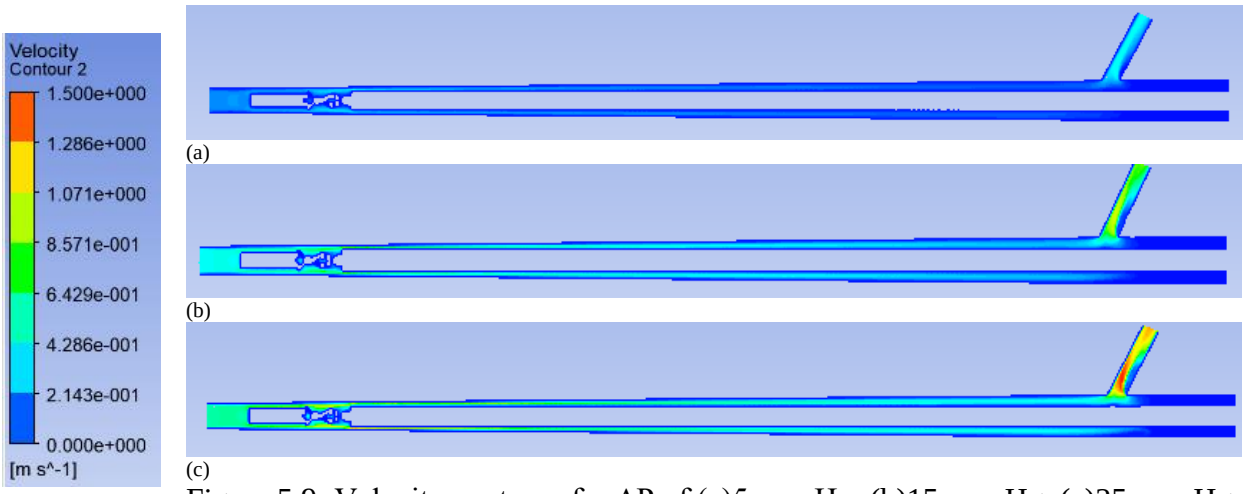

Figure 5.9: Velocity contours for ΔP of (a)5 mm Hg, (b)15 mm Hg, (c)25 mm Hg

The velocity contours for different ΔP are shown in Figure 5.9. The contours show that flow velocity in the device increases with an increase with ΔP as expected. The flow velocity assumes a zero value near the solid walls due to the no-slip condition and reaches a maximum away from the walls. The flow navigates around the jaws before assuming a reasonably developed profile until the protrusion at the outlet, where the velocity reaches its peak. A sharp change in the flow cross-section, particularly from the inlet to the jaws and at the protrusion near the outlet,

results in a local rise in the flow velocity. The fluid also stagnates beyond the location of the protrusion, near the outlet, and has negligible velocity.

ii) Pressure contours:

The pressure contours for different ΔP are shown in Figure 5.10. The contour plots show that the variation in pressure is more uniform compared to that of velocity. It primarily decreases along the flow direction towards the outlet, and a negligible variation is observed across a given section. Since the geometry is complex, particularly around the jaws and at the protrusion, more irregularities in the flow velocity are observed at these locations (Figure 5.9). This results in a larger pressure drop, as observed from the pressure contours. The pressure drop per unit length at any other location in the device is relatively less compared to that near the jaws and the protrusion. Therefore, one way to increase the efficiency of the flow aspect of the device is to design the geometry so that the internal components are more streamlined, particularly at the two mentioned locations.

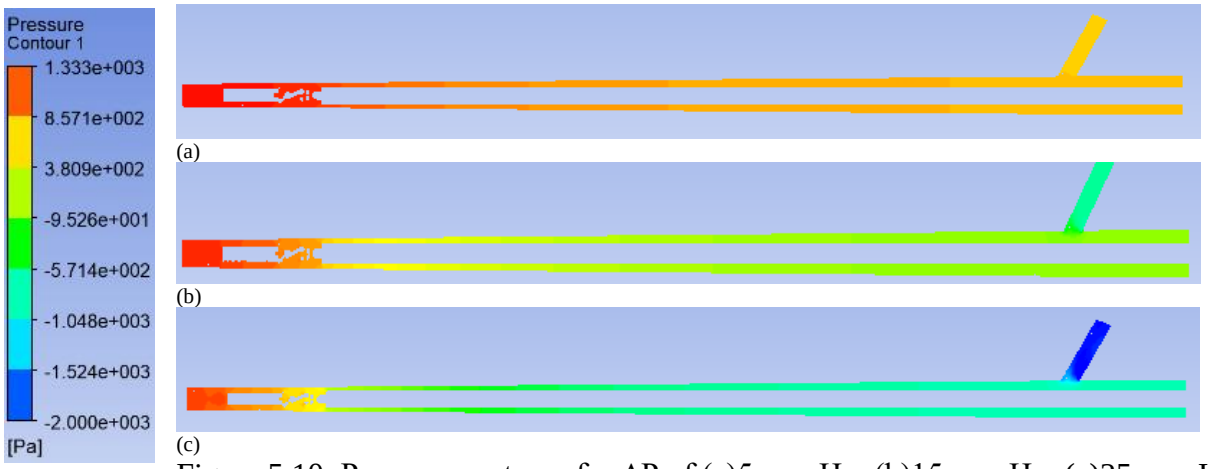

Figure 5.10: Pressure contours for ΔP of (a)5 mm Hg, (b)15 mm Hg, (c)25 mm Hg

iii) Strain rate contours:

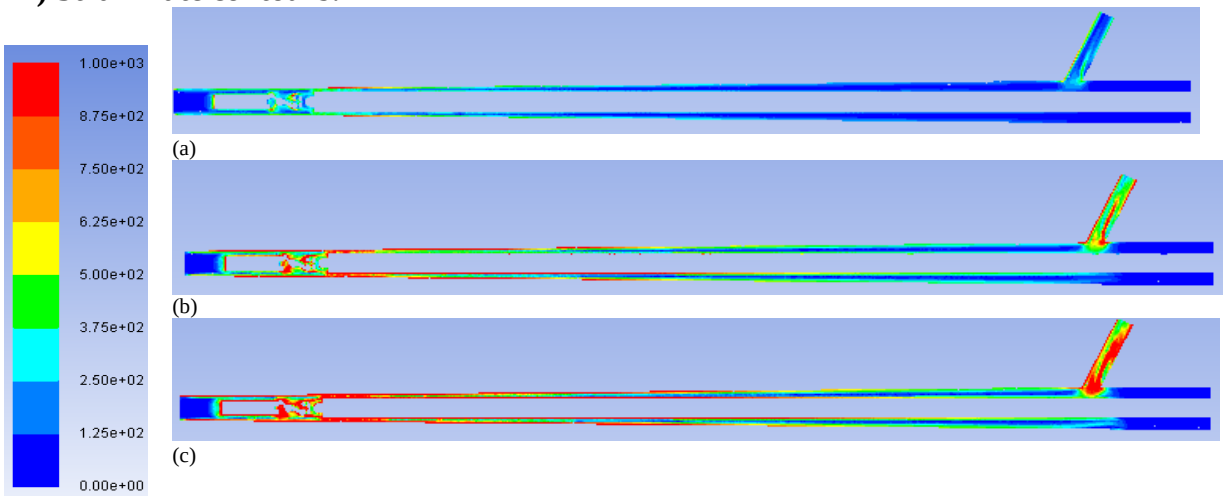

Figure 5.11: Strain rate contours for ΔP of (a)5 mm Hg, (b)15 mm Hg, (c)25 mm Hg

The strain rate contours for different ΔP are shown in Figure 5.11. These contours show that the strain rate in the channel increases with ΔP. The contours also have an opposite behavior as that of the velocity contours. For example, the strain rates are high near the walls and negligible near the center of the channel. This is expected as the flow velocity gradients are largest in the boundary layer, where it is subjected to high shear rates.

The near-wall high strain rates, in fact, aid the flow by reducing the fluid viscosity (from μ_0 to μ_∞Almost by a factor of 10), as governed by the Carreau model. This is because blood is a shear-thinning fluid. This is readily apparent in the variation of mass flow rate with respect to ΔP from Figure 5.8. The difference in the mass flow rate of blood and water through the S-I device, for example, increases with ΔP. This suggests that as ΔP (and hence shear rate) increases, the mass flow rate of a Carreau fluid-like blood also increases, as it offers lesser resistance at higher strain rates. This is, however, not so evident in the plots of flow through the forceps, owing to its complex geometry.

iv) Wall shear stress contours:

Figure 5.12 shows the contours of the wall shear stress plotted on the outer surface of the modified design. Wall shear stress denotes the degree of shearing action that the fluid layer near the wall undergoes.

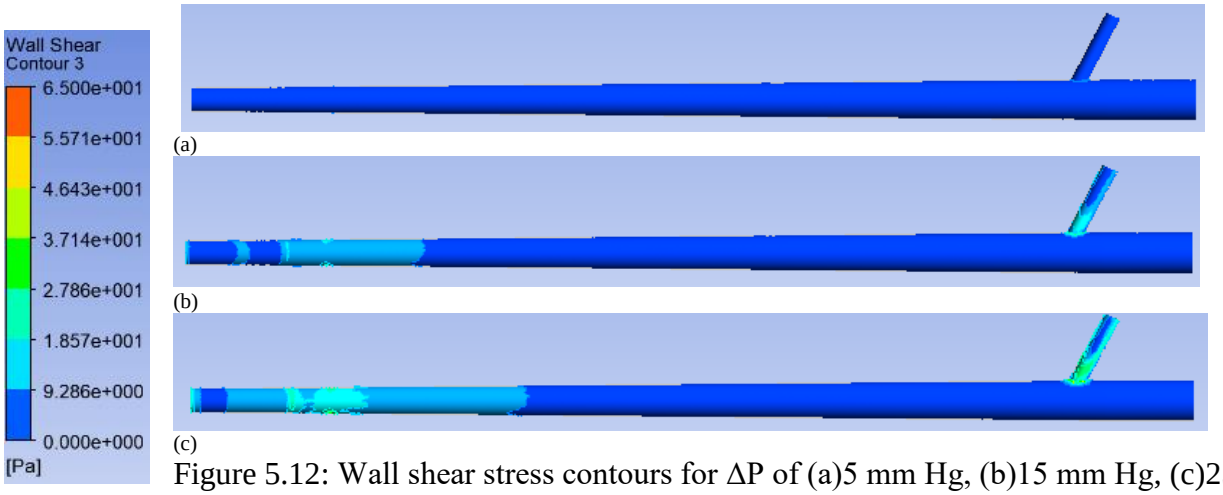

Figure 5.12: Wall shear stress contours for ΔP of (a)5 mm Hg, (b)15 mm Hg, (c)25 mm

As suggested by Figure 5.9 and Figure 5.11, the fluid near the jaws and protrusion flows over intricate parts of the device and is subjected to large gradients. This is reflected in the contours of wall shear stress, which locally assumes large magnitudes near the jaws and the protrusion. As expected, the peak wall shear stress near these two locations also increases with ΔP.

Figure 5.13 shows the contours of molecular viscosity inside the domain for different ΔP. For ΔP =25 mm Hg, as observed from Figure 5.11(c), the strain rates assume very high values of more than 800 s^{-1} in the middle of the domain. For these strain rates, the fluid viscosity computed using the Carreau model is close to $\mu_\infty = 0.00345$. Similarly, the strain rates near the jaws and protrusion are supposed to be high as the fluid squeezes past them. This results in a much smaller fluid viscosity of close to η_∞. In contrast, at the extreme right end of the device, where the flow is almost stagnant, the strain rates are expected to be negligible. Therefore, we

observe that the molecular viscosity at this end is close to $\mu_0 = 0.056$. For ΔP =25 mm Hg, the strain rates can be expected to be about five times higher than those for ΔP =5 mm Hg. This results in a value of molecular viscosity slightly less than μ_∞ as observed in Figure 5.13(c).

v) Molecular viscosity contours:

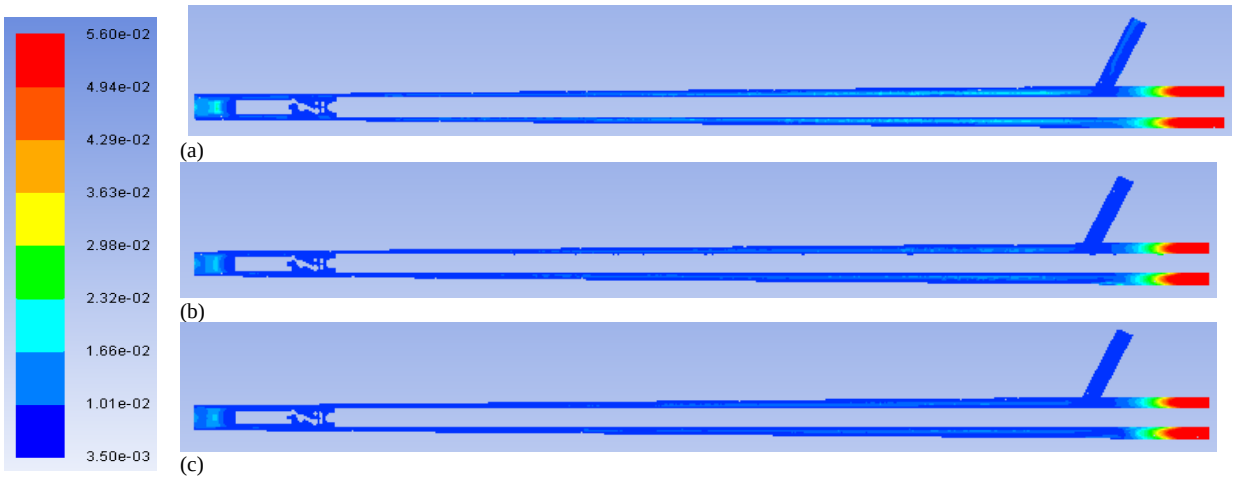

Figure 5.13: Molecular viscosity contours for ΔP of (a) 5 mm Hg, (b) 15 mm Hg, (c) 25 mm Hg

Conclusions from the above simulations can be summarized as follows:

- The Carreau model is chosen for the non-Newtonian simulation of blood flow.
- The 8 mm, 60° model is chosen as the preferred geometry, as it caters to the required flow rates of blood and water, similar to the Suction-Irrigation device.
- Based on this analysis, the fabrication is proposed for D= 8mm and $\phi = 60^\circ$ design model.

Chapter - 6

6 Flow Analysis of CO_2 insufflation in a Multi-functional Laparoscopic Forceps

6.1 Introduction

All the patients undergoing any kind of laparoscopic surgery have to undergo insufflation of gas into a peritoneal cavity to provide access to surgery by visualizing in the monitor. Insufflation of gas is termed as pneumoperitoneum, and carbon dioxide (CO_2) gas is most commonly used to insufflate the peritoneal cavity. The reasons for using CO_2 gas are that it is freely available, chemically stable, highly soluble, eliminates rapidly from the body, is a product of human metabolism, provides proper illumination, and is non-toxic. The surgeons must be aware of the challenges caused by CO_2 gas insufflation to maintain the desired flow rate and effective intra-abdominal pressure (IAP) to treat laparoscopic patients. From an exhaustive literature survey, it is found that CO_2 gas is insufflated at a flow rate of 2-6 lit/min to a standard intra-abdominal pressure of 10 mm Hg [127]-[138] in the peritoneal cavity. The IAP is maintained constant as any further increase may result in surgical complications, especially in patients suffering from heart disease, old age, and blood pressure problems [135]. However, the flow rate is varied from children to geriatric age patients, depending upon their age, due to variations in cardiovascular and respiratory systems.

6.2 Laparoscopic procedures and their devices

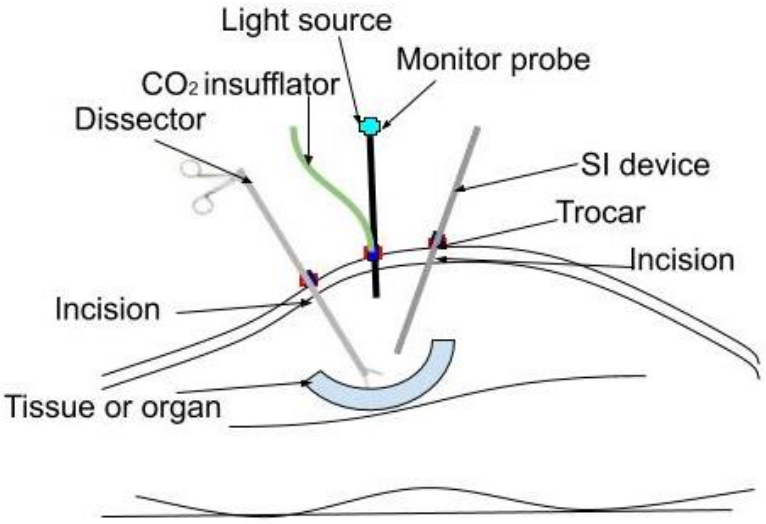

Figure 6.1: Overview of the laparoscopic procedure

Laparoscopic surgery involves multiple incisions around the belly button of a patient to introduce trocars of 5-12 mm sizes, as shown in Figure 6.1. Pneumoperitoneum is initiated by CO_2 gas insufflation through a veress needle. Then IAP is maintained at 10 mm Hg with desired flow rates. There are different instruments used for manipulating, dissecting, irrigating saline water to clean and sucking the blood and charred particle. Often, the affected tissue or organs of the human body is dissected and sealed off. But during dissection or cutting, blood oozes out, disrupting the view of surgeons. The surgeon is required to clean the operated area immediately to clear the field of view by using an irrigator. As the fluid comprising both blood and saline water gets accumulated inside the abdominal cavity, a suction device is used to suck the fluid and remove it. If the blood still oozes out, then the suction process is stopped, and the irrigation process continues again. Table 6.1 shows the most commonly used devices in laparoscopic surgical procedures.

Table 6.1: Devices commonly used in minimally invasive procedures

Laparoscopic device	**Function/ Purpose**	**Description**
1. Laparoscopes	To view organs inside the abdomen through a monitor.	It has a 5-10 mm diameter with a working length of 330 mm, having a high-resolution camera used for viewing organs in the abdominal cavity.
2. Trocar	To puncture and provide intra-abdominal access.	It has a 5-15 mm diameter and about 180 mm length used to rupture and make a hole to gain access to the peritoneal cavity. It is a cannula and allows multiple instruments to operate through it.
3. Forceps	Grasp and dissect tissue	It has a 5-10 mm diameter up to a length of 330 mm used for grasping and dissecting the tissue.
4. Suction-Irrigation device	Suck or irrigate the fluid	It has a 5-10 mm diameter and 330 mm length used as multipurpose equipment to either suck fluid inside the abdomen to clear the field of vision or to irrigate using saline water to clean the blood inside the abdomen.
5. Graspers/ Retractors	Hold the tissue	It consists of a traumatic (secure or firm holding) and atraumatic grasper (gentle holding) of 5 mm diameter up to a 300 mm length for holding and manipulating the tissue inside the abdominal cavity.

6. Ligature	Ligation	It has a 10mm tube diameter with a 30 mm length as its distal end for performing the surgical procedure of tying knots to bind tissues.
7. Probe	Examine the tissue	It is 3-5 mm in diameter, 330 mm in length used for separating detached tissue or organ. The blunt end of the probe is used to explore the operating field.
8. Dissecting scissors	Cutting tissue	It has a 5 mm diameter up to a working length of 450 mm that is used to dissect, coagulate the tissue with electrocautery procedure.

6.3 The proposed design and flow analysis using CO_2

The laparoscopic surgical tools, as listed in Table 6.1, are used for minimally invasive surgeries. In previous chapters, the diameter of the fluid domain, $D = 8mm$ design was chosen over $D = 10mm$ since it requires smaller incisions and standard trocar sizes. Further, $D = 8mm$ design, $\phi = 60^{\circ}$ geometry was chosen for the final proposed design using water as the working fluid. The same design is extended to serve as a multipurpose instrument to cut, cauterize, and grasp the tissue and act as a conduit for the CO_2 gas insufflation in the present work.

As shown in Figure 6.2, CO_2 gas can be insufflated into the peritoneal cavity through the annular region marked 'C.' Point 'A' acts as an entry of CO_2 gas, point 'C' is the CO_2 gas channel, and point 'B' acts as an outlet from where CO_2 gas is insufflated inside the patient's peritoneal cavity. Figure 6.3 shows the complete laparoscopic forceps. It adds safety by avoiding multiple

insertions and removing different instruments, and reducing the time during surgery. This instrument can be easily sterilized and has a provision of assembly and disassembly; hence can be used multiple times.

Figure 6.2: CO_2 gas insufflator unit from the proposed forceps

Figure 6.3: Proposed laparoscopic forceps

6.4 Scope of the present work

As mentioned in chapter 4, the proposed modified forceps design was carefully chosen out of different possible designs based on the flow analysis using water as the medium. This was done to mimic the blood flow during surgery; in the suction process, typically, the blood that oozes out of the tissue could also mix with the cleaning fluid.

In the current article, flow analysis is carried out for the CO_2 gas in the proposed forceps with $D = 8mm$ and $\phi = 60^{\circ}$. This is done to understand and quantify the flow behavior of the insufflation gas in the device. The results are plotted for pressure and velocity at varying mass flow rates across the device.

6.5 Geometry and mesh generation

The proposed CO_2 gas insufflator unit is 8 mm in diameter with a 5mm channel, with a length of 330 mm. The mesh independence studies were conducted for an extreme mass flow rate of 6 lit/min across the device. The velocity is selected as the defining parameter in the mesh independence studies for three meshes (M1, M2, and M3) and found to be consistently independent of elements and nodes. The deviation in velocity, measured with respect to that in the fine mesh M3, is less than 2%. So, an intermediate mesh M2 with 327,261 nodes and 880,257 elements is used for all simulations.

6.6 Boundary conditions used and proposed design parameters

The CO_2 gas through the fluid domain is simulated using a steady-state, pressure-based solver. As shown in Figure 6.2, while insufflating the abdomen in laparoscopic surgeries, the distal end (marked as B) acts as an outlet, the flow channel (marked as C) acts as the CO_2 gas passage area, the proximal end (marked as A) as an inlet. It means that the CO_2 gas is passed inside the peritoneal cavity from the proximal end of the forceps, comes into the flow channel, and leaves from the distal end. The distal end is fixed at a pressure of 1333 Pa, and the mass flow rate at the proximal end is varied from 2 lit/min to 6 lit/min. The density of CO_2 gas is taken as 1.7878 kg/m^3.

Table 6.2: Boundary conditions set at different mass flow rates.

S.No.	Volume flow rate (lit/min)	Mass flow rate (kg/s)
1	6	1.79e-4
2	5	1.49e-4
3	4	1.199e-4
4	3	0.894e-4
5	2	0.595e-4

6.7 Simulation methodology

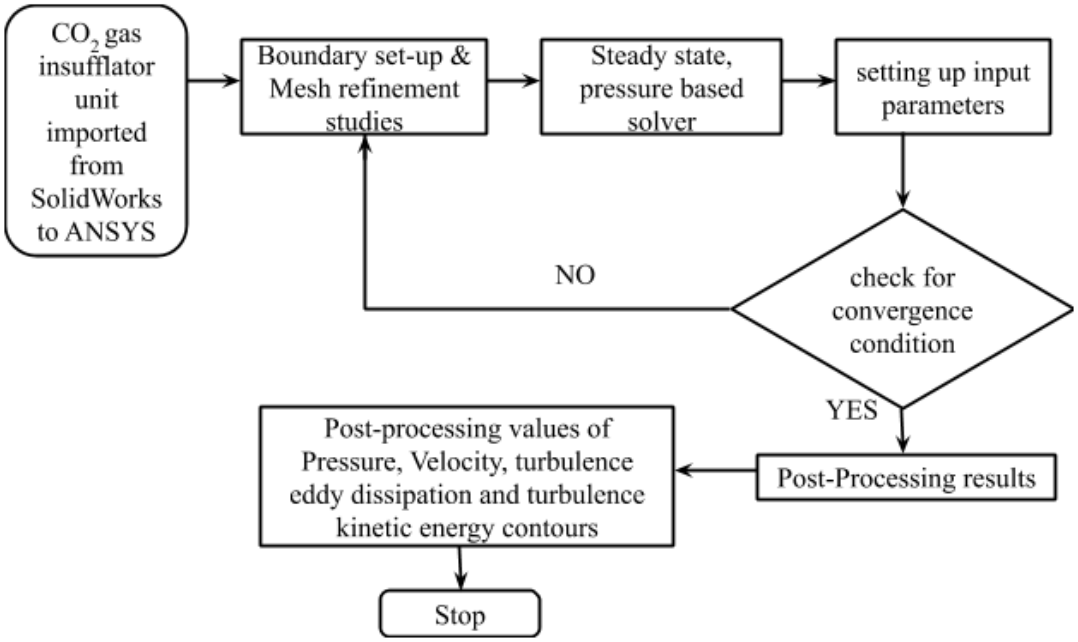

Figure 6.4: Flow chart of the simulation procedure adopted in the present analysis

In the present study, the ANSYS Fluent is used for flow analysis using a steady-state pressure-based Navier-Stokes solver. To simulate the gas flow, a standard $\kappa - \varepsilon$ turbulence model with an enhanced wall treatment method is used. Figure 6.4 shows the flow chart followed to run simulations by setting the input parameter, as shown in Table 6.2.

6.8 Result and Discussion

(a) Contours of pressure:

The contours shown in Figure 6.5 to Figure 6.7 are each for different mass flow rates with a constant IAP at the outlet. Figure 6.5(a-e) shows that the pressure continuously drops along the length of the flow channel due to a decrease in the volume flow rate from 6 lit/min to 2 lit/min insteps of 1 lit/min each. Due to the protrusion bend near the inlet, the gas flow takes a sharp turn, whereas, at the exit, the gas has to navigate the complex geometry around the jaw mechanism, resulting in pressure drops.

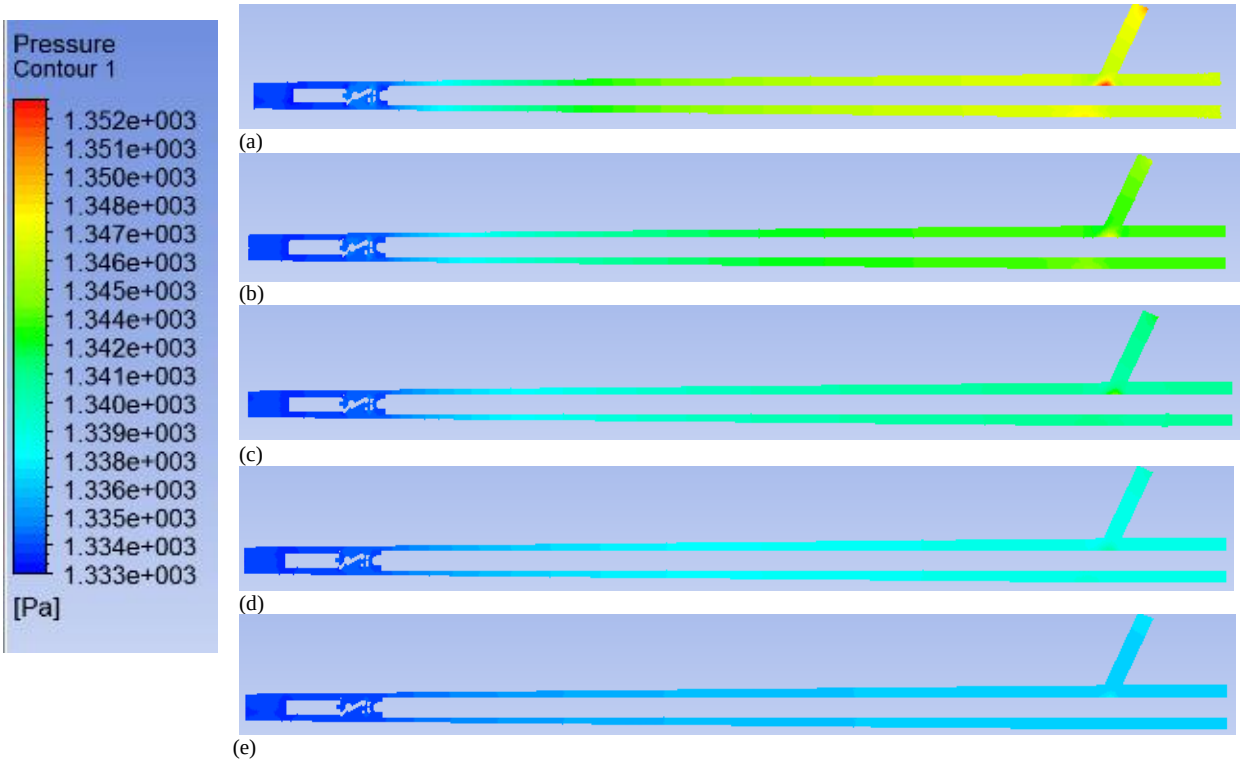

Figure 6.5: Pressure contours

(b) Contours of velocity:

The velocity contours are shown in Figure 6.6 for different mass flow rates. For all the cases, the flow velocity attains peak values at the protruding ends. However, the velocity of flow is almost similar in the annular region all along the length of the instrument. In addition, the magnitude of flow velocity in the fluid domain increases with an increase in the mass flow rate as observed from Figure 6.6(e) to Figure 6.6(a), respectively. A similar trend was observed for pressure drop between the inlet and outlet in Figure 6.5.

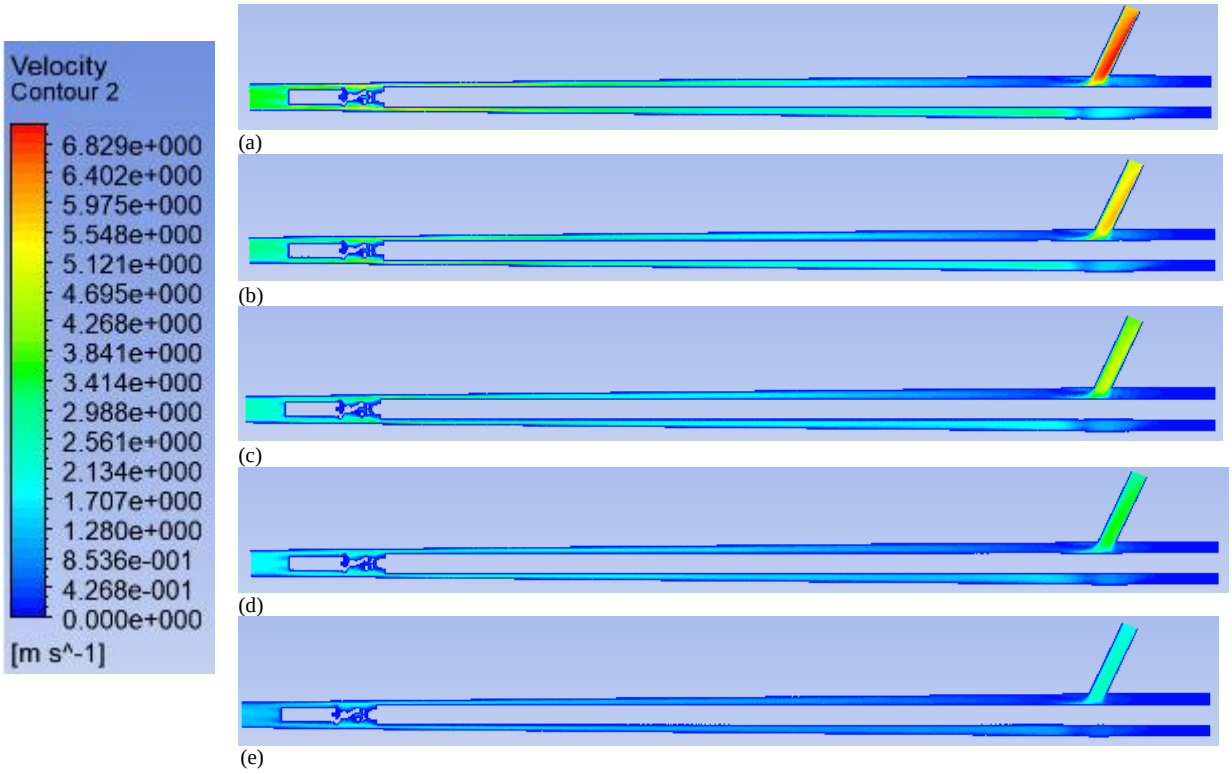

Figure 6.6: Velocity contours

(c) Contours of turbulence dissipation rate (ϵ):

Figure 6.7 shows turbulence eddy dissipation rate (ϵ) contours in the flow domain. ϵ assumes high magnitudes for all mass flow rates near the protrusion and around the jaws. This signifies large magnitudes of turbulence in the flow as the fluid navigates complex geometries in these regions of the instrument. A similar variation is observed for turbulence kinetic energy from the contours shown in Figure 6.9.

Figure 6.8 shows the increase in the applied pressure difference with respect to mass flow rate. It is evident as the mass flow rate increases in the device, there will be an increase in pressure and velocity as well. Table 3 shows the values corresponding to the marker points in Figure 6.8. The pressure difference across the device for the desired range of mass flow rates is well within the limits of the CO_2 insufflation pump. Therefore, the proposed instrument can

also cater to the required mass flow rate of CO_2 for an appropriate pressure difference that can be applied by the insufflation pump.

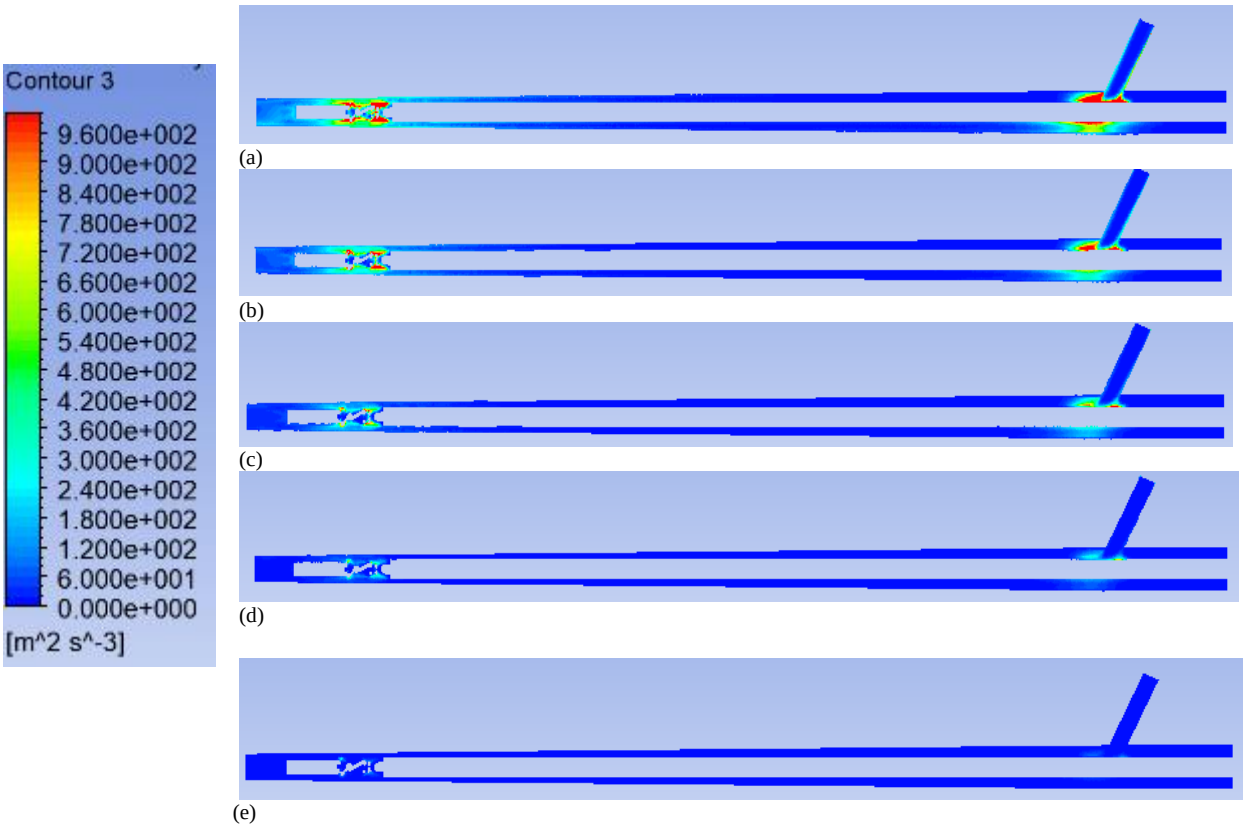

Figure 6.7: Turbulence eddy dissipation contours

Table 6.3: Mass flow rate variation across the device with respect to the applied pressure difference.

S.No	mass (L/min)	mass (g/s)	Pressure Variation (Pa)	Vmax (m/s)
1	6	0.179	97	7.11
2	5	0.149	71	5.98
3	4	0.1199	51	4.896
4	3	0.0894	34	3.74
5	2	0.0595	20	2.57

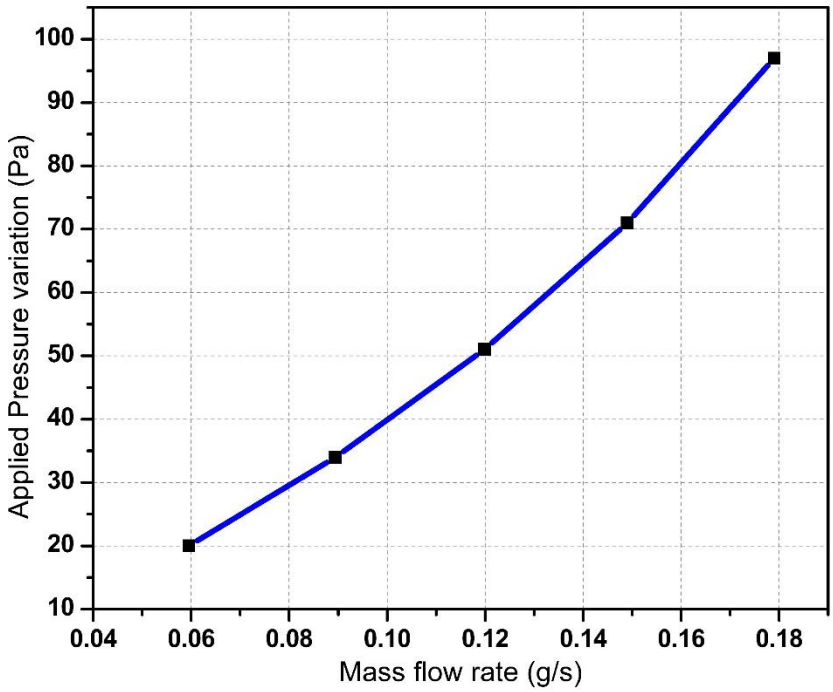

Figure 6.8: Variation of the mass flow rate of CO_2 with respect to the applied pressure difference

(d) Contours of turbulence kinetic energy (κ):

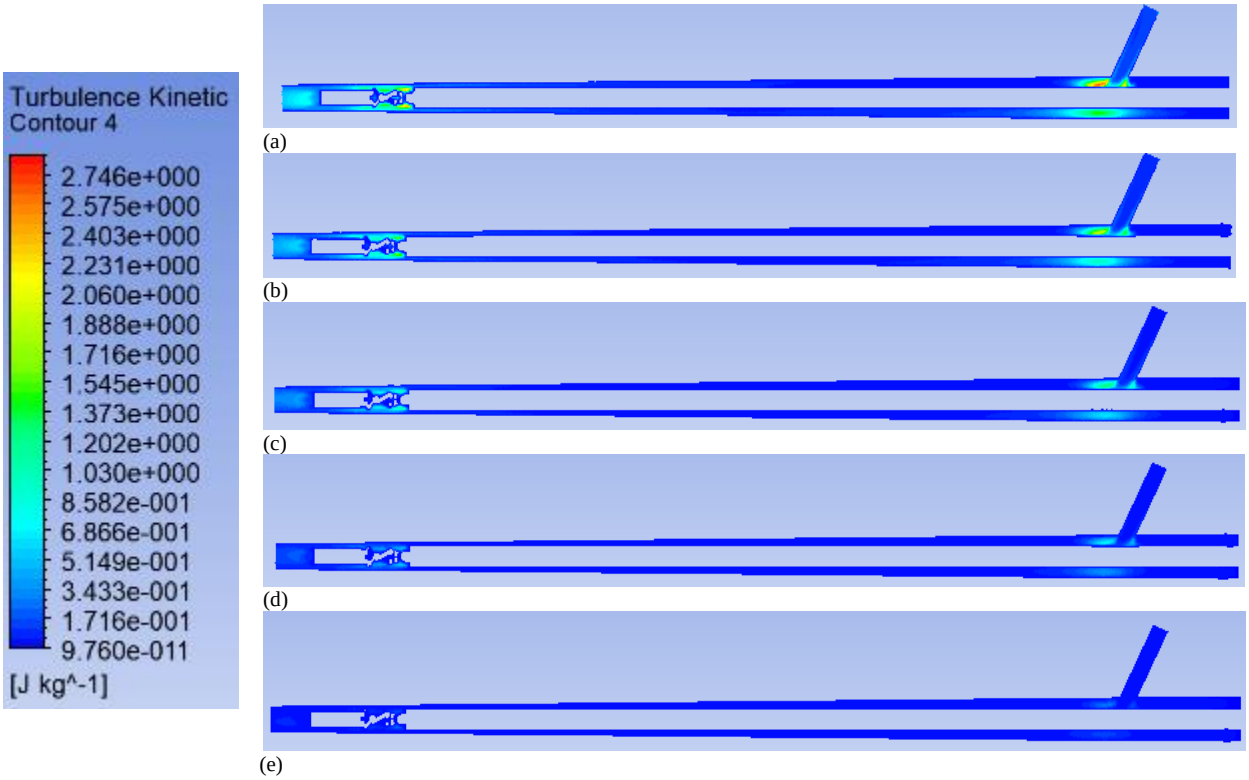

Figure 6.9: Turbulence kinetic energy contours

6.9 Advantages of the proposed design

In addition to all the existing features of the CO_2 insufflator device, the functionalities of the standard SI device and the dissector forceps are incorporated in the proposed design, thereby combining the functionality of all three individual devices into one. It helps avoid the insertion and removal of multiple devices, thereby reducing the possibility of leakage of CO_2 from the surgical area and saving time. Reduction in the use of multiple instruments can enhance the productivity of surgical procedures. Further, this device can reduce the risk of major injury due to loss of blood, discomfort, and pain to the patient. This device gives flexibility to the surgeon to use all the three features in whichever sequence is desired by the surgeon for better control of the surgical procedure. The new design is reusable as it can be completely dissembled and easily reassembled after sterilization.

Though this forceps is different from the commercially available devices, it can only be used if a dissection operation is also performed, as it is not a stand-alone CO_2 insufflator device. The present research work focuses only on numerical analysis. However, actual clinical trials are required to confirm the above-stated features of the device. In this analysis, optimization of the device is not performed. The design of this device can be further optimized from the fluid flow and CO_2 flow aspects in a more integrated sense.

Chapter - 7

7 Multi-phase simulations in a Multi-functional Forceps

7.1 Introduction

Liquid gas interaction is a common phenomenon in many engineering fields like nuclear, chemical, petroleum, and pharmaceutical industries. Multi-phase simulations can help achieve a more accurate and comprehensive analysis of the problem and is close to the actual physical characteristics. Different phases, such as all three-phase flows, gas-liquid, liquid-solid, and gas-solid, come under four main multi-phase flow categories. These classifications can usually be done as per the flow regimes as dispersed, mixed, or separated flow. In dispersed flow, one phase is widely spread in another continuous phase, whereas, in the separated flow, the flow has a distinct boundary between all phases. The best example of a separated flow is stratified flow. Our case is considered as a separated flow where water is flowing on the bottom of the annular flow in a pipe with a liquid film along the pipe and a gas core at the top section of a fluid domain. CFD models can predict the combination of water and air mixtures, allowing to evaluate and predict flow characteristics at any point of the simulation domain. This powerful tool is applied for several types of flows by different approaches. However, for a multi-phase flow problem, there are two approaches, namely Euler-Euler and Euler-Lagrange approaches. The Euler-Lagrange approach is computationally expensive and increases the computational time for even a low volume fraction of the dispersed phase. On the other hand, the Euler-Euler model is suitable for separated flows. This Euler-Euler model can be used for dispersed flow if the volume fraction is high and the flow is dense. The sum of volume fraction is unity.

7.2 Geometry and mesh generation

The designed laparoscopic forceps have 8 mm to 13 mm varying diameter with a 5mm channel, with a length of 330 mm. The mesh independence studies were conducted for an extreme mass pressure drop of 25mm Hg across the device. The velocity is selected as the defining parameter in the mesh independence studies for three meshes (M1, M2, and M3) and found to be consistently independent of elements and nodes. The deviation in velocity, measured to that in the fine mesh M3, is less than 2%. So, an intermediate mesh M2 with 115,224 nodes and 277,140 elements is used for all simulations.

7.3 Flow configuration

The laparoscopic surgical tools, as listed in Table 6.1, are used for minimally invasive surgeries. In Chapter 4, the diameter of fluid domain, $D = 8mm$ design was chosen over $D = 10mm$ since it requires smaller incisions and standard trocar sizes. Further, $D = 8mm$ design, $\phi = 60^{\circ}$ geometry was chosen for the final proposed design as it caters to the required flow conditions when used in place of the SI device. The same design is extended to serve as a multipurpose instrument and act as a conduit for multi-phase analysis in this chapter.

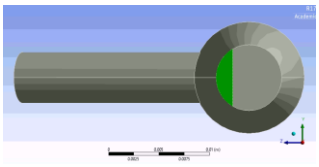

Figure 7.1: Fluid domain from the proposed forceps. Figure 7.2: Forceps view showing two divided regions on the inlet of the fluid domain

. Figure 7.2 shows the left side view of the fluid domain that is divided into two partitions. Partition highlighted (in green) signifies the provision of CO_2 gas escapes from the peritoneal cavity through the annular region. As shown in Figure 7.1, Point 'B' acts as an entry of a mixture

of CO_2 gas and water, point 'C' is the combination of CO_2 gas channel and water channel, and point 'A' acts as an outlet from where CO_2 gas and water exits from the patient's peritoneal cavity.

7.4 Simulation methodology

In the current chapter, multi-phase flow analysis is carried out for the CO_2 gas and water in the proposed forceps for $D = 8mm$ and $\phi = 60^{\circ}$. The results are plotted for different pressure drops across the device.

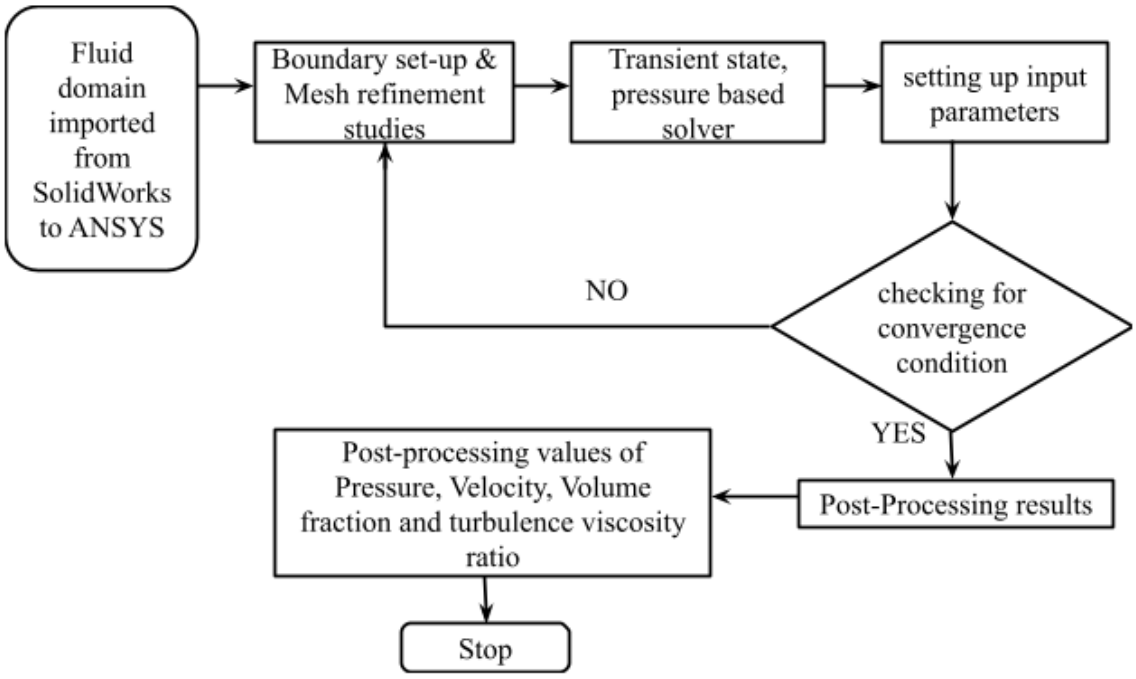

Figure 7.3: Flow chart of the simulation procedure adopted in the present analysis

In the present study, ANSYS Fluent is used for a flow analysis of two-phase fluid flow. The two-phase simulation involves three steps: defining a number of phases and possible flow regimes. The second step is forming governing equations obtained from conservation laws of physics. The last step is solving these equations that describe the mass, momentum, and energy conservation principles. ANSYS uses all these steps in CFD simulations. To simulate a two-phase

fluid flow, a VOF model is opted to predict the interface region between two immiscible phases. Also, by using this model, tracing the void fraction of individual phases is possible by using only a single set of equations. In the VOF method, the sum of volume fraction of air and water is considered to be unity and evaluated by solving continuity and momentum equations. Figure 7.3 shows the flow chart followed to run simulations by setting the input parameter, as shown in Table 7.1.

7.5 Boundary conditions and simulation parameters

Table 7.1: Boundary conditions used for the device operating in suction mode.

S.No.	Pressure drop (Pa)	Intra-abdominal pressure (Pa)	Outlet pressure for both fluids Pressure (Pa)
1	666	1333	666
2	1333	1333	0
3	2000	1333	-666
4	2666	1333	-1333
5	3333	1333	-2000

The two-phase fluid model is simulated using an implicit transient-state, pressure-based solver. VOF model was considered with two Eulerian phases. Water is taken as the primary phase, and CO_2 gas is taken as the secondary phase. The pressure inlet of 1333 Pa is maintained constant for both phases as it is the standard pressure to be maintained in the patient's abdomen during the surgery. The pressure at the outlet was varied by 5 mm Hg (666 Pa) from 666 Pa to -2000 Pa. Negative pressure sign indicates suction pressure. In this type of boundary condition, both pressure and volume fraction need to be quantified. The distal end (marked as B) surface, which acts as an inlet, is split into 20 percent area to allow the entry of CO_2 gas passage area and 80 percent area to allow the water passage. This means that CO_2 gas enters the upper part of the fluid domain, and

water enters the lower part. The SIMPLE scheme solution method is used for pressure velocity coupling, and a second-order upwind scheme is used to determine fluid flow characteristics.

Table 7.2: Number of time steps used

S.No.	Pressure Drop	Number of time steps	Time step size	Max iteration/time steps	Sampled time (sec)
1	666	2500	0.002	350	5
2	1333	2500	0.001	350	2.5
3	2000	3340	0.0005	250	1.67
4	2666	4167	0.0003	250	1.25
5	3333	3334	0.0003	250	1

7.6 Result and discussion

a) Contours of pressure:

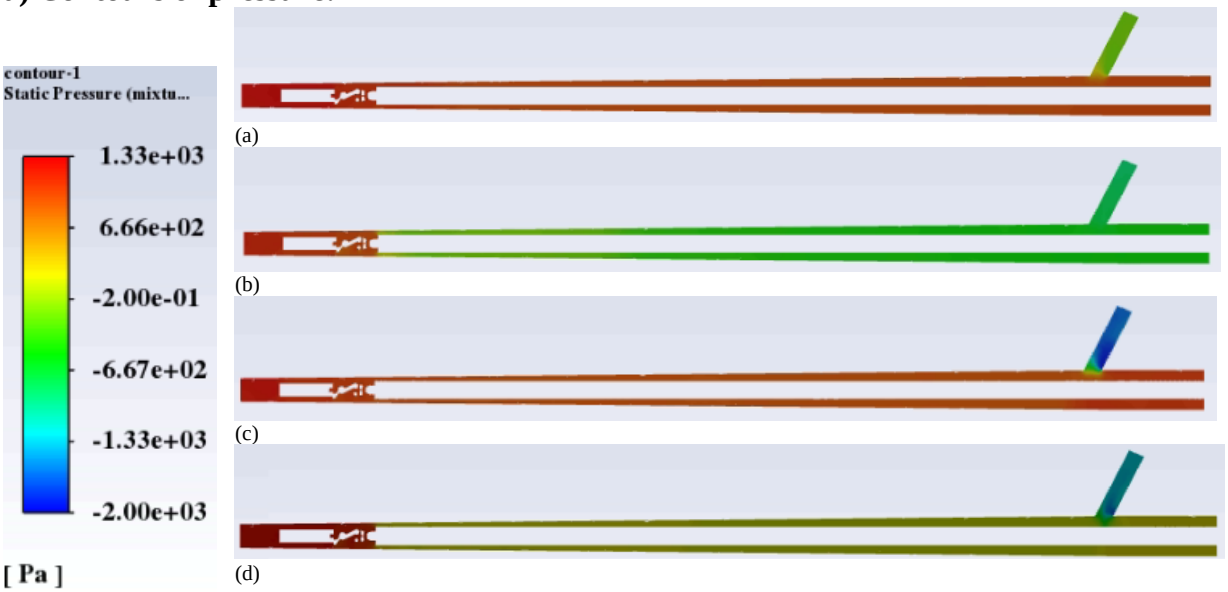

Figure 7.4: Pressure contours

The two-phase fluid model is simulated using an implicit transient-state, pressure-based solver. VOF model was considered with two Eulerian phases. Water is taken as the primary phase, and CO_2 gas is taken as the secondary phase. The pressure inlet of 1333 Pa is maintained constant for both phases as it is the standard pressure to be maintained in the patient's abdomen during the

surgery. The pressure at the outlet was varied by 5 mm Hg (666 Pa) from 666 Pa to -2000 Pa. Negative pressure sign indicates suction pressure. In this type of boundary condition, both pressure and volume fraction need to be quantified. The distal end (marked as B) surface, which acts as an inlet, is split into 20 percent area to allow the entry of CO_2 gas passage area and 80 percent area to allow the water passage. This means that CO_2 gas enters the upper part of the fluid domain, and water enters the lower part. The SIMPLE scheme solution method is used for pressure velocity coupling, and a second-order upwind scheme is used to determine fluid flow characteristics.

Table 7.2 shows the number of time steps for which the simulation data is sampled to obtain the averaged flow variables like pressure, velocity, volume fraction, and turbulent viscosity ratio for each of the cases. Since the problem considered is transient, visualizing the contours of the averaged flow variables gives good insight into the overall flow features. The contours of these flow variables are shown in Figure 7.4 to Figure 7.7 for different pressure drops from inlet to outlet with a constant IAP at the inlet (as shown in Table 7.1).

Figure 7.4(a-d) shows that the pressure continuously drops along the length of the flow channel. Due to the protrusion bend near the exit, the mixture takes a sharp turn, whereas, at the inlet, the mixture has to navigate the complex geometry around the jaw mechanism resulting in higher pressure drops near these two regions. The pressure drop in the straight (middle) section is much less in comparison.

(b) Contours of velocity:

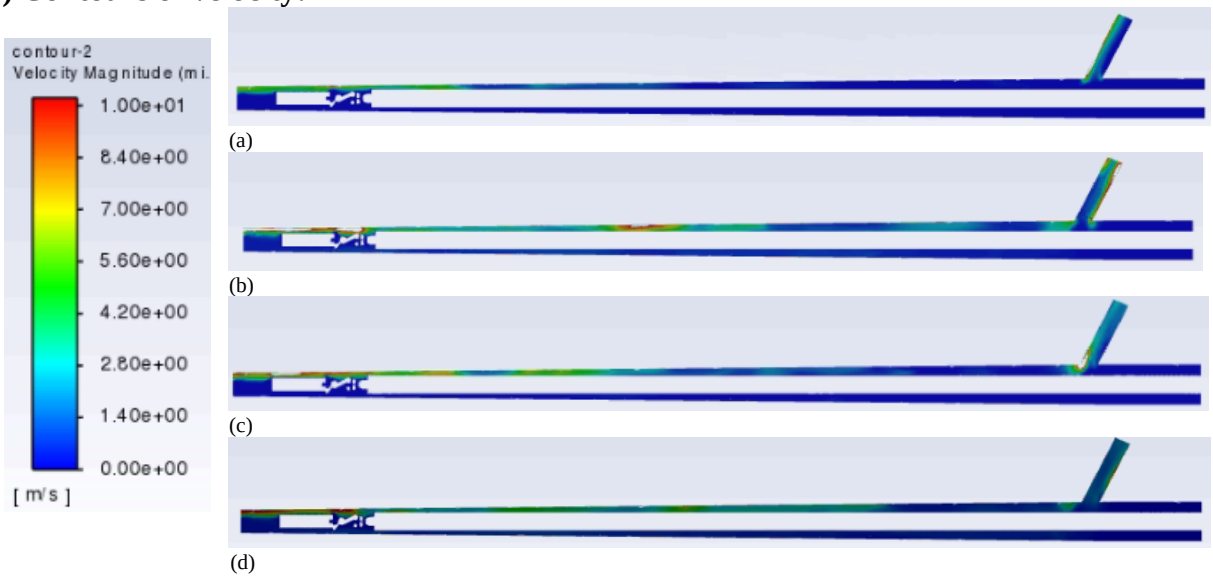

Figure 7.5: Velocity contours

The velocity contours are shown in Figure 7.5 for different pressure variation across the device. For all the cases, the flow velocity attains peak values at the protruding ends and near the jaws. However, the flow velocity is almost similar in the annular region all along the length of the instrument. In addition, the magnitude of flow velocity in the fluid domain increases with an increase in the applied pressure difference, as observed from Figure 7.5(d) to Figure 7.5(a), respectively.

Figure 7.6 shows the volume fraction of CO_2, clearly showing both phases. The CO_2 phase is indicated by the red region where as the blue region indicates the presence of water. In all the cases, CO_2 primarily occupies the upper region of the flow domain as it enters from the upper portion of the inlet. As the flow progresses, the gas also occupies some of the lower regions of the device, particularly towards the outlet. Owing to the large difference in densities of CO_2 and water, their velocities are also significantly different. This manifests as regions of high velocity (occupied by CO_2 gas bubbles) in parts of the flow domain, as observed in Figure 7.5.

(c) Contours of volume fraction of CO_2:

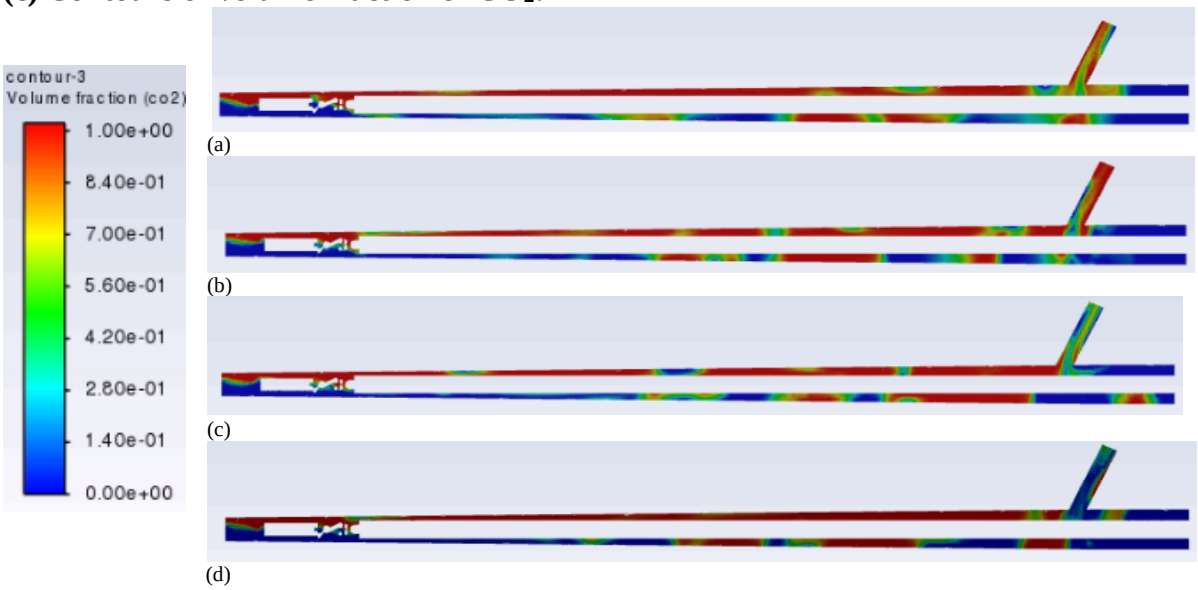

Figure 7.6: Volume fraction of CO_2 contours

(c) Contours of turbulence viscosity ratio:

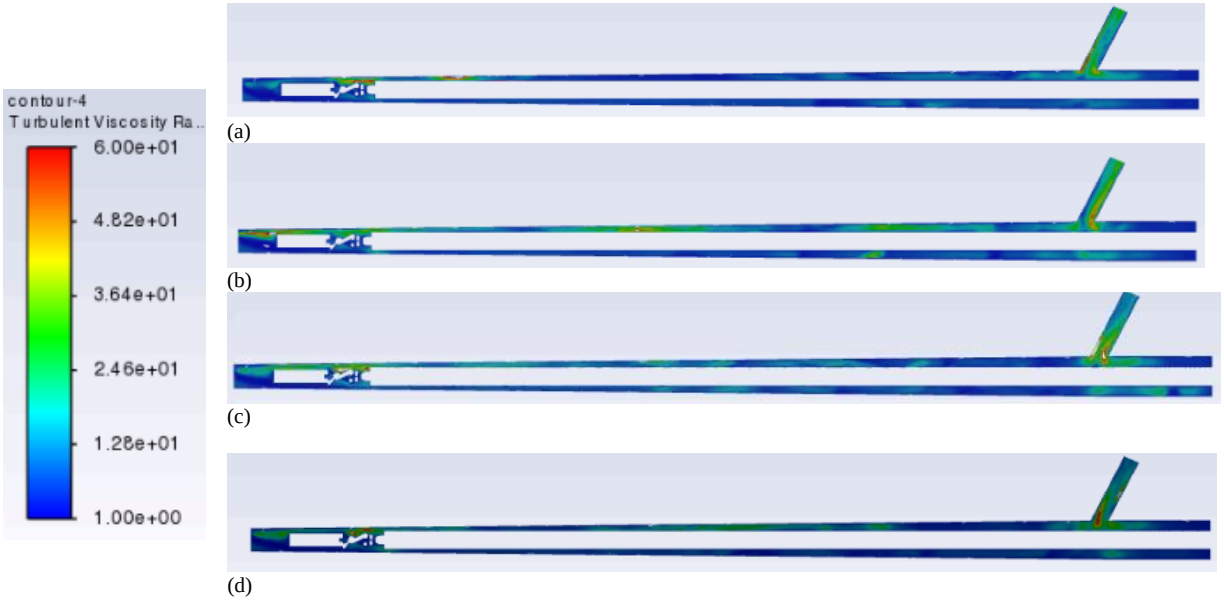

Figure 7.7: Turbulence viscosity ratio contours

Figure 7.7 shows turbulence viscosity ratio contours in the flow domain. It assumes high magnitudes for all cases near the protrusion and around the jaws. This signifies large magnitudes

of turbulence in the flow as the fluid navigates complex geometries in these relatively narrow cross-sections of the instrument.

Figure 7.8 to Figure 7.15 illustrate the average variation of different flow variables for the two phases for different pressure drops. The area-weighted average is calculated by dividing the summation of the product of the selected field variable and facet area by the total area of the surface as below in equation 3 [139].

$$\frac{1}{A}\int \phi \, dA = \frac{1}{A}\sum_{i=1}^{n} \phi_i |A_i| \qquad \text{- (3)}$$

The mass-weighted average of a quantity is computed as in equation 4 below

$$\frac{\int \emptyset\rho|\vec{v}\cdot\overrightarrow{dA}|}{\int \rho|\vec{v}\cdot\overrightarrow{dA}|} = \frac{\sum_{i=1}^{n} \emptyset_i\cdot\rho_i|\overrightarrow{v_i}\cdot\overrightarrow{A_i}|}{\sum_{i=1}^{n} \rho_i|\overrightarrow{v_i}\cdot\vec{A}_i|} \qquad \text{-(4)}$$

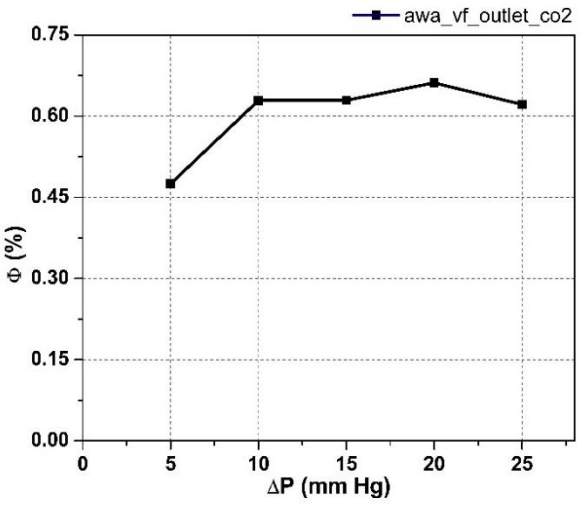

Figure 7.8

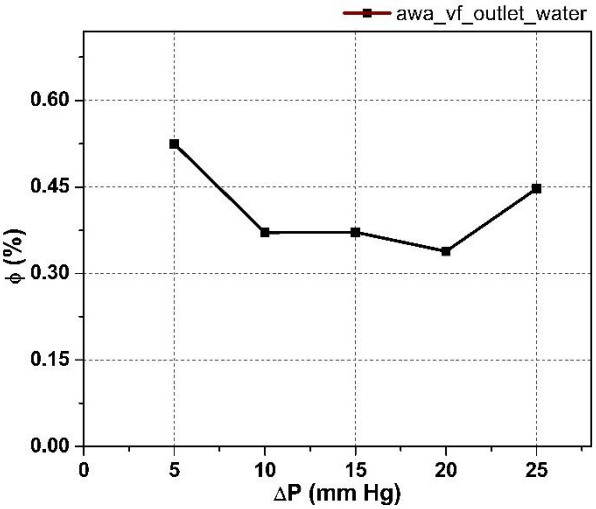

Figure 7.9

Figure 7.8: Area weighted average volume fraction of CO_2 at the outlet
Figure 7.9: Area weighted average volume fraction of water at the outlet

Figure 7.8 and Figure 7.9 show the area-weighted average volume fraction for CO_2 and water, respectively. The area-weighted average volume fraction for water at the outlet has exactly the opposite trend as that of CO_2 as together they sum up to unity. The variation of the volume

fraction with respect to the applied pressure difference follows a more complex trend as the flow is highly transient and multiphase.

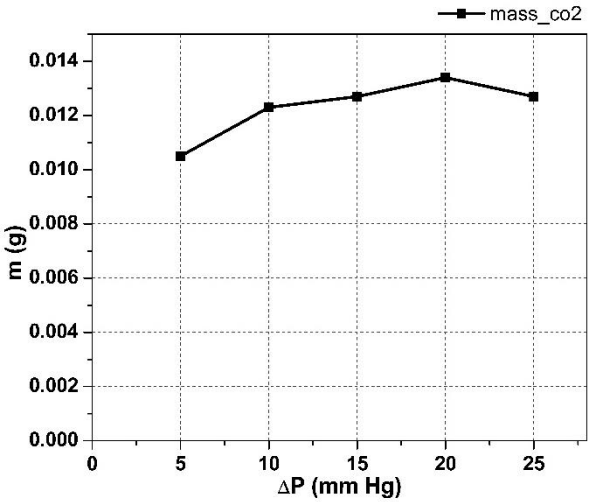

Figure 7.10: Mass of CO_2

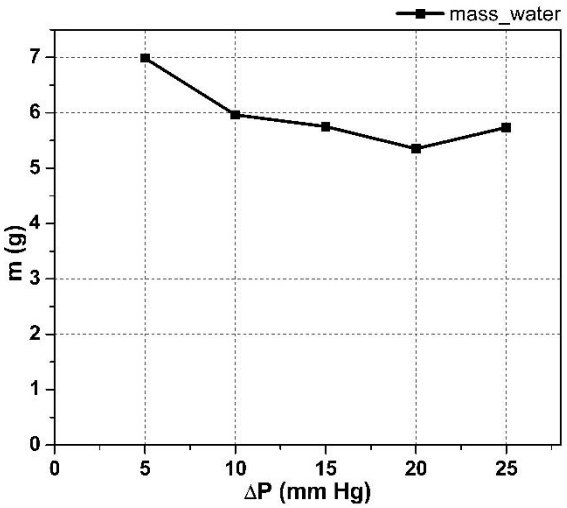

Figure 7.11: Mass of water

As shown in Figure 7.10 and Figure 7.11, similarly, the mass of CO_2 and mass of water follow opposite trends as the total volume = $\boldsymbol{m_{CO_2}/\rho_{CO_2} + m_{water}/\rho_{water}}$ = constant.

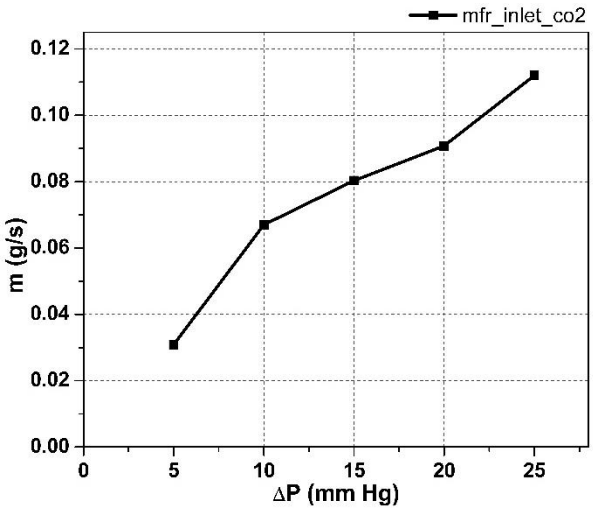

Figure 7.12: Mass flow rate of CO_2 at the inlet.

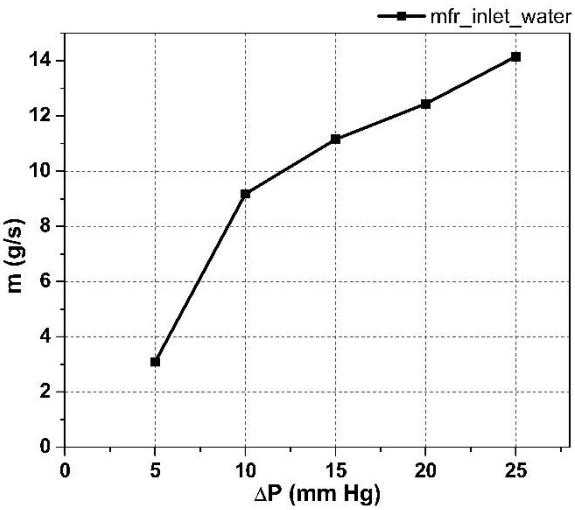

Figure 7.13: Mass flow rate of water at the inlet

Mass flow rates and the velocities plotted in Figure 7.12 to Figure 7.15 increase with ΔP because the pressure difference is responsible for driving the flow in this problem. The values in

the graphs of mass flow rates and mass weighed average x-velocities of the fluids (shown in Figure 7.12 to Figure 7.15) are related to each other as $\frac{\dot{m}_{CO_2}}{\dot{m}_{water}} \approx \frac{(\rho A u_{mean})_{CO_2}}{(\rho A u_{mean})_{water}}$ (from definition).

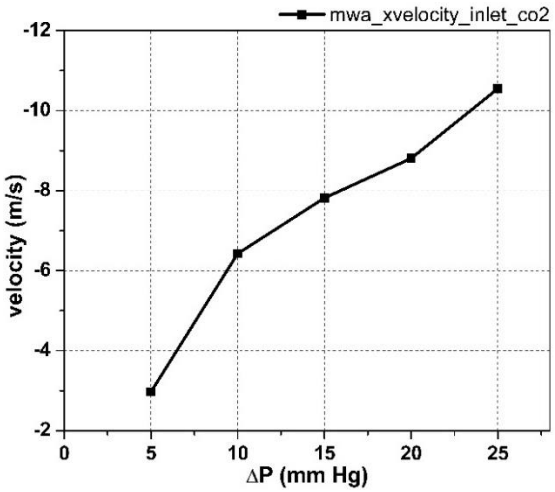

Figure 7.14

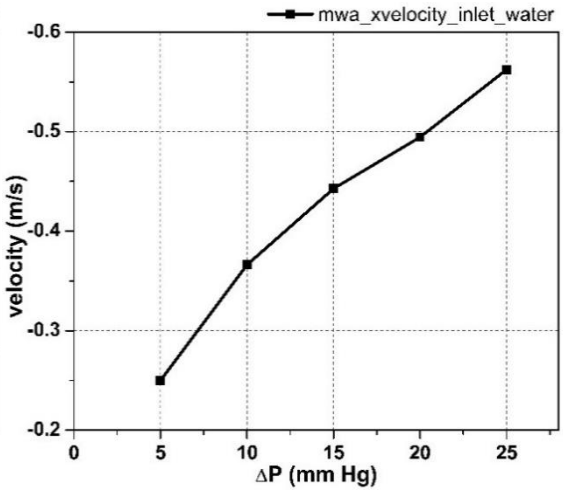

Figure 7.15

Figure 7.14: Mass weighted average x-velocity of CO_2 at the inlet
Figure 7.15: Mass weighted average x-velocity of water at the inlet

The x-velocity of both the fluids increases with ΔP as expected, as shown in Figure 7.14 and Figure 7.15**.**

Limitations of the present study:

Following are the limitations of the present study.

- The area fraction of CO_2 (the region through which CO_2 passes) at the inlet is assumed to be 20%. Other values of area fractions like 40%, 60%, and 80% can also be simulated to investigate the effect it has on the flow field inside the device and the resulting mass flow rates of the two fluids.
- The current work is carried out for the CO_2 gas and water mixture. The problem may be simulated with a mixture of blood and water for more realistic and accurate results.

Chapter-8

8 CONCLUSIONS

8.1 General Conclusions

In the recent scenario, the application of laparoscopic surgery is necessary for the convenient survival of humans. The enriching activities of laparoscopic surgery are accomplished due to the attainable different laparoscopic instruments with their technical specifications and design modifications. The literature survey presented in the thesis contributes to different trends of laparoscopic instruments in this modern technological world. This thesis has offered the existing reviews of a few designing methods of laparoscopic surgical devices. It permits the benefits to entire designers of the laparoscopic instrument as reducing the brainstorming issues and time consumption while designing or redesigning the laparoscopic surgical devices.

From the literature review, we noticed that limited work had been carried out for analyzing the characteristics of laparoscopic surgical instruments in terms of simulation. In the review, we mainly focussed on a certain number of laparoscopic instruments, namely, laparoscopic grasper, suction irrigation type instrument, laparoscopic handles, and the forceps. From analyzing the overall accomplished performances, the design and technical contributions are very limited in the suction and irrigation types of laparoscopic instruments. Besides, the simulation of Newtonian analysis and non-Newtonian analysis in the existing and our modified laparoscopic instrument is not available in the existing research. This approach achieves efficient ways for abdominal surgeries such as removing the spleen, uterus, etc. We hope that this perspective supports for enrich the related ongoing or the forecasting of further laparoscopic surgical instrumentation research

works and promotes a supreme pathway for enhancing the operation characteristics of the instruments in the way of surgeons' satisfaction.

The existing research on laparoscopic instrumental enhancement between the years 2011 and 2020 is symbolized in this thesis. The review promotes direction to several surgical device designers by adopting the additional innovative methodology for designing novel laparoscopic instruments. Literature surveys and feedback from practicing surgeons suggest that the existing design faces prolonged time and can be avoided by improving the current design of forceps. Based on the work carried out and the results obtained, the following conclusions are drawn:

1. The proposed laparoscopic forceps shall function as the existing instruments and facilitates the surgeon ergonomically.
2. The present device comprises an outer sleeve over the laparoscopy forceps. A gap between the outer tube of laparoscopy forceps and the outer sleeve serves as an annular region through which the suction irrigation fluids flow. The suction irrigation fluid and carbon dioxide (CO_2) can be fed to or removed from the device through a small pipe protruding from the outer tube at the distal end.
3. This development provides a multi-purpose laparoscopic surgical device that can suck, irrigate, cut, grasp, and cauterize the tissue.
4. This development facilitates a laparoscopic surgical device to reduce the time lost in switching between them during laparoscopic surgery.
5. The present device enables manipulating, dissecting the tissue, then irrigating and sucking the fluid from the abdomen, thereby avoiding the insertion of multiple instruments multiple times, keeping the inert gas level pumped inside the abdomen stable, and minimizes the risk to the patient as well as the surgeon.

6. The laparoscopic forceps increase the efficiency of the laparoscopic surgical process.
7. It avoids the exchange of instruments, which prevents fatigue/injury to the surgeon, patient, or both.
8. This device can be easily assembled/disassembled, is reusable, and can be easily sterilized.
9. The present work can be further extended for commercialization under the "Make in India" initiative aimed toward affordable and indigenously manufactured multi-functional instruments.

8.2 Specific Conclusions

In our work, a modified laparoscopic instrument is proposed to ensure a reduced number of incisions over the abdominal region. This design requires only one incision to play a role as both a suction-irrigation device and as forceps, thus reducing the risk of postoperative injuries which can happen due to multiple incisions. The fluid flow is simulated using water from which we concluded the following salient points:

- For the S-I device, the suction and irrigation mass flow rates are the same as the device is symmetric from both ends. In the modified instrument, the suction and irrigation mass flow rates are slightly different as the flow from both ends is not symmetric.
- The mass flow rate provided by the new design is larger than the suction irrigation device that is already under use by the surgeons and hence meets the requirements from the flow perspective.
- Prototype fabrication of the new design is evaluated which is used for experimental validation with the numerical analysis results.

Different designs of the modified form of laparoscopic forceps have been analyzed for the flow aspects in chapter 4. All the modified designs of laparoscopic forceps (with different pipe diameters and protrusion angles) cater to the mass flow requirements if they are used in place of the S-I device.

The initial design in Table 4.2 is not considered as it gives lesser flow rates. The diameter of the flow tube also reduces abruptly near the protrusion, which could cause blockages due to the formation of unwanted organic deposits. $8mm$ diameter design is narrower towards the distal end and hence would be better suited for practical use when compared with the $10mm$ diameter design. 45° protrusion angle design results in a lesser mass flow rate when compared with the 60° protrusion angle design due to higher turbulence in the flow tube. Despite this, 45° protrusion angle design might be better suited for practical purposes as the induced turbulence can aid in the removal of any unwanted organic deposits near the jaws and protrusion. Based on the above discussion, the design with $8mm$ diameter and 45° protrusion angle was initially proposed as a suitable improvement to the dissector forceps. The proposed design is compared with the standard SI device and tabulated in Table 4.2, and the following conclusions are drawn.

- All the features of the standard SI device are already incorporated in the modified design. In addition, the modified design is versatile and acts both as a forceps and a suction irrigation device, thereby combining the functionality of two devices into one.
- The mass flow rate obtained using the modified design in suction irrigation mode is marginally higher compared to that of the standard SI device.

- It helps avoid two additional steps of re-inserting the SI device and removing it, consequently decreasing the chances of CO_2 leakage from the abdomen and saving time of surgery.
- This device gives flexibility to the surgeon to use the SI feature more frequently for quick removal of blood or other body fluids in the field of view.
- This device helps reduce the risk of significant injury due to the usage of multiple laparoscopic instruments, thereby reducing the blood loss, discomfort, and pain to the patient.

This instrument is designed in such a way that it can be completely disassembled part by part, similar to the dissector forceps currently in use. The inner rod – jaws assembly, outer tube, outer sleeve, handle, and other smaller components can all be taken apart. This way, they can be individually cleaned and sterilized without compromising the patient's safety. This feature allows for ease of sterilization so that it can be used multiple times.

In chapter 5, flow analysis of blood (modeled as a non-Newtonian fluid) has been carried out in the alternate design of surgical forceps, and the results are compared with those obtained previously in the case of water (a Newtonian fluid). This new device has functionalities of both dissector forceps and S-I device. The mass flow rates computed using shear-thinning flow models like Carreau and Carreau-Yasuda models, which are used to simulate the blood flow, are found to be almost identical. Compared to the $8mm, 45^{\circ}$design, $8mm, 60^{\circ}$ design better caters to the mass flow rate delivered by the S-I device. The results also show that $8mm, 60^{\circ}$ design can effectively cater to the mass flow requirements of both the S-I cleaning fluid in irrigation mode and blood in

suction mode. Therefore, this is proposed as a suitable improvement to the dissector forceps and is finalized for fabrication.

This new design is expected to:

- avoid the exchange of multiple instruments, consequently decreasing the chances of CO_2 leakage from the abdomen.
- reduce the time of surgery.
- reduce the risk of fatigue to the surgeon and trauma to the patient due to the exchange of multiple instruments.
- give flexibility to the surgeon to use the SI feature more frequently for quick removal of blood or other body fluids in the field of view.

Many surgeries like Myomectomy, diagnostic laparoscopy, appendectomy, Nephrectomy, cholecystectomy, Hysterectomy, splenectomy, Single-incision laparoscopic surgery, etc., are time-critical and need to be carried out with precision with little time for instrument exchange. Therefore, the proposed forceps can find practical applications potentially in all such procedures.

In chapter 6, the new design of the CO_2 insufflators unit is designed and simulated in a systematic methodology. Firstly, the design necessities are reviewed based on the characteristics of the existing three instruments, namely, dissector forceps, Suction-Irrigator unit, and CO_2 insufflators unit. Then, the new designs are obtained through simulation approaches using Newtonian flow and non-Newtonian fluid behaviors, as discussed in our previous chapters 4 and 5. New designs combine all the functions of dissector forceps, CO_2 insufflators units and suction-irrigation instruments. Finally, the feasibility of the new designs is verified by simulating the gas flow over the instrument at different mass flow rates. The result has shown that the proposed design

can potentially benefit almost all laparoscopic surgeries by reducing the time exchange of instruments, making multi-functional, decreasing trauma, improving patient morbidity, and saving time during surgery than the existing instruments.

8.3 Limitations of the Current Study

1. The surgeon has to physically remove the pin and reinsert it to switch between modes of the instrument. Thus, the designs can be improved over the existing mechanism by fitting the switch with a spring or electrically-operated toggle switch.
2. The proposed design has a long, inflexible shaft, which makes some regions inside the abdomen inaccessible and restricts the grasper head in an axial orientation. Adding shaft flexibility will allow an additional degree of freedom to the head.
3. The concept of the S-I device presently used in surgeries is incorporated in our proposed design. Currently used designs use the same tube for simultaneous suction and irrigation, which could pose the risk of cross-contamination in the intra-abdominal regions. The presence of jaws and other mechanisms in the S-I pathways may possibly increase this risk. In our present work, this problem has not been addressed and can be taken as future work.
4. The proposed laparoscopic forceps is not clinically tested or trialed on living beings.

8.4 Future Scope of Work

1. The proposed design has a long, inflexible shaft, which makes some regions inside the abdomen inaccessible and restricts the grasper head in an axial orientation. Adding shaft flexibility will allow an additional degree of freedom to the head.

2. Since the CO_2 insufflation and S-I processes require the same passage area in our proposed design so as to facilitate the surgeon and does not compromises the patient's safety. So, using a three-way valve (as a separate unit) can allow the S-I fluids and CO_2 to flow through the same pathway. Thus, we can have a three-way valve attached at the protrusion end of the proposed device.
3. The proposed design can further be universalized by standardizing laparoscopic and endoscopic devices so that the outer sleeve can be slid over them to enhance their individual capabilities with the S-I feature.
4. In the current design, the jaws, the four-bar mechanism, and the inner rod constitute a single assembly. To change the laparoscopic functionality with a different set of jaws, the entire assembly must be replaced. This design can be improved by ensuring that the jaws can be easily detached from the four-bar mechanism.
5. A specially designed miniature 3-axis distal force sensor can be added to perform tissue palpation and measure tissue interaction forces at the tip of a surgical instrument. This feature will lead to the widespread adaption of the proposed design in robot-assisted laparoscopic surgery.
6. Further experimentation can be carried out to validate the predicted results. For instance the device can be experimented with and tested for blood flow, CO_2 gas flow, or a combination of water and CO_2 fluid flow inside the instrument.
7. Because of the increased friction due to the extra cylinder of the outer sleeve, there would be an additional force required to operate the finger handles significantly more and therefore leading to muscle fatigue. The required force can be studied and compared with the existing forceps.

BIBLIOGRAPHY

[1]. Kryztopher D. Tung, Rami M. Shorti, Earl C. Downey, Donald S. Bloswick, Andrew S. Merryweather, 2015, The Effect of Ergonomic Laparoscopic Tool Handle Design on Performance and Efficiency, Surg Endoscopy, 29(9), pp. 2500-2505.

[2]. Vicdan Sari, Theodoor E. Nieboer, Mark E. Vierhout, Dick F. Stegeman & Kirsten B. Kluivers, 2010, The operation room as a hostile environment for surgeons: Physical complaints during and after laparoscopy, Minimally Invasive Therapy & Allied Technologies, 19(2), pp. 105-109.

[3]. M.A. van Veelen, and D.W. Meijer, 1999, Ergonomics and Design of Laparoscopic Instruments: Results of a Survey Among Laparoscopic Surgeons, Journal of Laparoendoscopic & Advanced Surgical Techniques, 9(6), pp. 481-489.

[4]. Valerio Cigaina, David Jenkins,2000, Medical Device Handle for Use in Laparoscopic Surgery, US Patent 6165180 A.

[5]. D.B. Jones et al., 2015, Safe Energy Use in the Operating Room, Current Problems in Surgery, 52(11), pp. 447–468.

[6]. Tailin Fan, Kester Batchelor, John R. Mensch, Richard A. Thompson, 2015, Laparoscopic Forceps Assembly, US Patent 9216030 B2, 22.

[7]. Moran, Peter, Moran, Stuart, White, Michael,2008, Laparoscopic Forceps, US Patent 2001/013803.

[8]. Salvatore Castro, Robert E. Welt, 2011, Flexible Dissecting Forceps, US Patent 20110029010 A1.

[9]. William P. McVay,1996, Laparoscopic Irrigation Bottle Pump, US Patent US 08/115,068.

[10]. Abraham Frech, Conor J. Walsh, 2016, Laparoscopic Suction Device and Method, US Patent 20160206369 A1.

[11]. Jin U. Kang, Peter L. Gehlbach, 2015, Motion-Compensated Micro-Forceps System and Method, US Patent 20150305761 A1.

[12]. Rashann Coleman, 2014, Surgical Needle Locks that Cooperate with Laparoscopic Forceps and Related Methods, US Patent 20140135821 A1.

[13]. Sven Schneider, Tobias Unger, 2014, Endoscopic Instruments, and Shafts for an Endoscopic Instruments, US Patent 20140236147 A1.

[14]. Haining William Dai, Brian Hess, Francis M. Reynolds, David Kosh, Fioleda Prifti, 2014, Cupped Forceps, US Patent WO2014005063 A1.

[15]. Justin Collins, 2014, Laparoscopic Surgery, US Patent 8821377 B2.

[16]. Andrea Pietrabissa Cesare Stefanini Arianna Menciassi Paolo Dario, 2008, Auxiliary Forceps for Hand-Assisted Laparoscopic Surgery (HALS), US Patent 20040153121A1.

[17]. Hock Lim Tan, Sven Schneider, 2016, Forceps Insert for Laparoscopic Procedures, US Patent D761961S.

[18]. Patrick L. Dumbauld Paul Guerra Roger F. Smith Scott DePierro, 2010, Insulating Boot for Electrosurgical Forceps, US Patent 20070078458A1.

[19]. Michael A. Schellp Feffer, 1998, Laparoscopic Tissue Retrieval Forceps, US Patent US 08/786,634.

[20]. Michael Esposito, 2015, Bowed Tip for Laparoscopic Surgery, US Patent 20150105820 A1.

[21]. Hand Andrea, Cesare, Arianna, Paolo, Bardini, Marco, Luigi, 2001, Auxiliary Forceps for Assisted Laparoscopic Surgery (HALS), US Patent WO / 2002/100281.

[22]. Daniel A. Joseph, Covidien L.P, 2015, Forceps, US Patent US9039039704 B2.

[23]. Kevin W. Smith, 1992, Maryland Dissector Laparoscopic Instrument, US Patent US5156633 A.

[24]. Melzer, A., 1996, Endoscopic instruments: conventional and intelligent. Endosurgery. New York: Churchill Livingstone, pp. 69-95.

[25]. Sakurazawa N,Harada J, Ando F, et al., 2020, Evaluation of the safetyand efficacy of suction-tip forceps, a new tool for laparoscopic surgery, for gastric cancer. Asian Journal of Endoscopic Surgery, 2021(14), pp.232–240.

[26]. Rosen JE, Size A, Yang Y, Sharon A, Sauer-Budge A., 2015, Artificial hand for minimally invasive surgery: design and testing of initial prototype. Surg Endosc., 29(1), pp. 61-67.

[27]. Geryane, M. H., Hanna, G. B., & Cuschieri, A., 2004, Time–motion analysis of operation theater time use during laparoscopic cholecystectomy by surgical specialist residents. Surgical Endoscopy, 18(11), pp. 1597–1600.

[28]. Siu, J., Hill, A. G., & MacCormick, A. D., 2017, Systematic review of reusable versus disposable laparoscopic instruments: costs and safety. ANZ journal of surgery, 87(1-2), pp. 28–33.

[29]. Dimitrios K Manatakis, Nikolaos Georgopoulos, 2014, Reducing the Cost of Laparoscopy: Reusable versus Disposable Laparoscopic Instruments, Hindawi Publishing Corporation Minimally Invasive Surgery Volume 2014, Article ID 408171, pp. 1-4.

[30]. Boylu, Sukru, 2013, Forceps, European Patent EP 2422720 B1.

[31]. Boni, L., David, G., Mangano, A., Dionigi, G., Rausei, S., Spampatti, S., Cassinotti, E., & Fingerhut, A., 2015, Clinical applications of indocyanine green (ICG) enhanced fluorescence in laparoscopic surgery. Surgical endoscopy, 29(7), pp. 2046–2055.

[32]. Santos, B. F., Enter, D., Soper, N. J., & Hungness, E. S., 2011, Single-incision laparoscopic surgery (SILS™) versus standard laparoscopic surgery: A comparison of performance using a surgical simulator. Surgical endoscopy, 25(2), pp. 483-490.

[33]. Chambers, W. M., Bicsak, M., Lamparelli, M., & Dixon, A. R., 2011, Single-incision laparoscopic surgery (SILS) in complex colorectal surgery: a technique offering potential and not just cosmesis. Colorectal disease : the official journal of the Association of Coloproctology of Great Britain and Ireland, 13(4), pp. 393–398.

[34]. Jeong, S. Y. et al., 2014, Open versus laparoscopic surgery for mid-rectal or low-rectal cancer after neoadjuvant chemoradiotherapy (COREAN trial): survival outcomes of an open-label, non-inferiority, randomised controlled trial. The Lancet. Oncology, 15(7), 767–774.

[35]. Yiannakopoulou E, Nikiteas N, Perrea D, Tsigris C., 2015, Virtual reality simulators and training in laparoscopic surgery. International Journal of Surgery (London, England). Jan;13, pp. 60-64.

[36]. Chen, W. T., Chang, S. C., Chiang, H. C., Lo, W. Y., Jeng, L. B., Wu, C., & Ke, T. W., 2011, Single-incision laparoscopic versus conventional laparoscopic right hemicolectomy: a comparison of short-term surgical results. Surgical endoscopy, 25(6), pp. 1887–1892.

[37]. Yamashita, T., Tomifuji, M., Araki, K., Kurioka, T., & Shiotani, A., 2011, Endoscopic transoral oropharyngectomy using laparoscopic surgical instruments. Head & neck, 33(9), pp. 1315–1321.

[38]. Dapri, G., Casali, L., Dumont, H., Van der Goot, L., Herrandou, L., Pastijn, E., Sosnowski, M., Himpens, J., & Cadière, G. B., 2011, Single-access transumbilical laparoscopic appendectomy and cholecystectomy using new curved reusable instruments: a pilot feasibility study. Surgical endoscopy, 25(4), pp. 1325–1332.

[39]. Friedersdorff, F., Aghdassi, S. J., Werthemann, P., Cash, H., Goranova, I., Busch, J. F., Ebbing, J., Hinz, S., Miller, K., Neymeyer, J., & Fuller, T. F., 2013, Laparoendoscopic single-site (LESS) varicocelectomy with reusable components: comparison with the conventional laparoscopic technique. Surgical endoscopy, 27(10), pp. 3646–3652.

[40]. Van den Dobbelsteen, J.J., Lee, R.A., van Noorden, M. and Dankelman, J., 2012. Indirect measurement of pinch and pull forces at the shaft of laparoscopic graspers. Medical & biological engineering & computing, 50(3), pp.215-221.

[41]. Ibrahim, Khalil, Ahmed Ramadan, Mohamed Fanni, Yo Kobayashi, Ahmed Abo-Ismail, Masakatus G. Fujie, 2015, "Development of a new 4-DOF endoscopic parallel manipulator based on screw theory for laparoscopic surgery." Mechatronics 28, pp. 4-17.

[42]. Lai, E. C., Yang, G. P., & Tang, C. N., 2013, Robot-assisted laparoscopic liver resection for hepatocellular carcinoma: short-term outcome. American journal of surgery, 205(6), pp. 697–702.

[43]. S. A. Elprama, K. Kilpi, P. Duysburgh, A. Jacobs, L. Vermeulen and J. van Looy, 2013, "Identifying barriers in telesurgery by studying current team practices in robot-assisted surgery," 2013 7th International Conference on Pervasive Computing Technologies for Healthcare and Workshops, pp. 224-231.

[44]. Mocan B., Bintintan V.V., Brad S., Ciuce C., Mocan M., Murar M., 2016, Development of a Robotic Driven Handheld Laparoscopic Instrument for Non-invasive

Intraoperative Detection of Small Endoluminal Digestive Tumors. In: Wenger P., Chevallereau C., Pisla D., Bleuler H., Rodić A. (eds) New Trends in Medical and Service Robots. Mechanisms and Machine Science, vol 39. Springer, Cham, pp. 197-210.

[45]. Mirbagheri, A., F. Farahmand, A. Meghdari, F. Karimian, 2011, "Design and development of an effective low-cost robotic cameraman for laparoscopic surgery: RoboLens." Scientia Iranica 18(1), pp. 105-114.

[46]. Gehrman, J., Angenete, E., Björholt, I., Lesén, E., and Haglind, E., 2020, Cost-effectiveness analysis of laparoscopic and open surgery in routine Swedish care for colorectal cancer. Surgical endoscopy, 34(10), pp.4403-4412.

[47]. Gehrman, J., Björholt, I., Angenete, E., Andersson, J., Bonjer, J., & Haglind, E., 2017, Health economic analysis of costs of laparoscopic and open surgery for rectal cancer within a randomized trial (COLOR II). Surgical endoscopy, 31(3), pp. 1225–1234.

[48]. Talha, A., El-Haddad, H., Ghazal, A. E., & Shehata, G., 2020, Laparoscopic versus open appendectomy for perforated appendicitis in adults: randomized clinical trial. Surgical endoscopy, 34(2), pp. 907–914.

[49]. Lim, J.J. and Erdman, A.G., 2003, A review of mechanism used in laparoscopic surgical instruments. Mechanism and Machine Theory, 38(11), pp.1133-1147.

[50]. Herati, A.S., Andonian, S., Rais-Bahrami, S., Atalla, M.A., Srinivasan, A.K., Richstone, L. and Kavoussi, L.R., 2011. Use of the valveless trocar system reduces carbon dioxide absorption during laparoscopy when compared with standard trocars. Urology, 77(5), pp.1126-1132.

[51]. Lee, W.J., Chan, C.P. and Wang, B.Y., 2013, Recent advances in laparoscopic surgery. Asian journal of endoscopic surgery, 6(1), pp.1-8.

[52]. Crist, D.W. and Gadacz, T.R., 1993, Complications of laparoscopic surgery. Surgical Clinics of North America, 73(2), pp.265-289.

[53]. Ohtani, H., Tamamori, Y., Azuma, T., Mori, Y., Nishiguchi, Y., Maeda, K. and Hirakawa, K., 2011, A meta-analysis of the short-and long-term results of randomized controlled trials that compared laparoscopy-assisted and conventional open surgery for rectal cancer. Journal of Gastrointestinal Surgery, 15(8), pp.1375-1385.

[54]. Burhan Hakan Kanat, Abdullah Böyük, Mustafa Girgin, Yavuz Selim Ilhan, Ferhat Çay, İbrahim Erdemay, 2018, "Obtaining a hook from a disposable laparoscopic suction/irrigation system." Laparoscopic Endoscopic Surgical Science (LESS) 25(1), pp. 23-25.

[55]. Siotos, C., Stergios, K., Prasath, V., Seal, S. M., Duncan, M. D., Sakran, J. V., & Habibi, M., 2019, Irrigation Versus Suction in Laparoscopic Appendectomy for Complicated Appendicitis: A Meta-analysis. The Journal of surgical research, 235, 237–243.

[56]. St Peter SD, Adibe OO, Iqbal CW, et al. Irrigation versus suction alone during laparoscopic appendectomy for perforated appendicitis: a prospective randomized trial. Ann Surg. 2012; 256:581–585.

[57]. Sun, F., Wang, H., Zhang, F., Zhang, X., Xing, Z., Zhang, S., Zhang, H., & Wang, Y., 2018, Copious Irrigation Versus Suction Alone During Laparoscopic Appendectomy for Complicated Appendicitis in Adults. Journal of investigative surgery : the official journal of the Academy of Surgical Research, 31(4), pp. 342–346.

[58]. Junaidi, M., Kalluri, R., Rao, Y., Gokhale, A., & Patel, A., 2021, Design and fluid flow simulation of modified laparoscopic forceps. Computer methods in biomechanics and biomedical engineering, 24(8), pp. 844–863.

[59]. Lee, D., Kim, U., Gulrez, T., Yoon, W., Hannaford, B., & Choi, H., 2016, A Laparoscopic Grasping Tool With Force Sensing Capability. IEEE/ASME Transactions on Mechatronics, 21, pp. 130-141.

[60]. Susmitha Wils, K., Devasahayam, S. R., Manivannan, M., & Mathew, G., 2017, Force model for laparoscopic graspers: implications for virtual simulator design. Minimally invasive therapy & allied technologies : MITAT : official journal of the Society for Minimally Invasive Therapy, 26(2), pp. 97–103.

[61]. Hardon, S. F., Schilder, F., Bonjer, J., Dankelman, J., & Horeman, T., 2019, A new modular mechanism that allows full detachability and cleaning of steerable laparoscopic instruments. Surgical endoscopy, 33(10), pp. 3484–3493.

[62]. Uysal, D., Gasch, C., Behnisch, R., Nickel, F., Müller-Stich, B. P., Hohenfellner, M., & Teber, D., 2021, Evaluation of new motorized articulating laparoscopic instruments by laparoscopic novices using a standardized laparoscopic skills curriculum. Surgical endoscopy, 35(2), pp. 979–988.

[63]. Haraguchi, D., Kanno, T., Tadano, K., & Kawashima, K., 2015, A Pneumatically Driven Surgical Manipulator With a Flexible Distal Joint Capable of Force Sensing. IEEE/ASME Transactions on Mechatronics, 20, pp. 2950-2961.

[64]. T. Kanno, D. Haraguchi, M. Yamamoto, K. Tadano and K. Kawashima, 2015, "A Forceps Manipulator With Flexible 4-DOF Mechanism for Laparoscopic Surgery," in IEEE/ASME Transactions on Mechatronics, 20(3), pp. 1170-1178,

[65]. Zhang, Boyu, Zhuxiu Liao, and Hongen Liao, 2017, "Visible forceps manipulator with novel linkage bending mechanism for neurosurgery." 39th Annual International Conference of the IEEE Engineering in Medicine and Biology Society (EMBC). IEEE, 2017.

[66]. Tapia-Araya, A. E., Usón-Gargallo, J., Sánchez-Margallo, J. A., Pérez-Duarte, F. J., Martin-Portugués, I. D., & Sánchez-Margallo, F. M., 2016, Muscle activity and hand motion in veterinarians performing laparoscopic training tasks with a box trainer. American journal of veterinary research, 77(2), pp. 186–193.

[67]. Atsuro Sawada, Jin Kono, Atsushi Sengiku, Naoto Kume, Junichi Fukuda, Toshinari Yamasaki et al., 2018, "Laparoscopic Forceps with Force Feedback." International Conference on Human-Computer Interaction, Springer, Cham, 10902, pp. 83-95.

[68]. Hemmati S. H., 2014, How to build a simple and safe laparoscopic hydatid evaluation system. JSLS : Journal of the Society of Laparoendoscopic Surgeons, 18(3), e2014.00314, pp. 1-5.

[69]. Tixier, F., Garçon, M., Rochefort, F., & Corvaisier, S., 2016, Insulation failure in electrosurgery instrumentation: a prospective evaluation. Surgical endoscopy, 30(11), pp. 4995–5001.

[70]. Espada, M., Munoz, R., Noble, B. N., & Magrina, J. F., 2011, Insulation failure in robotic and laparoscopic instrumentation: a prospective evaluation. American journal of obstetrics and gynecology, 205(2), pp. 121.e1–121.e1215.

[71]. Yunlei Liang, Zhijiang Du, Weidong Wang, Zhiyuan Yan, Lining Sun, 2019, An improved scheme for eliminating the coupled motion of surgical instruments used in laparoscopic surgical robots." Robotics and Autonomous Systems 112, pp. 49-59.

[72]. Van Duren, B. H., van Boxel, G. I., Hart, A., & Newton, N., 2016, A novel safety mechanism to reduce the risk of inadvertent electrosurgical injury. Journal of Medical Engineering & Technology, 40(5), pp. 239–244.

[73]. Kazuya Kawamura, Hiroto Seno, Yo Kobayashi, Satoshi Ieiri, Makoto Hashizume & Masakatsu G. Fujie, 2016, Design parameter evaluation based on human operation for tip mechanism of forceps manipulator using surgical robot simulation, Advanced Robotics, 30(7), pp. 476-488.

[74]. Barrie, J., Russell, L., Hood, A. J., Jayne, D. G., Neville, A., & Culmer, P. R., 2018, An in vivo analysis of safe laparoscopic grasping thresholds for colorectal surgery. Surgical endoscopy, 32(10), pp. 4244–4250.

[75]. Kim, F. J., Sehrt, D., da Silva, R. D., Gustafson, D., Nogueira, L., & Molina, W. R., 2015, Evaluation of emissivity and temperature profile of laparoscopic ultrasonic devices (blades and passive jaws). Surgical endoscopy, 29(5), pp. 1179–1184.

[76]. Prince, S. W., Kang, C., Simonelli, J., Lee, Y., Gerber, M. J., Lim, C., … Tsao, T., 2019, A Robotic System for Telementoring and Training in Laparoscopic Surgery. The International Journal of Medical Robotics and Computer Assisted Surgery, 16(2), pp. 1-13.

[77]. Seehofer, D., Mogl, M., Boas-Knoop, S., Unger, J., Schirmeier, A., Chopra, S., & Eurich, D., 2012, Safety and efficacy of new integrated bipolar and ultrasonic scissors compared to conventional laparoscopic 5-mm sealing and cutting instruments. Surgical endoscopy, 26(9), pp. 2541–2549.

[78]. Seehofer, D., Mogl, M., Boas-Knoop, S., Unger, J., Schirmeier, A., Chopra, S., & Eurich, D., 2012, Safety and efficacy of new integrated bipolar and ultrasonic scissors compared to conventional laparoscopic 5-mm sealing and cutting instruments. Surgical endoscopy, 26(9), pp. 2541–2549.

[79]. Shimomura, Y., Minowa, K., Kawahira, H., & Katsuura, T., 2016, Ergonomic design and evaluation of the handle for an endoscopic dissector. Ergonomics, 59(5), pp. 729–734.

[80]. Tsai, Y. C., Lin, V. C., Chung, S. D., Ho, C. H., Jaw, F. S., & Tai, H. C., 2012, Ergonomic and geometric tricks of laparoendoscopic single-site surgery (LESS) by using conventional laparoscopic instruments. Surgical endoscopy, 26(9), pp. 2671–2677.

[81]. A. Hassan-Zahraee, B. Herman and J. Szewczyk, 2011, "Mechatronic design of a hand-held instrument with active trocar for laparoscopy," 2011 IEEE International Conference on Robotics and Automation, INSPEC No 12288636 , pp. 1890-1895.

[82]. Tung, K. D., Shorti, R. M., Downey, E. C., Bloswick, D. S., & Merryweather, A. S., 2015, The effect of ergonomic laparoscopic tool handle design on performance and efficiency. Surgical endoscopy, 29(9), pp. 2500–2505.

[83]. González, A. G., Barrios-Muriel, J., Romero-Sánchez, F., Salgado, D. R., & Alonso, F. J., 2020, Ergonomic assessment of a new hand tool design for laparoscopic surgery based on surgeons' muscular activity. Applied ergonomics, 88(103161), pp. 1-10.

[84]. S. Guo, J. Cui, N. Xiao and X. Bao, 2018, "Simulation Analysis of Catheter Bending in Vascular Intervention Robot Based on ANSYS," 2018 IEEE International Conference on Mechatronics and Automation (ICMA), INSPEC No. 18162807 pp. 585-590.

[85]. Friedrich, M. G., Tirilomis, T., Kollmeier, J. M., Wang, Y., & Hanekop, G. G., 2018, Modifications of Surgical Suction Tip Geometry for Flow Optimisation: Influence on Suction-Induced Noise Pollution. Surgery research and practice, 2018, 3074819, pp. 1-8.

[86]. Wain, R. A. J., Whitty, J. P. M., Dalal, M. D., Holmes, M. C., & Ahmed, W., 2014, Blood flow through sutured and coupled microvascular anastomoses: A comparative

computational study. Journal of Plastic, Reconstructive & Aesthetic Surgery, 67(7), pp. 951–959.

[87]. Wu, Z. J., Gellman, B., Zhang, T., Taskin, M. E., Dasse, K. A., & Griffith, B. P., 2011, Computational Fluid Dynamics and Experimental Characterization of the Pediatric Pump-Lung. Cardiovascular engineering and technology, 2(4), pp. 276–287.

[88]. Suhwan Park, Cheongjun Kim, Suyong Kim & Doo Yong Lee, 2018, Improved estimation of torque between a surgical instrument and environment in multi-DOF motion, Journal of Mechanical Science and Technology 32(6), pp. 2817-2828.

[89]. Centenero, Samir Aboul-Hosn, and Federico Hernández-Alfaro, 2012, "3D planning in orthognathic surgery: CAD/CAM surgical splints and prediction of the soft and hard tissue results–our experience in 16 cases." Journal of Cranio-Maxillofacial Surgery 40(2), pp. 162-168.

[90]. Mehta, N. Y., Haluck, R. S., Frecker, M. I., & Snyder, A. J., 2002, Sequence and task analysis of instrument use in common laparoscopic procedures. Surgical endoscopy, 16(2), pp. 280–285.

[91]. Hartwich, J. E., Carter, R. F., Wolfe, L., Goretsky, M., Heath, K., St. Peter, S. D., & Lanning, D. A., 2013, The effects of irrigation on outcomes in cases of perforated appendicitis in children. Journal of Surgical Research, 180(2), pp. 222–225.

[92]. Elnaz Shariati, Jalal Bakhtiari, Alireza Aminsharifi, Amir Niasari-Naslaji, Ebrahim Shariati, 2014, Comparison of Laparoscopic Versus Conventional Open Partial Nephrectomy in Dogs, Iranian Journal of Veterinary Surgery, 9(2), pp. 51-56.

[93]. Zemlyak, A. Y., Colavita, P. D., El Djouzi, S., Walters, A. L., Hammond, L., Hammond, B., Heniford, B. T., 2012, Comparative study of wound complications: Isolated

panniculectomy versus panniculectomy combined with ventral hernia repair. Journal of Surgical Research, 177(2), pp. 387–391.

[94]. Melendez, M. M., Vosswinkel, J. A., Shapiro, M. J., Gelato, M. C., Mynarcik, D., Gavi, S., McNurlan, M., 2007, Wall Suction Applied to Needle Muscle Biopsy—A Novel Technique for Increasing Sample Size. Journal of Surgical Research, 142(2), pp. 301–303.

[95]. Aesculap, Inc.3773 Corporate Parkway Center Valley, PA 18034, United States. https://www.aesculapusa.com/assets/base/doc/DOC465REV_M_Laparoscopic_Catalog.pdf

[96]. Karl Leblanc, 2003, Laparoscopic Hernia Surgery: An Operative Guide, Taylor & Francis, CRC Press, pp. 136. Vimex endoscopy,

https://vimex-endoscopy.com/wp-content/uploads/2017/12/EN-Laparoscopic-pum-PV-5512LAP-ver.1.2.pdf

[97]. Li, Jeremy., 2012, Design and Development of Biomedical and Surgical Instruments in Biomedical Applications. IntechOpen, Chapter 9, pp. 213-222.

[98]. Barry, S. L., Fransson, B. A., Spall, B. F., & Gay, J. M., 2012, Effect of two instrument designs on laparoscopic skills performance. Vet Surg, 41(8), pp. 988–993.

[99]. Md. Abdul Raheem Junaidi, Harsha Sista, Ram Chandra Murthy Kalluri, YV Daseswara Rao, 2020, Laparoscopic Surgical Device, IN Patent Application: 202011034072.

[100]. Md. Abdul Raheem Junaidi, Harsha Sista, Ram Chandra Murthy Kalluri, YV Daseswara Rao, 2020, Laparoscopic Surgical Device, IN Design Patent Application: 334185-001.

[101]. Abdelsalam, S. I., Mekheimer, K. S., & Zaher, A. Z., 2020, Alterations in blood stream by electroosmotic forces of hybrid nanofluid through diseased artery: Aneurysmal/stenosed segment. Chinese Journal of Physics, 67, pp. 314–329.

[102]. Abumandour, R., Eldesoky, I., Kamel, M., Ahmed, M. & Abdelsalam, S., 2020, Peristaltic thrusting of a thermal-viscosity nanofluid through a resilient vertical pipe. Zeitschrift für Naturforschung A, 75(8), pp. 727-738.

[103]. Bhatti MM, Marin M, Zeeshan A, Ellahi R and Abdelsalam SI, 2020, Swimming of Motile Gyrotactic Microorganisms and Nanoparticles in Blood Flow Through Anisotropically Tapered Arteries. Front. Phys. 95(8), pp. 1-9.

[104]. Junaidi, M., Kalluri, R., Rao, Y., Gokhale, A., & Patel, A., 2021, Design and fluid flow simulation of modified laparoscopic forceps. Computer methods in biomechanics and biomedical engineering, 24(8), pp. 844–863.

[105]. A.D. Caballero & S. Laín, 2015, Numerical simulation of non-Newtonian blood flow dynamics in human thoracic aorta, Comput Methods Biomech Biomed Engin., 18(11), pp. 1200-1216.

[106]. Seta, B., Torlak, M., & Vila, A., 2017, Numerical Simulation of Blood Flow Through the Aortic Arch. CMBEBIH 2017, IFMBE Proceedings, Springer, Singapore, 62, pp. 259–268.

[107]. Abdollahzadeh Jamalabadi MY, Daqiqshirazi M, Nasiri H, Safaei MR, Nguyen TK, 2018, Modeling and analysis of biomagnetic blood Carreau fluid flow through a stenosis artery with magnetic heat transfer: A transient study.PLoS ONE 13(2), pp. e0192138.

[108]. Qiao, Y., Zeng, Y., Ding, Y., Fan, J., Luo, K., & Zhu, T., 2019, Numerical simulation of two-phase non-Newtonian blood flow with fluid-structure interaction in aortic dissection. Computer methods in biomechanics and biomedical engineering, 22(6), pp. 620–630.

[109]. Razavi, A., Shirani, E., & Sadeghi, M. R., 2011, Numerical simulation of blood pulsatile flow in a stenosed carotid artery using different rheological models. J. Biomech, 44(11), pp. 2021–2030.

[110]. Quanyu, W., Xiaojie, L., Lingjiao, P., Weige, T., & Chunqi, Q., 2017, Simulation Analysis Of Blood Flow In Arteries Of The Human Arm. Biomed. Eng.: Appl. Basis Commun., 29(04), pp. 1750031.

[111]. Carreau, P. J. (1972). Rheological Equations from Molecular Network Theories. J Rheol., 16(1), pp. 99–127.

[112]. Cho, Y. I., & Kensey, K. R., 1991, Effects of the non-Newtonian viscosity of blood on flows in a diseased arterial vessel. Part 1: Steady flows. Biorheology, 28(3-4), pp. 241–262.

[113]. Chan, W.Y., Ding, Y., & Tu, J., 2007, Modeling of non-Newtonian blood flow through a stenosed artery incorporating fluid-structure interaction. Anziam J, 47, 507-523.

[114]. Siebert, M., & Fodor, P.S., 2009, Newtonian and Non-Newtonian Blood Flow over a Backward- Facing Step - A Case Study, Proceedings of the COMSOL Conference 2009 Boston. Corpus ID: 2940769.

[115]. S. Tabakova, E. Nikolova, and St. Radev, 2014, Carreau model for oscillatory blood flow in a tube, AIP Conference Proceedings 1629, pp. 336.

[116]. Molla, M. M., & Paul, M. C., 2012, LES of non-Newtonian physiological blood flow in a model of arterial stenosis. Med Eng Phys., 34(8), pp. 1079–1087.

[117]. Liu, B., & Tang, D., 2011, Influence of non-Newtonian properties of blood on the wall shear stress in human atherosclerotic right coronary arteries. MCB Mol. Cell. Biomech., 8(1), pp. 73–90.

[118]. Fisher, C., & Rossmann, J. S., 2009, Effect of non-newtonian behavior on hemodynamics of cerebral aneurysms. J. Biomech. Eng., 131(9), pp. 091004.

[119]. Hammoud, A., Sharay, E. Y., & Tikhomirov, A. N., 2019, Newtonian and non-Newtonian pulsatile flows through carotid artery bifurcation based on CT image geometry. AIP Conference Proceedings 2171, pp. 110022.

[120]. Johnston, B. M., Johnston, P. R., Corney, S., & Kilpatrick, D., 2004, Non-Newtonian blood flow in human right coronary arteries: steady state simulations. J. Biomech., 37(5), pp. 709–720.

[121]. Gijsen, F. J., Allanic, E., van de Vosse, F. N., & Janssen, J. D., 1999, The influence of the non-Newtonian properties of blood on the flow in large arteries: unsteady flow in a 90 degrees curved tube. J. Biomech., 32(7), pp. 705–713.

[122]. Leuprecht, A., Perktold, K., 2001, Computer Simulation of Non-Newtonian Effects on Blood Flow in Large Arteries. Comput Methods Biomech Biomed Engin., 4(2), pp. 149–163.

[123]. Sarifuddin, 2020, CFD Modelling of Casson Fluid Flow and Mass Transport Through Atherosclerotic Vessels. Differ Equ Dyn Syst., springer, pp. 1-17.

[124]. A. Jon'aˇsov'a; J.,2008, Vimmr. Numerical simulation of non-Newtonian blood flow in bypass models. Proceedings in Applied Mathematics and Mechanics, 79thAnnual Meeting of the International Association of Applied Mathematics and Mechanics, Bremen, 8(1), pp. 10179–10180.

[125]. Yong Hyun Kim, Pamela J. Vande Vord, Joon Sang Lee., 2008, Multiphase non-Newtonian effects on pulsatile hemodynamics in a coronary artery, Int. J. Numer. Methods Fluids; 58(7), pp. 803–825.

[126]. Yeleswarapu, K. K., Kameneva, M. V., Rajagopal, K. R., & Antaki, J. F., 1998, The flow of blood in tubes: theory and experiment. Mech. Res. Commun., 25(3), pp. 257–262.

[127]. Mandy Perrin, Anthony Fletcher, 2004, Laparoscopic abdominal surgery, Continuing Education in Anaesthesia Critical Care & Pain, 4(4), 107–110.

[128]. Jiang, R., Sun, Y., Wang, H., Liang, M., &Xie, X., 2019, Effect of different carbon dioxide (CO_2) insufflation for laparoscopic colorectal surgery in elderly patients. Medicine, 98(41), pp. 1-10.

[129]. Makkieh N, 2017, Bradycardia and Cardiac Arrest during Laparoscopic Surgery. J CardiolCurr Res 8(1), pp. 00271(1-2).

[130]. Sood J, Kumra VP., 2003, Anaesthesia for laparoscopic surgery. Indian J Surg; 65(3), pp. 232-240.

[131]. McHoney, M., Corizia, L., Eaton, S., Kiely, E. M., Drake, D. P., Tan, H. L., Spitz, L., &Pierro, A., 2003, Carbon dioxide elimination during laparoscopy in children is age dependent. Journal of pediatric surgery, 38(1), 105–110.

[132]. Choi, S., Yang, S. Y., Choi, G. J., Kim, B. G., & Kang, H., 2019, Comparison of pressure- and volume-controlled ventilation during laparoscopic colectomy in patients with colorectal cancer. Scientific reports, 9(1), pp. 17007(1-10).

[133]. ShylaEndojet CO_2 insufflator manual, http://www.compamed-tradefair.com/prod_file_download/k-U2FsdGVkX19XOqBwdvm-Naw-EU3kRGDYwuEkmWCnQek/2/26398_1

[134]. Jung, K. T., Kim, S. H., Kim, J. W., & So, K. Y., 2013, Bradycardia during laparoscopic surgery due to high flow rate of CO2 insufflation. Korean journal of anesthesiology, 65(3), pp. 276–277.

[135]. Veekash, G. & Wei, L.X. & Su, M.., 2010, Carbon dioxide pneumoperitoneum, physiologic changes and anesthetic concerns. Ambulatory Surgery. 16. pp. 41-46.

[136]. Sherwani, Nzar,Kareem, Tayeb, 2019, The effect of intra-abdominal carbon dioxide pressure on blood pressure in laparoscopic surgeries, Medical Journal of Babylon, 16(4), pp. 286-291.

[137]. Pacilli, M., Pierro, A., Kingsley, C., Curry, J. I., Herod, J., & Eaton, S., 2006, Absorption of carbon dioxide during laparoscopy in children measured using a novel mass spectrometric technique. British journal of anaesthesia, 97(2), pp. 215–219.

[138]. Pelizzo, G., Bernardi, L., Carlini, V., Pasqua, N., Mencherini, S., Maggio, G., De Silvestri, A., Bianchi, L., & Calcaterra, V., 2017, Laparoscopy in children and its impact on brain oxygenation during routine inguinal hernia repair. Journal of minimal access surgery, 13(1), pp. 51–56.

[139]. Ansys Fluent 12.1 user help manual guide, 2012, topic 20.3.1, area-weighted average, mass-weighted average.

https://www.afs.enea.it/project/neptunius/docs/fluent/html/th/node416.htm

APPENDICES

NOTE: All dimensions are in mm only.

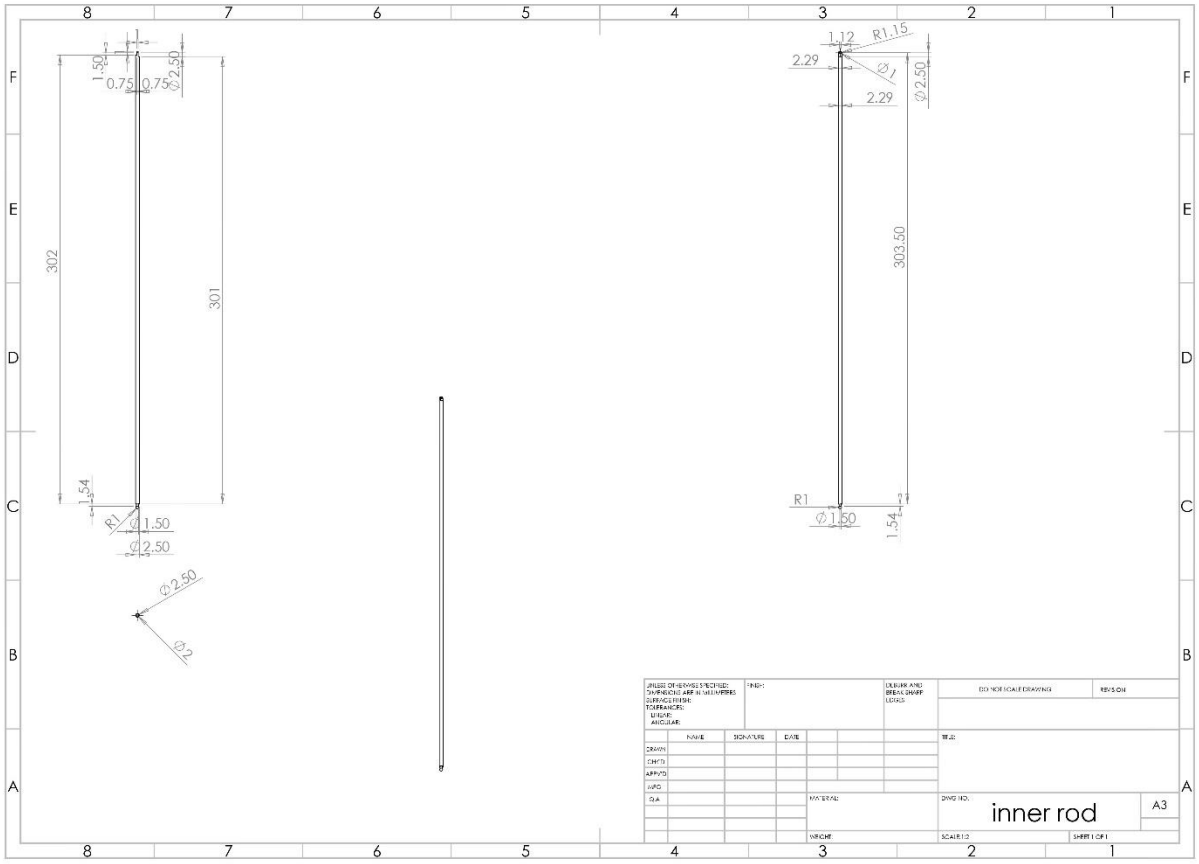

Fig. 1: Inner rod

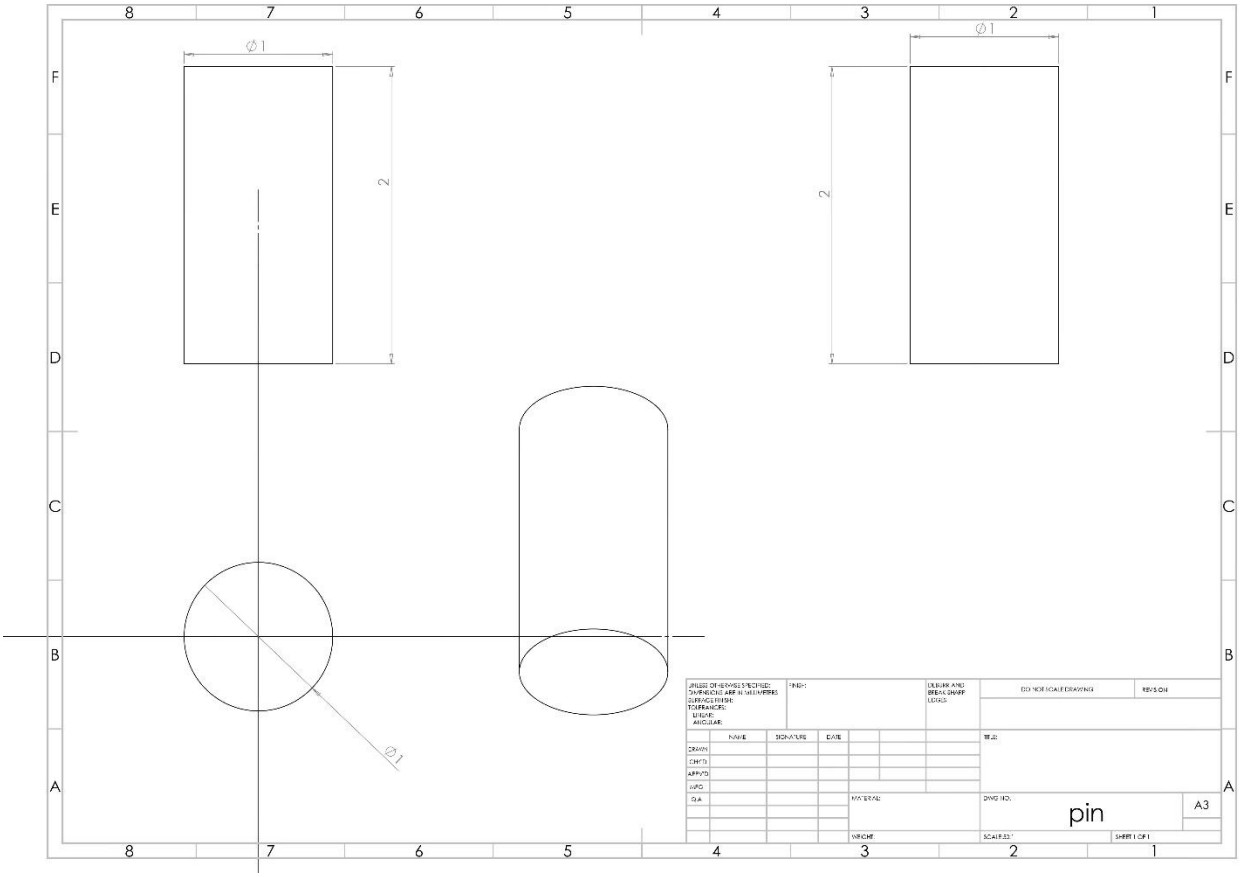

Fig. 2: Pin

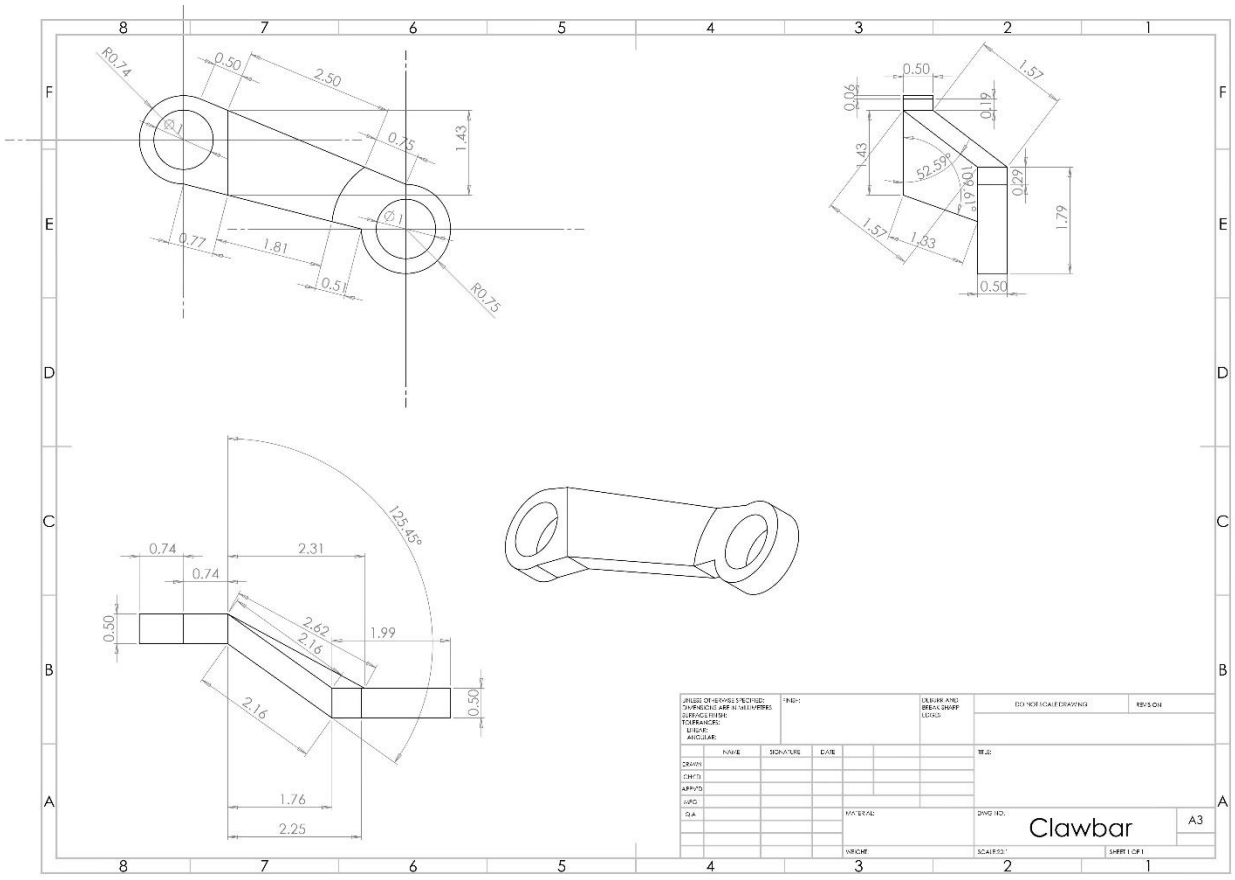

Fig. 3: Clawbar

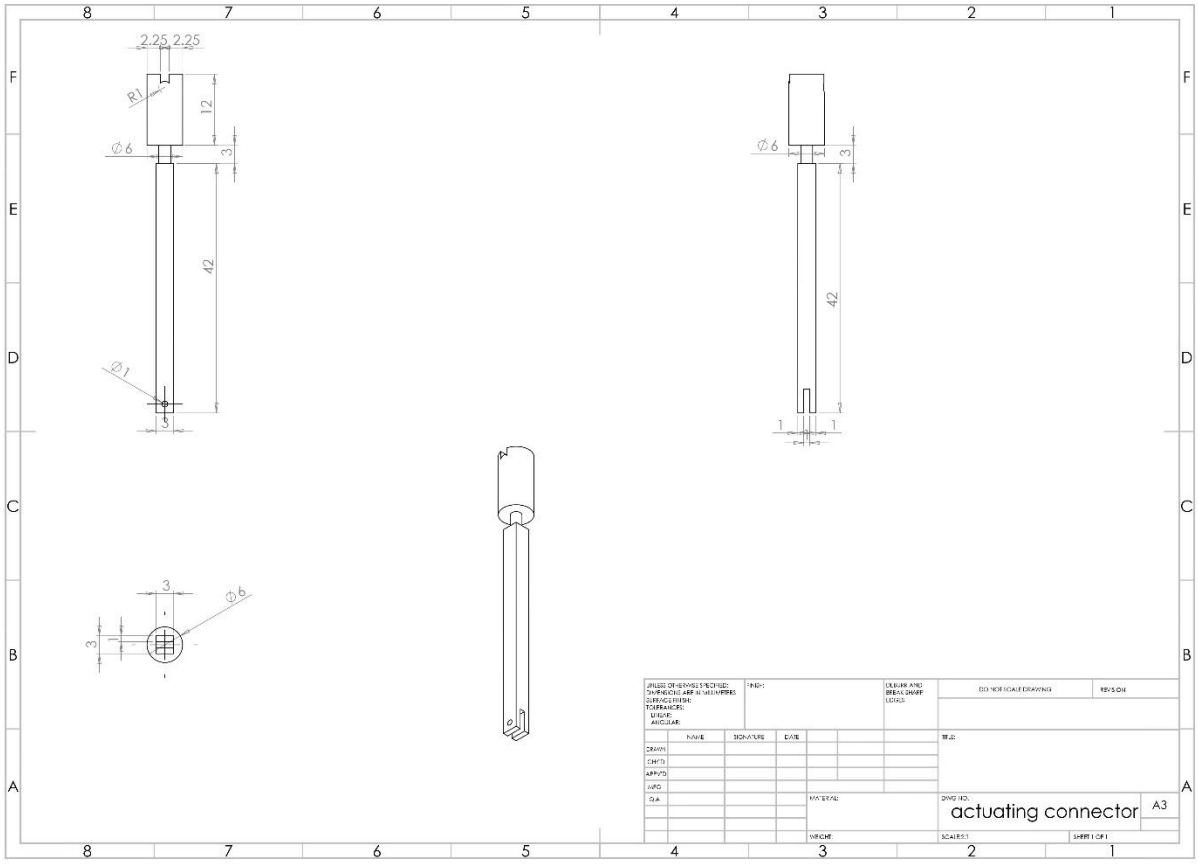

Fig. 4: Actuating connector

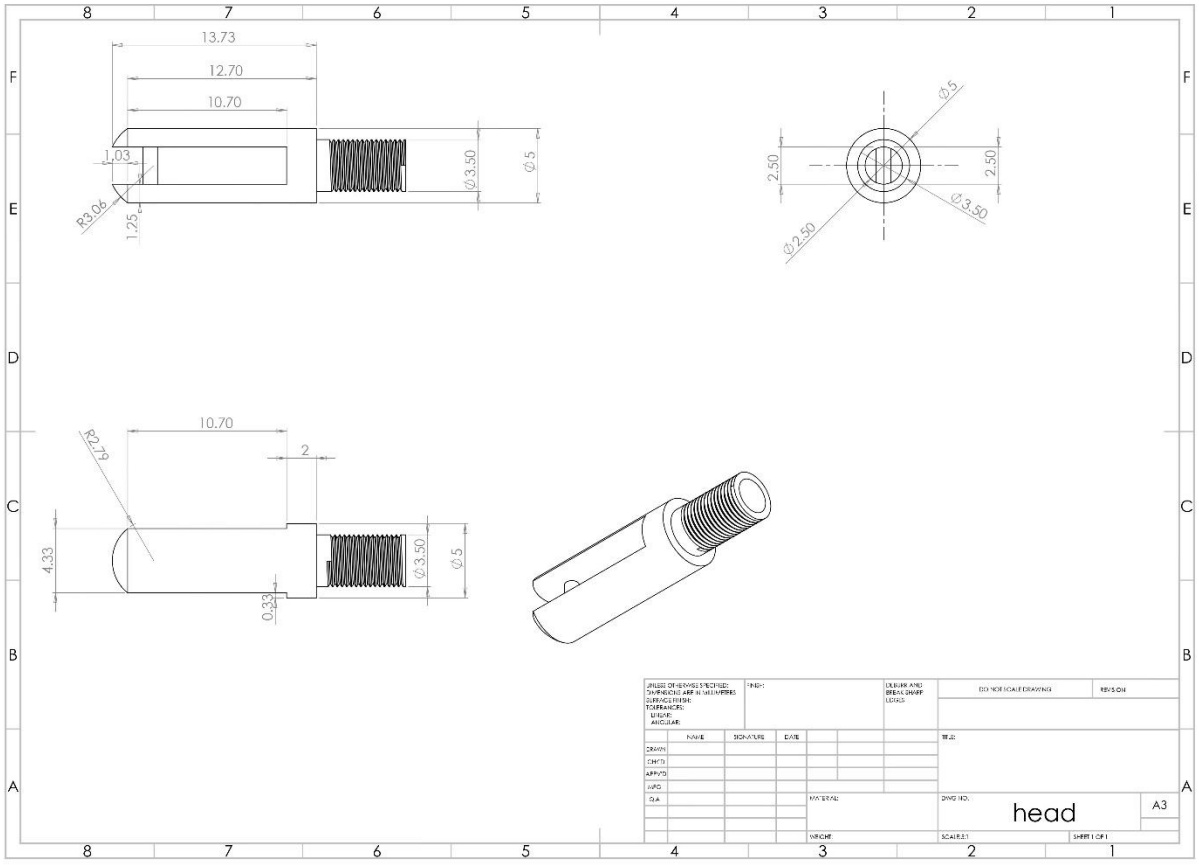
13.73
12.70
10.70
1.03
R3.06
1.25
Ø3.50
Ø5
Ø5
2.50
2.50
Ø3.50
Ø2.50
10.70
2
R2.79
4.33
0.33
Ø3.50
Ø5
head
A3

Fig. 5: Head

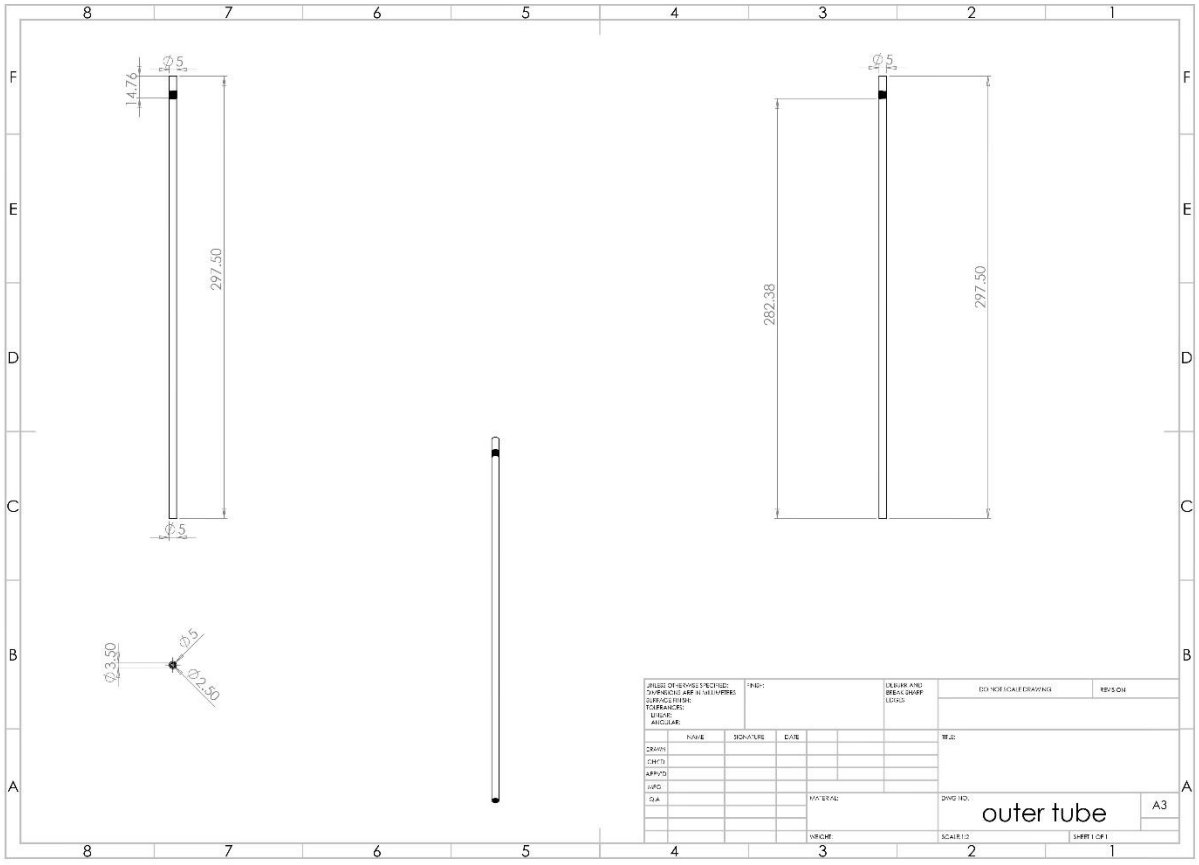

Fig. 6: Outer tube

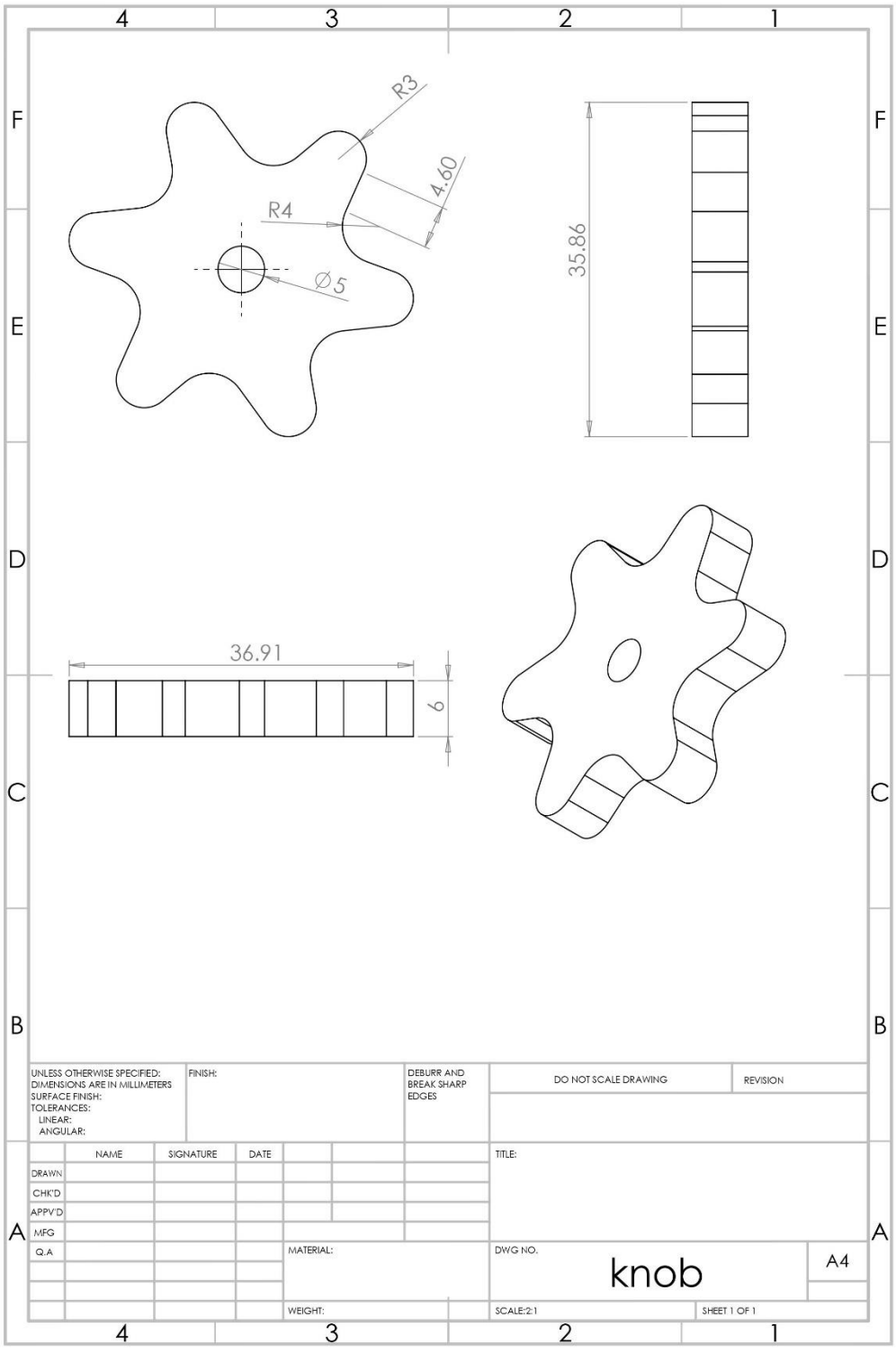
R3
4.60
R4
Ø5
35.86
36.91
6
UNLESS OTHERWISE SPECIFIED:
DIMENSIONS ARE IN MILLIMETERS
SURFACE FINISH:
TOLERANCES:
LINEAR:
ANGULAR:
FINISH:
DEBURR AND BREAK SHARP EDGES
DO NOT SCALE DRAWING
REVISION
NAME
SIGNATURE
DATE
TITLE:
DRAWN
CHK'D
APPV'D
MFG
Q.A
MATERIAL:
DWG NO.
knob
A4
WEIGHT:
SCALE:2:1
SHEET 1 OF 1

Fig. 7: knob

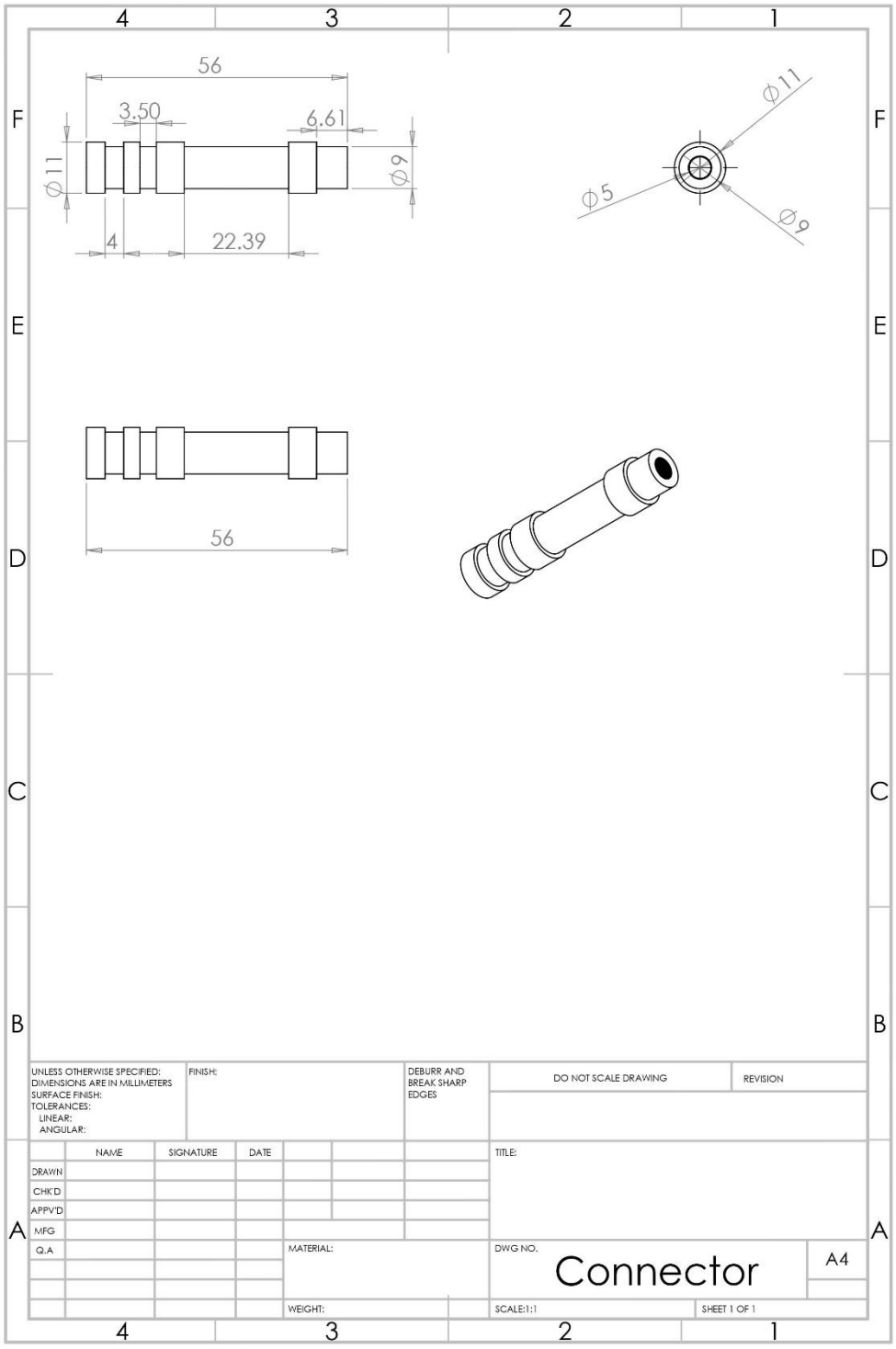

Fig. 8: Connector

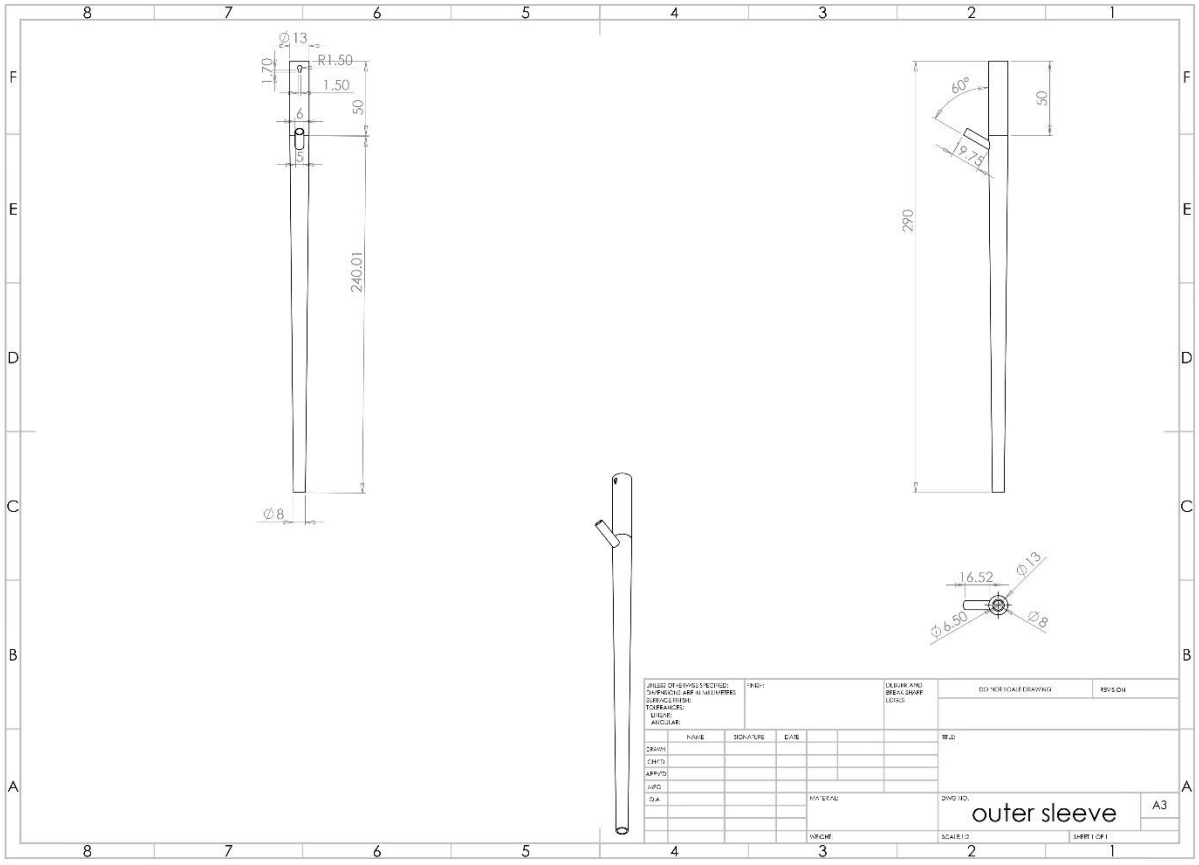

Fig. 9: Outer sleeve

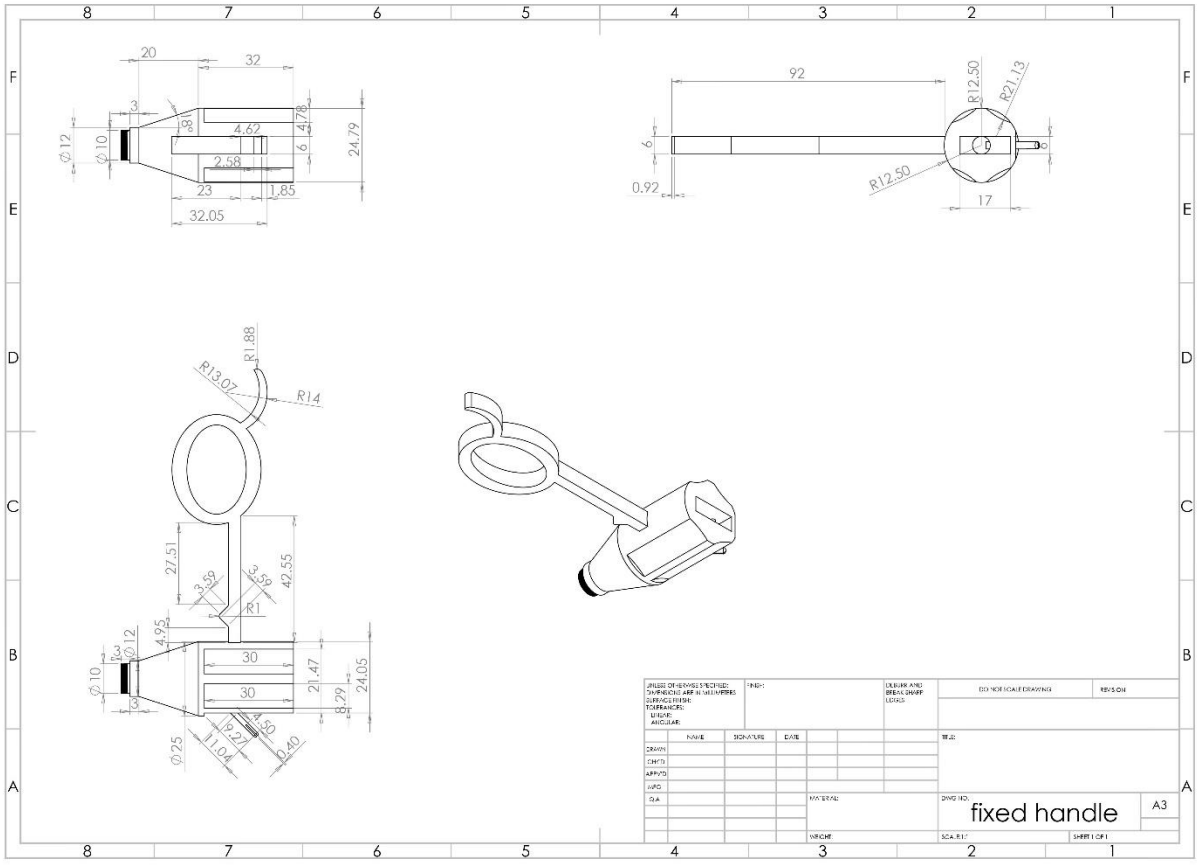

Fig. 10: Fixed handle

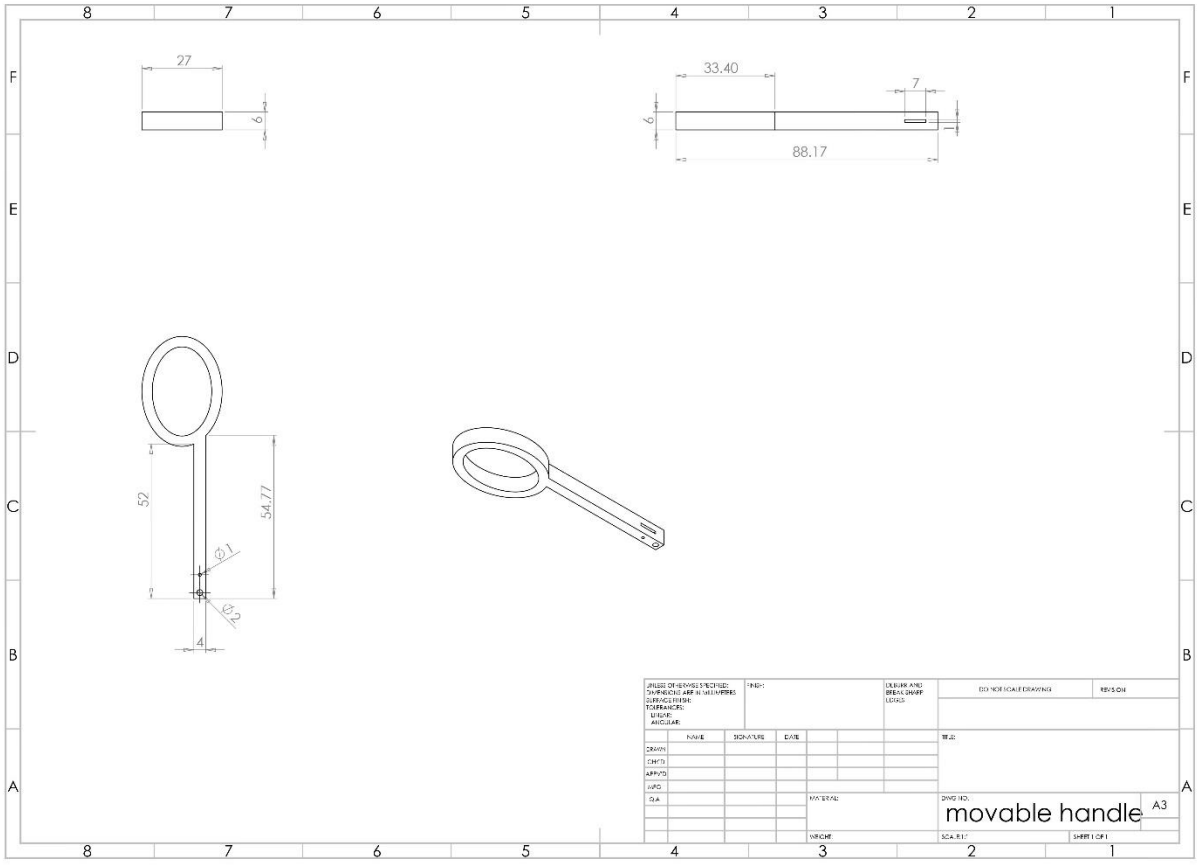

Fig. 11: Movable handle

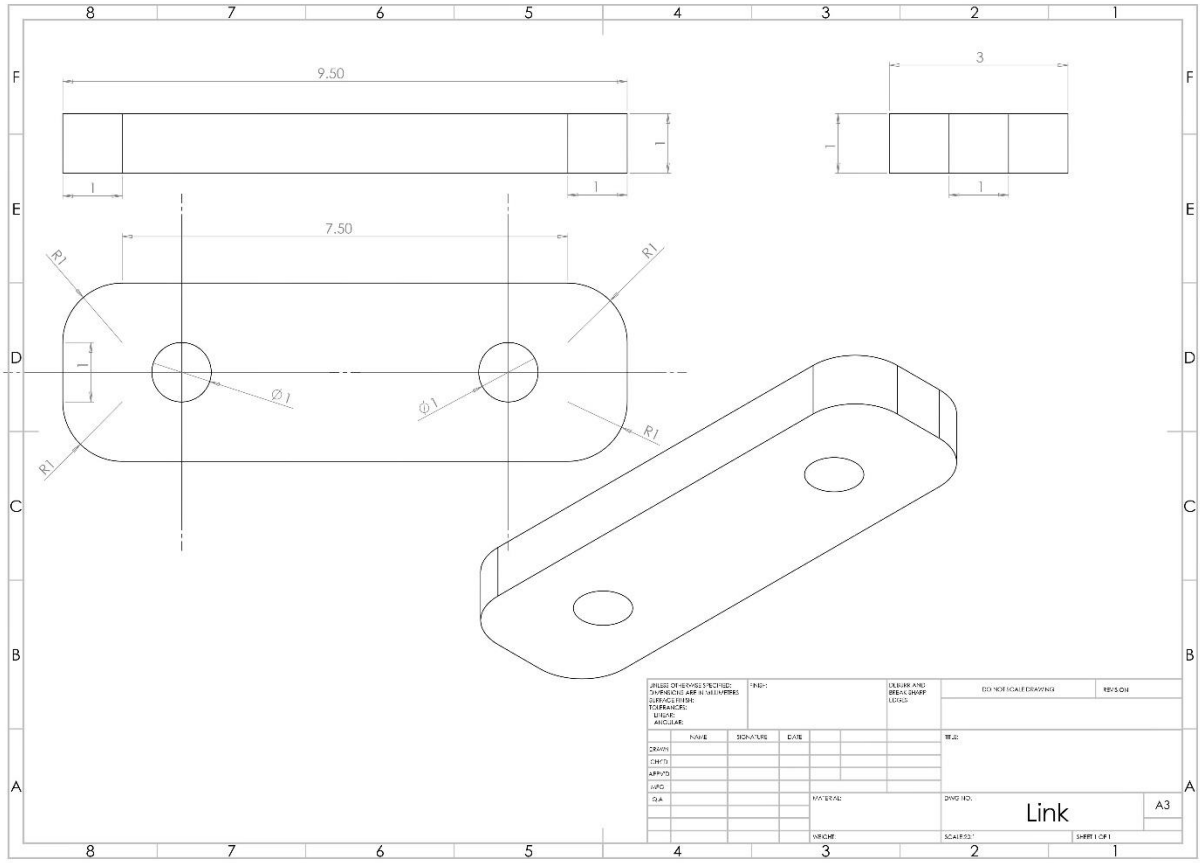

Fig. 12: Link

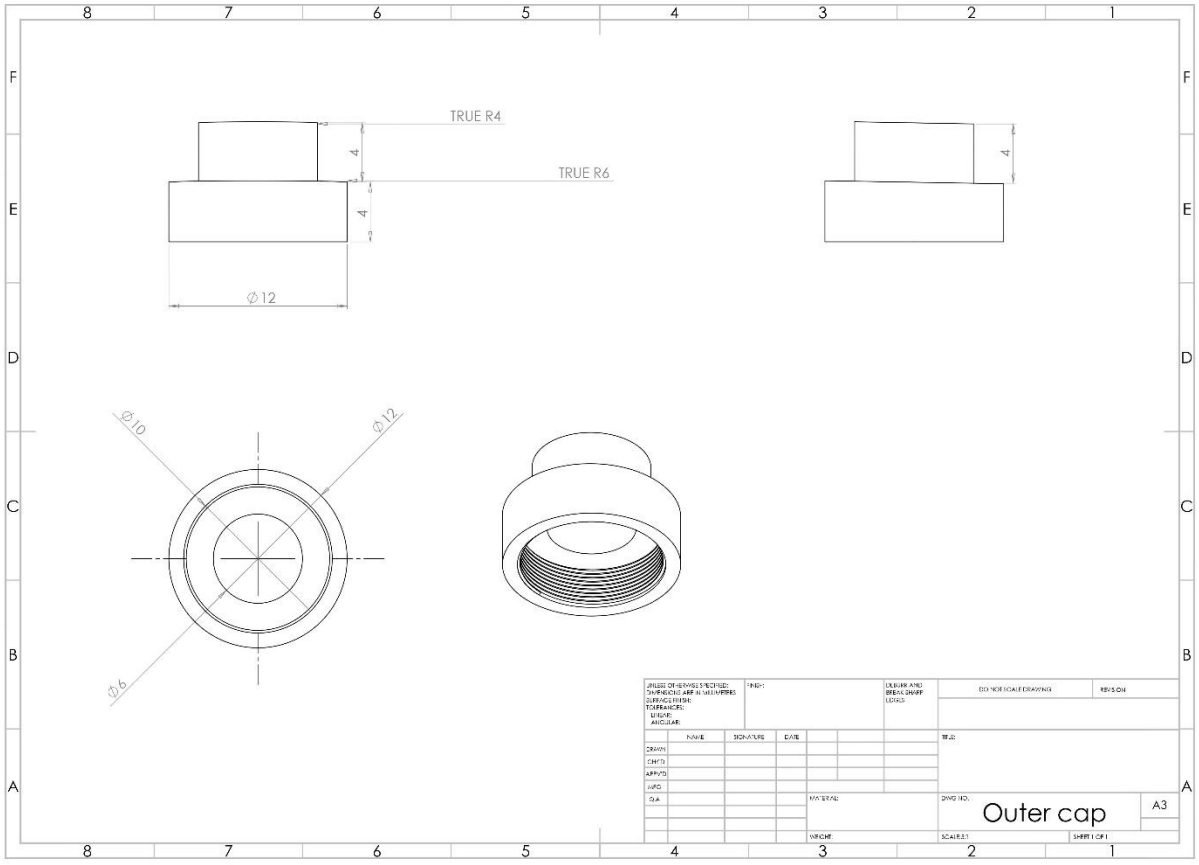

Fig. 13: Outer cap

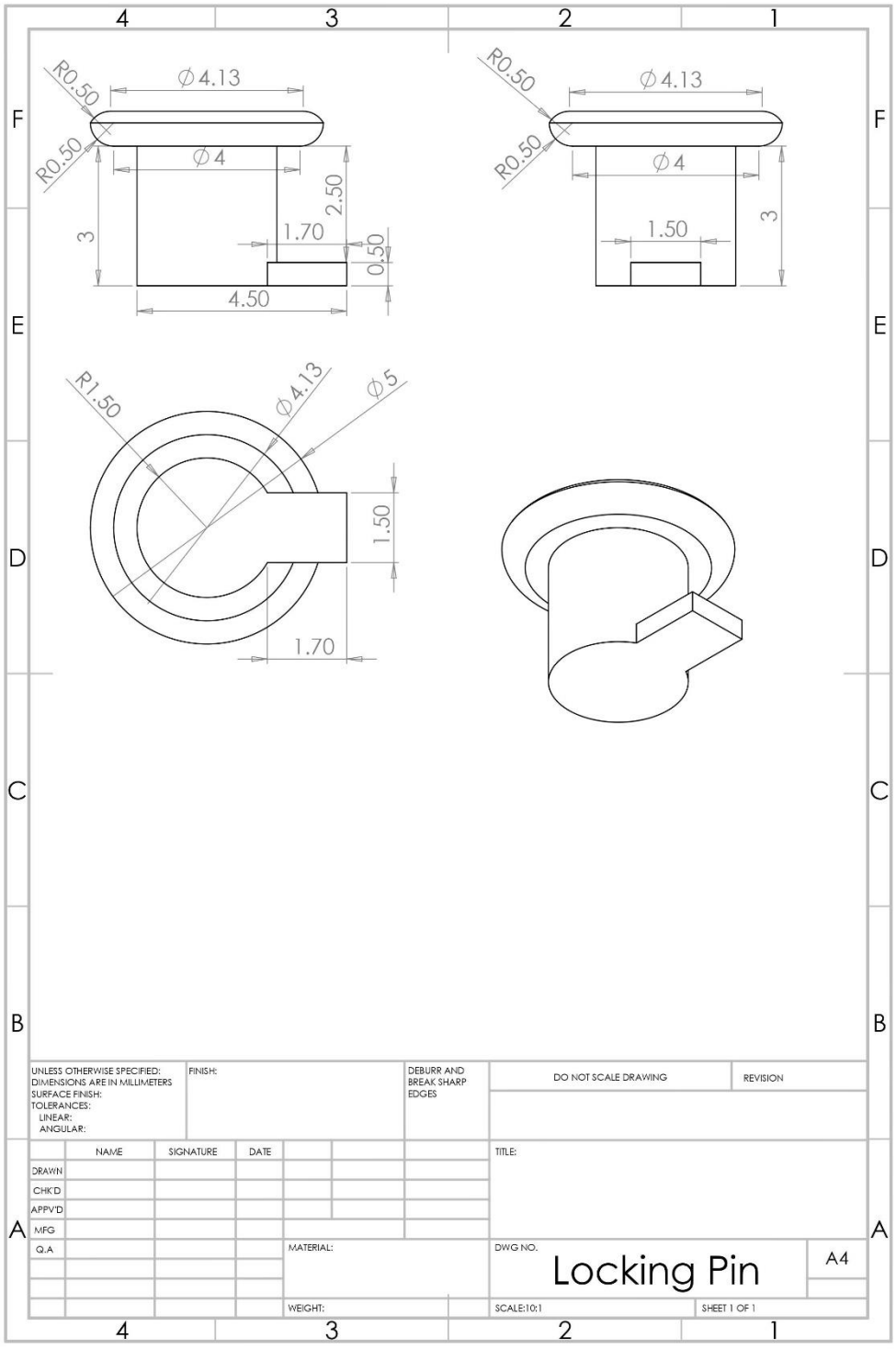

Fig. 14: Locking pin

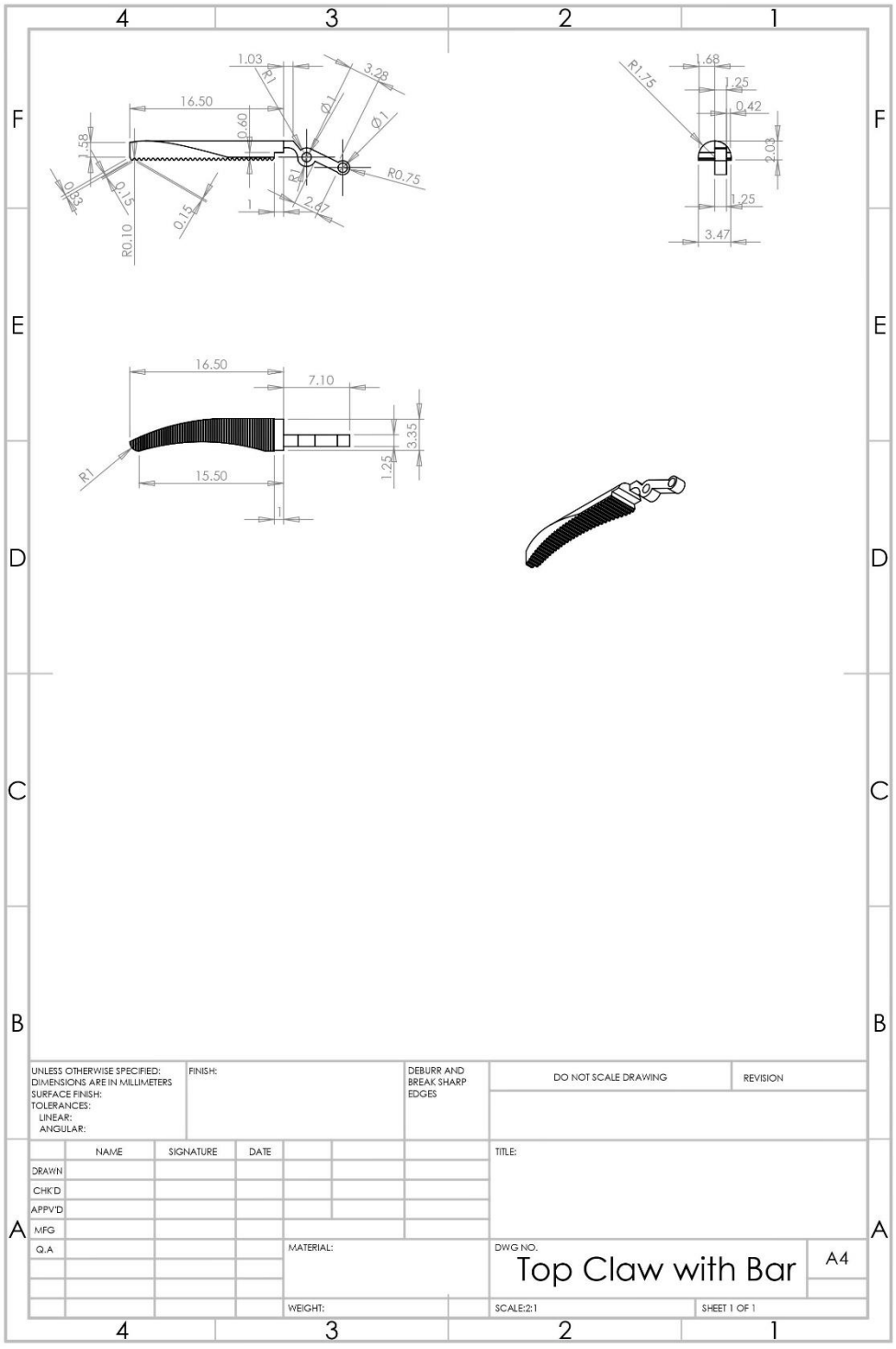

Fig. 15: Top claw with bar

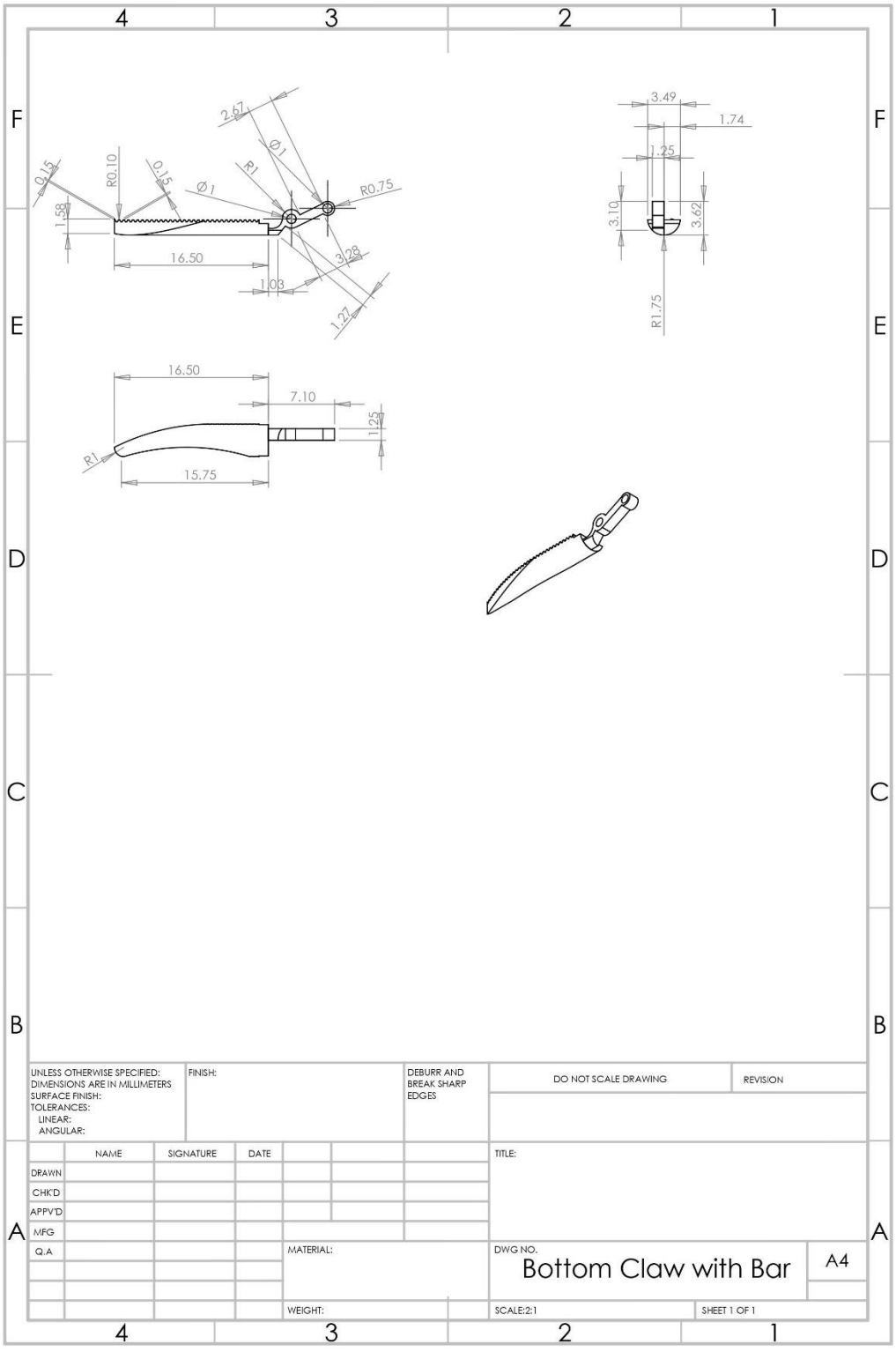

Fig. 16: Bottom claw with bar

Fig. 17: SolidWorks rendering of the model of the proposed laparoscopic forceps

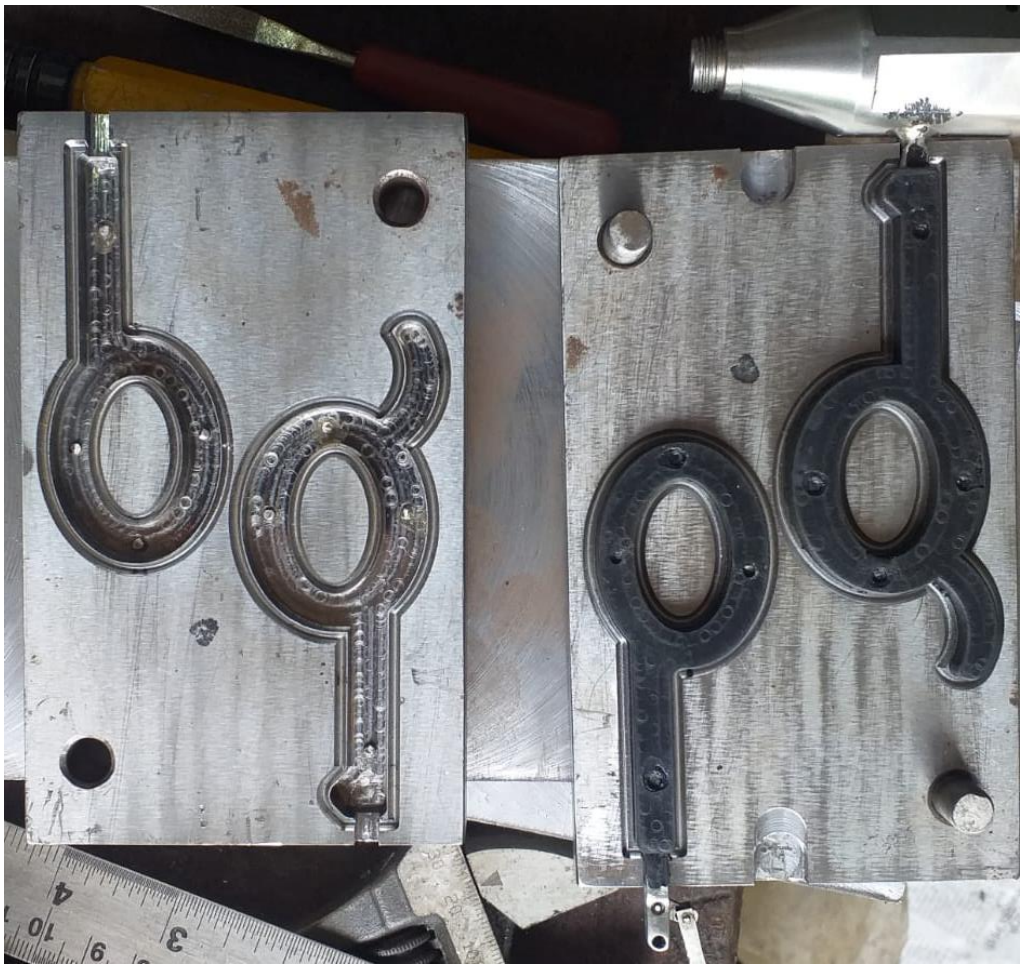

Fig. 18: Die pattern making and molding

User defined function for using Carreau-Yasuda model in ANSYS FLUENT

```
/* Carreau-Yasuda Viscosity Model */

#include "udf.h"

DEFINE_PROPERTY(cell_viscosity,c,t)

{

real mu_inf=0.00345;

real mu_zero=0.16;

real lambda=8.2;

real p=0.64;

real n=0.2128;

real mu_lam;

real rate=(C_STRAIN_RATE_MAG(c,t));

mu_lam=mu_inf + (mu_zero-mu_inf) * pow(1.0 + pow( lambda*rate , p ) , (n-1)/p );

return mu_lam;

}
```

List of publications and presentations

PATENTS:

1. Md. Abdul Raheem Junaidi, Harsha Sista, Ram Chandra Murthy Kalluri, Y. V. Daseswara Rao, (2020). Laparoscopic Surgical Device, IN Patent Application: 202011034072.
2. Md. Abdul Raheem Junaidi, Harsha Sista, Ram Chandra Murthy Kalluri, Y. V. Daseswara Rao, (2020). Laparoscopic Surgical Device, IN Design Patent Application: 334185-001.

INTERNATIONAL JOURNALS:

3. Junaidi MAR, Kalluri RCM, Rao YVD, Gokhale AGK, Patel A., (2021), Design and fluid flow simulation of modified laparoscopic forceps. Comput Methods Biomech Biomed Engin. 24(8), pp. 844-863. doi: 10.1080/10255842.2020.1855331. Epub 2020 Dec 11. PMID: 33305607. **(SCIE indexed).**
4. Junaidi, M., Sista, H., Kalluri, R., Rao, Y., & Gokhale, A. (2021). Simulation of non-Newtonian flow of blood in a modified laparoscopic forceps used in minimally invasive surgery. Computer methods in biomechanics and biomedical engineering, 24(16), 1794–1806. https://doi.org/10.1080/10255842.2021.1919884 **(SCIE indexed).**
5. Md. Abdul Raheem Junaidi, Harsha Sista, Ram Chandra Murthy Kalluri, Y. V. Daseswara Rao, "International Journal of Biomedical Engineering and Technology" on topic " CO_2 Gas Flow Simulation in a Multi-functional Forceps used in Laparoscopic Surgeries" (Accepted). **(SCI indexed).**

BOOK CHAPTERS:

6. Junaidi M.A.R., Pandey G., Ram Chandra Murthy K., Daseswara Rao Y.V. (2021) CFD Studies on the Modified Laparoscopic Instrument Used in Minimally Invasive Surgeries. In:

Sikarwar B.S., Sundén B., Wang Q. (eds) Advances in Fluid and Thermal Engineering. Lecture Notes in Mechanical Engineering. Springer, Singapore. https://doi.org/10.1007/978-981-16-0159-0_56. **(SCOPUS indexed)**.

7. Junaidi M.A.R., Sista H., Rao Y.V.D., Murthy K.R.C. (2021) Challenges in the Design of a Laparoscopic Surgical Forceps. In: Rao Y.V.D., Amarnath C., Regalla S.P., Javed A., Singh K.K. (eds) Advances in Industrial Machines and Mechanisms. Lecture Notes in Mechanical Engineering. Springer, Singapore. https://doi.org/10.1007/978-981-16-1769-0_40. **(SCOPUS indexed)**.

INTERNATIONAL CONFERENCE PUBLICATIONS

8. Abdul Raheem Junaidi, Aakrit Patel, Ram Chandra Murthy, Y. V. Daseswara Rao, Advances in Laparoscopic Surgeries and CFD Perspective of Suction-Irrigation Devices, AIP Conference Proceedings 2317, 030025 (2021); https://doi.org/10.1063/5.0036257 (Received **Best Paper award**). **(SCOPUS indexed)**.

CONFERENCE PRESENTATIONS

1. Md. Abdul Raheem Junaidi, Harsha Sista, Ram Chandra Murthy K and Y. V. Daseswara Rao, "A Versatile Reusable Laparoscopic Instrument for Minimally Invasive Surgeries", SWAYAM, Aug 2020.
2. Md. Abdul Raheem Junaidi, Gourabh Pandey, Ram Chandra Murthy K and Y. V. Daseswara Rao, "CFD Studies on the Modified Laparoscopic Instrument used in Minimally Invasive Surgeries", Aug 2020, 2nd International Conference on Future Learning Aspects of Mechanical Engineering (FLAME - 2020), 5th – 7th August 2020

3. Abdul Raheem Junaidi, Aakrit Patel, K. Ram Chandra Murthy, and Y. V. Daseswara Rao, "Advances in Laparoscopic surgeries and CFD perspective of suction-irrigation devices", AIP Conference Proceedings 2317, 030025 (2021)
4. Md. Abdul Raheem Junaidi, Harsha Sista, Y. V. Daseswara Rao and Ram Chandra Murthy K, “Challenges in the design of a laparoscopic surgical forceps”, IPRoMM, Sep 2020.

Brief biography of the Candidate

Md. Abdul Raheem Junaidi is currently a research scholar working under the supervision of Dr. Ram Chandra Murthy and co-supervision of Prof. Y. V. Daseswara Rao. He is working as an Assistant Professor in the Department of Mechanical Engineering at Muffakham Jah College of Engineering and Technology (MJCET) past nine years. He obtained his B.E (Mechanical Engineering) and M.E (Turbomachinery) from the University College of Engineering (UCE), Osmania University (Autonomous). He obtained gold medal in Tenth SSC board exam, and Intermediate from respective institutes. He bagged many prizes at graduation level in academics and extra-curricular activities. His previous work experience includes being a Technical Writer at the SIA Group of companies, Hyderabad, and a Programmer Analyst in Cognizant Technology Solutions, Chennai. He has filed seven patents and published more than 30 International Journals. He also reviewed reputed international journals like Journal of Complementary and Alternative Medical Research, Journal of The Institution of Engineers (India): Series C, etc., Recently, he received best paper award for his research paper work in an international conference.

Brief biography of the Supervisor

Dr. Ram Chandra Murthy is currently an Assistant Professor at the Department of Mechanical Engineering, Birla Institute of Technology and Science (BITS), Pilani Hyderabad campus. He obtained his B.Tech (Mechanical Engineering) from the Indian Institute of Technology, Madras, and M.S., and Ph.D. from the Rutgers, The State University of New Jersey. His previous experiences include as a Graduate Engineer Trainee at Tata Motors, Pimpri, Pune, and CFD Specialist at Altair Engineering, Bangalore. His teaching and research interests include Computational Fluid Dynamics, Fluid-Structure Interaction, and Rarefied Gas Dynamics. He has published around 20 papers in reputed international journals and presented more than 20 research works in National and International Conferences. Dr. Ram Chandra Murthy K is presently guiding 02 Ph.D. and guided/guiding several graduate and undergraduate students.

Brief biography of the Co-supervisor

Prof. Y. V. Daseswara Rao is currently a Professor at the Department of Mechanical Engineering, Birla Institute of Technology and Science (BITS), Pilani Hyderabad campus. He obtained his B. Tech (Mechanical Engineering) from National Institute of Technology, Surathkal (Known that time as Regional Engineering College), and M. Tech. (Design Eng.) from the Indian Institute of Technology, Delhi (IITD), and Ph.D. from the Government College of Engineering, Raipur (Known now as NIT Raipur). His major areas of research interest include topological synthesis and analysis of Gear trains and Robotic structures. Robot-Assisted Incremental Sheet Metal Forming. Vibration and Shock Isolation. Robotic Dental Implantation. Crashworthiness in automobile vehicles under axial impacts. He has published more than 20 papers in peer-reviewed international journals. He has so far published 40 plus research works in national and international conferences. Prof. Y. V Daseswara Rao is guided 05 Ph.D. and guided/guiding several graduate and undergraduate students.